Biomaterials Science

REVIEW

View Article Online
View Journal

Cite this: DOI: 10.1039/c5bm00085h

A survey of state-of-the-art surface chemistries to minimize fouling from human and animal biofluids

Christophe Blaszykowski,*[a] Sonia Sheikh[b] and Michael Thompson[a,b]

Received 16th March 2015,
Accepted 22nd June 2015

DOI: 10.1039/c5bm00085h

www.rsc.org/biomaterialsscience

Upon contact with bodily fluids, synthetic materials spontaneously acquire a layer of various species (most notably proteins) on their surface. The concern with respect to biomedical equipment, implants or devices resides in the possibility for biological processes with potentially harmful effects to ensue. In biosensor technology, the issue with this natural fouling phenomenon is that of non-specific adsorption to sensing platforms, which generates an often overwhelming interference signal that prevents the detection, not to mention the quantification, of target analytes present at considerably lower concentration. To alleviate this ubiquitous, recurrent problem – this genuine biotechnological plague – considerable research efforts have been devoted over the last few decades to engineer antifouling coatings. Extensive literature now exists that describes stealth organic adlayers capable of reducing fouling surface coverage Γ down to a few ng cm^{-2} – however from biotechnologically irrelevant buffered solutions free or nearly depleted of any potentially interfering species. Regrettably indeed, few coatings are known to display/retain such level of performance when exposed to otherwise more complex, real-life biosamples (even diluted). Herein, we comprehensively review the state-of-the-art surface chemistries developed to date (January 2015) to minimize fouling from 8 such uncomparatively more challenging biological media (blood plasma, blood serum, cell lysate, cerebrospinal fluid, egg, milk, saliva, and urine) – whether of human or animal origin. Literature search for another 25 biological milieux generated no (exploitable) hit. Also discussed in this Review are the identification of the species responsible for fouling, and the dependence of antifouling properties on biosample source variability.

I. Introduction – fouling: a genuine biotechnological plague

The 21st century will be that of Biotechnology. Already, not a week passes without a breakthrough, or a usually more modest contribution to the field, to see the light of day. Whether in *in-* or *ex-vivo* applications, certain aspects of Biotechnology require biofluids – a broad definition of which would be those 'biological media produced by living organisms' – to become exposed to exogenous synthetic materials. Upon contact, these artificial surfaces spontaneously acquire a layer of various accumulated species, most notably (but not only) proteins – a natural, ubiquitous adsorption phenomenon known as 'fouling'. The first event to take place (which is often overlooked or simply ignored) is actually the adsorption of water molecules, followed by ions, to form a hydrated electrostatic layer physically distinct from the local bulk environment.[1] It is only shortly thereafter that proteins start sequentially adsorbing, upon migration from the bulk medium (where they reside solvated) according to their diffusability in solution and affinity for the surface.[1] The adhesion of the much larger, less motile entities that are biological cells happens last, through the adsorbed aqueous layer of ions and proteins.[1–3]

Situations exist where the biofluid-foreign material interaction has a detrimental effect through the surface-mediated activation[4] of adverse biological processes/responses, such as thrombosis and the 'foreign body reaction'.[5–13] This issue has potentially severe, short- or long-term repercussions, which healthcare professionals employing biomedical equipment, implants or devices (most of which are manufactured from exogenous materials such as titanium, stainless steel or plastic) inevitably face during their career and are therefore unfortunately familiar with.[5–13] Negative effects by no means are restricted to the health of the recipients of a medical intervention however, but also may compromise the functionality and performance not to forget the longevity and integrity of biofluid-contacting objects. In biosensor technology too, fouling – more often referred to as 'non-specific adsorption' (NSA) – is notoriously problematic as biofluid matrix components have the propensity to adsorb non-specifically to

[a]Econous Systems Inc., 80 St. George Street, Toronto, Ontario, Canada M5S 3H6. E-mail: cblaszyk@chem.utoronto.ca
[b]University of Toronto, Department of Chemistry – St. George campus, 80 St. George Street, Toronto, Ontario, Canada M5S 3H6

sensing platforms thereby generating often overwhelming interference signals that prevent the detection – let alone the quantification – of target analytes present at considerably lower concentration (several orders of magnitude).[14–16] Indeed, NSA species also produce physicochemical stimuli that are indiscriminately detected by the sensor and interfere with the specific response of the target analyte. From an analytical point of view, the consequence is the possibility for the occurrence of 'false positives', *i.e.* responses incorrectly interpreted as genuine binding events between analytes and sensor recognition elements. Conversely, erroneous 'false negative' readings might result if analyte binding is prevented. Both these situations, understandably, pose serious dangers, most particularly in clinical diagnostics for detection interfaces intending to perform analysis with biosamples possessing highly interfering matrices, such as blood plasma and serum.[14–16] Fouling constitutes arguably the single most important technical reason why biosensors still have not found a prominent place as alternative screening/diagnostic tools in clinical analysis despite tremendous promise notably in terms of cost and ease of operation as well as miniaturization capability for point-of-care testing. In many respects, it is no exaggeration to compare fouling to a 'plague', one Biotechnology deeply suffers from.

Understandly, preventing surfaces that come into intimate contact with biofluids from fouling is paramount in many fields of Biotechnology, and considerable research efforts have consequently been dedicated over many years to engineer antifouling coatings able to reduce, or ideally eliminate entirely, the (non-specific) adsorption of biofluid matrix components – most particularly proteins. Many different types of organic adlayers have been reported for this purpose, oligo- and polyethylene glycol (OEG and PEG) constructs being historically the most prevalent coating materials.[17–23] 'Ultralow' fouling (<5 ng cm^{-2}) has now been achieved for single-protein buffered solutions. Advances are unfortunately limited in scope as few coatings in actuality attain/retain such level of performance when challenged by highly proteinaceous complex media (even diluted), examples of which being blood plasma and serum.[23] Literally hundreds, perhaps even thousands, of articles have been published that praise the antifouling properties of coatings against buffered solutions spiked with a single type – or an extremely simple mixture – of model proteins. When it comes to practical relevance however,[19,24] the literature pertaining to otherwise more demanding real-world biological milieux is, in stark contrast, considerably much more limited.[23]

Herein, we present an up-to-date literature survey of state-of-the-art antifouling surface chemistries developed to minimize fouling from both human and animal biosamples through the implementation of (sub)nanometer thin self-

Christophe Blaszykowski

Dr Christophe Blaszykowski earned an MSc (2001) and a PhD (2005) in Organic Chemistry from Pierre et Marie Curie University (Paris – France). His research focused on developing new radical cyclization, dianionic annulation, and Pt-catalyzed cycloisomerization reactions. In 2006, he then completed a postdoctoral fellowship at the University of Toronto (Toronto – Canada), where he investigated Pd-catalyzed/norbornene-mediated annulation reactions. Since 2006, his multidisciplinary research interests also include Surface Chemistry – notably that of new ultrathin molecular coatings, which he has been collaboratively developing for various companies to modify/tailor the surface properties (e.g. wettability, work function, antifouling, biocompatibility) of different substrate materials of (bio)technological relevance (e.g. ITO, quartz, gold, plastics, stainless steel) for application in such varied areas as molecular optoelectronics, bioanalytical sensors, and biomedical equipment/implants/devices. He is presently a Senior Research Scientist holding the position of Research & Development Manager at Econous Systems Inc. – a biotech startup such company for which he has designed and synthesized the diverse (novel) surface-modifying building block molecules (over 40 to date) necessary for ultrathin adlayer formation.

Sonia Sheikh

Dr Sonia Sheikh received her BSc in Nutritional Science and Chemistry (2007), MASc in Biomaterials and Biomedical Engineering (2009), and PhD in Bioanalytical Chemistry (2014) from the University of Toronto (Canada). Her PhD Thesis focused on the development of antifouling and antithrombogenic ultrathin surface chemistries against biological fluids for bioanalytical and biomedical applications. Dr Sheikh is currently a Postdoctoral Fellow in the Laboratory of Professor Michael Thompson at the University of Toronto, where she is developing real-time and label-free biosensors as advanced alternatives to current clinical diagnostic techniques for various diseases/conditions. Always of great interest for Dr Sheikh are both the fundamental and applied research on novel antifouling and biocompatible coatings, which she is also currently investigating.

assembled monolayers (SAM) or thicker polymer films/brushes (Fig. 1).[23] Among the 33 biological media searched, only the following 8 generated exploitable hits – to date (January 2015) and our knowledge – and will be described in this Review: blood plasma, blood serum, cell lysate, cerebrospinal fluid, egg, milk, saliva, and urine. The remaining 25 biological milieux are listed later on. Literature relating to special architectures (*e.g.* membranes,[25] fluidic channels,[26,27] array chips,[28] (nano)particulate systems/quantum dots and beads,[29] wires/electrodes,[30] polymer suspensions[31]), to the additional use of sacrificial blocking biomolecules or surfactants,[28,32,33] and to biofouling[18,34] is not covered. Also not treated are the adsorption dynamics of biofluid multi-components (both global and individual aspects),[4,23] as well as the physicochemical mechanistic hypotheses put forth to try and rationalize the antifouling properties of surfaces.[17–21,35,36] In every instance, interested readers are kindly invited to consult the provided literature. At the exception of some key references, this Review is restricted to biosample solutions containing ≥10 vol% of biofluid, and to fouling surface coverage $\Gamma < 30$ ng cm^{-2} (*quantified* with a suitable technique[37]). At greater dilution, fouling certainly may become negligible;[14] nevertheless, from a practical standpoint, such solutions and testing conditions definitively lose relevance with respect to most real-life applications.[38] The same holds true for too high a fouling surface coverage. This Review intends to constitute a comprehensive treatment of pertinent literature. We apologize however to those researchers, whose scientific contribution(s) may have been inadvertently omitted.

Michael Thompson

Professor Michael Thompson obtained his undergraduate degree from the University of Wales, UK and his PhD in analytical chemistry from McMaster University. In 1971, he was appointed Lecturer in Instrumental Analysis at Loughborough University. He then moved to the University of Toronto where he is now Professor of Bioanalytical Chemistry. He has held a number of distinguished research posts including the Leverhulme Fellowship at the University of Durham and the Science Foundation Ireland E.T.S Walton Research Fellowship at the Tyndall National Institute, Cork City. He is recognized internationally for his pioneering work over many years in the area of research into new biosensor technologies and the surface chemistry of biochemical and biological entities. Thompson has served on the Editorial Boards of a number of major international journals including Analytical Chemistry and The Analyst and is currently Editor-in-Chief of the monograph series "Detection Science" for the Royal Society of Chemistry, UK. He has been awarded many prestigious international prizes for his research including The Robert Boyle Gold Medal of the Royal Society of Chemistry and the E.W.R. Steacie Award of the Chemical Society of Canada. He was made a Fellow of the Royal Society of Canada in 1999.

II. Antifouling surface chemistries against blood plasma/serum

II.A. Blood: the biofluid of life

Blood is a complex biofluid in which bathe both cellular and non-cellular species that are essential in sustaining life as they provide a means of delivering vital nutrients and gases to cells (or conversely disposing of metabolic waste products), of regulating the internal environment (*e.g.* pH, osmosis), of protecting the organism against foreign bodies (through the action of the immune system), or of preventing blood loss (*via* haemostasis and coagulation).[39–42] Considering the importance of blood in maintaining an organism healthy and functional, it is not surprising that the daily production of blood cells reaches approximately 1 trillion.[41] On average, the volume of blood in human adults is about 5 liters, or ~7% of the body weight.[42] Whole blood is essentially composed of three parts, which easily separate upon centrifugation.[39–42] The lightest fraction is 'blood plasma', a viscous aqueous liquid that accounts for ~55% of the volume of blood. The second, thinner phase is called 'buffy coat' (~1% in volume) and contains platelets and white blood cells (WBCs). Lastly, red blood cells (RBCs) make up the densest fraction, which accounts for the remaining ~45% of blood volume. Buffy coat and RBCs collectively constitute the cellular fraction of blood (the 'formed elements'). RBCs or 'erythrocytes', WBCs or 'leukocytes', and non-nucleated platelets or 'thrombocytes' each have their own special purpose.[39–44] While RBCs for instance contain haemoglobin to transport oxygen fuel and carbon dioxide waste, WBCs provide protection against pathogens and other foreign entities through the body's immune response. Platelets finally are a key factor in haemostasis and coagulation with the formation of blood clots ('thrombosis') at the site of an injury. On the other hand, plasma gathers the non-cellular components of blood and is mainly composed of water (~90%), the remaining dry matter consisting of such elements as ions, lipids, vitamins, and thousands of proteins[45] including albumin, globulins and fibrinogen.[42,46] Albumin – the most profuse plasma protein (30–50 g L^{-1}) – is an osmotic regulator as well as functions as a carrier for various species such as ions, fatty acids, amino acids, and enzymes.[39,46] Immunoglobulins (commonly known as 'antibodies') – that are characterized by great structural diversity – are the next most abundant plasma proteins, followed by fibrinogen that has an approximate blood concentration of 1.5–4 g L^{-1} and is essential for the formation of blood clots.[39,46] When fibrinogen and other clotting factors are removed from plasma (upon coagulation then centrifugation of whole blood), the remaining medium is known as 'blood serum'.[39]

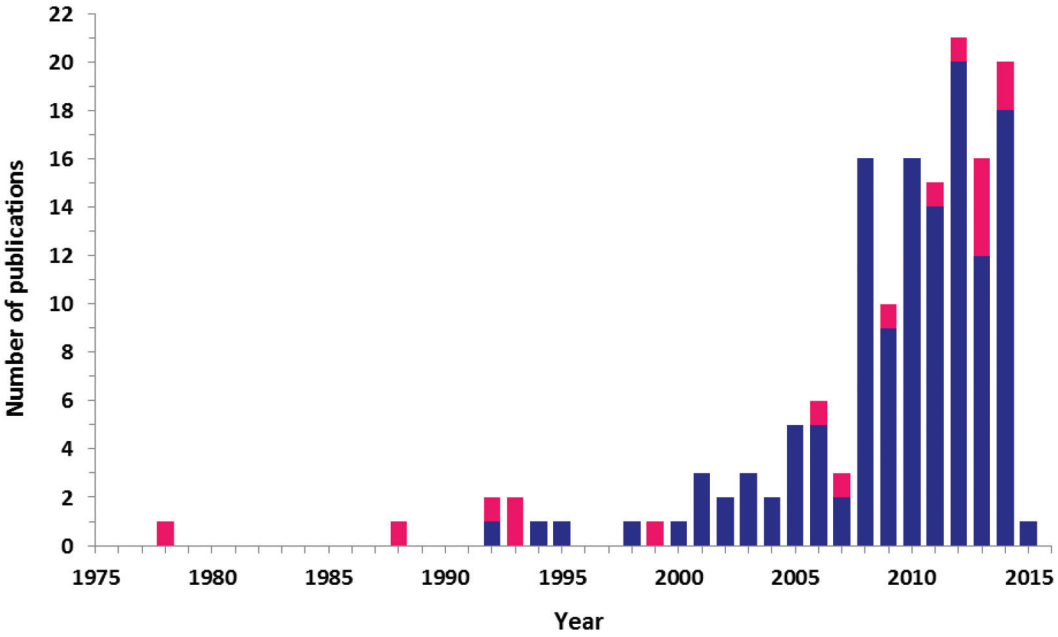

Fig. 1 40 years of antifouling surface chemistry: histogram showing the distribution by year of the publications inventoried in this Review containing the keywords 'antifouling', 'low-fouling', 'non-fouling', or 'fouling' associated with 'plasma', 'serum', 'cell lysate', 'cerebrospinal fluid', 'egg', 'milk', 'saliva', or 'urine' (from Scifinder® database – last updated January 2015). The colour code is as follows: blue (blood plasma/serum) and pink (other biological media). Adapted from ref. 23 with permission of the Royal Society of Chemistry.

Even cleared of the cellular components of blood (*vide supra*), blood plasma and serum still constitute highly complex matrices of strongly adhesive proteins at high concentration (~60–80 g L^{-1}).[47] Let us now first explore the various antifouling surface chemistry strategies developed to date to combat fouling from blood plasma/serum biosamples.

II.B. 'Bioinspired' constructs: single amino acids, peptides and peptoids

We begin our survey of state-of-the-art antifouling surface chemistries with the work of Lundström and co-workers, who 'as early as' 1995 used *in situ* ellipsometry to study the antifouling properties of L-cysteine (Fig. 2A) monolayers directly attached on gold, against 10% human plasma diluted in phosphate buffered saline (PBS).[48] After exposure for 10 min followed by successive PBS/water rinsings, the amount of adsorbed proteins was estimated to be $\Gamma \sim 200$ ng cm^{-2} – a value slightly lower than that recorded on bare gold. [A very recent 2014 account, describing ~1.1 nm-thick L-cysteine coatings on gold-sputtered stainless steel substrates, appears to have been more successful at reducing fouling either from undiluted human serum or sheep plasma, as assessed by BCA protein assay upon 15 min exposure at 37 °C.[49]] However, a real significant difference ($\Gamma < 50$ ng cm^{-2}) was observed for gold derivatized with a monolayer of glutathione tripeptide (Fig. 2B). This work was an extension of previous studies by the investigators, wherein total and individual protein adsorption from 10% human plasma/serum on these nanometer-thick monolayers (~0.6 and 1.3 nm, respectively) had been probed using ellipsometry combined with antisera binding experiments.[50,51]

Further investigations on the antifouling properties of single amino acid-based monolayers – tethered to gold substrates through *N*-3-mercaptopropionic acid (3-MPA) graft residues – were conducted by Masson's group in 2008.[52] NSA upon exposure to undiluted bovine serum (76 mg protein per mL) for 20 min was quantified by means of surface plasmon resonance (SPR). Among the 19 natural amino acids studied, the lowest amount of NSA ($\Gamma \sim 418$ ng cm^{-2}) was monitored for SAMs made of polar (L-Asn, L-Ser) or

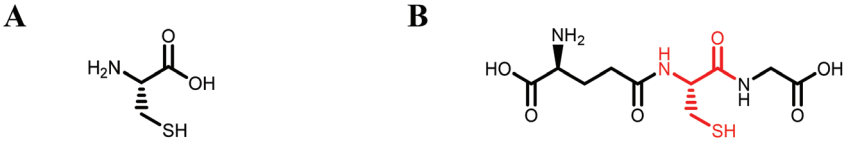

Fig. 2 Molecular structure of (A) L-cysteine amino acid, and (B) glutathione tripeptide. Adapted from ref. 23 with permission of the Royal Society of Chemistry.

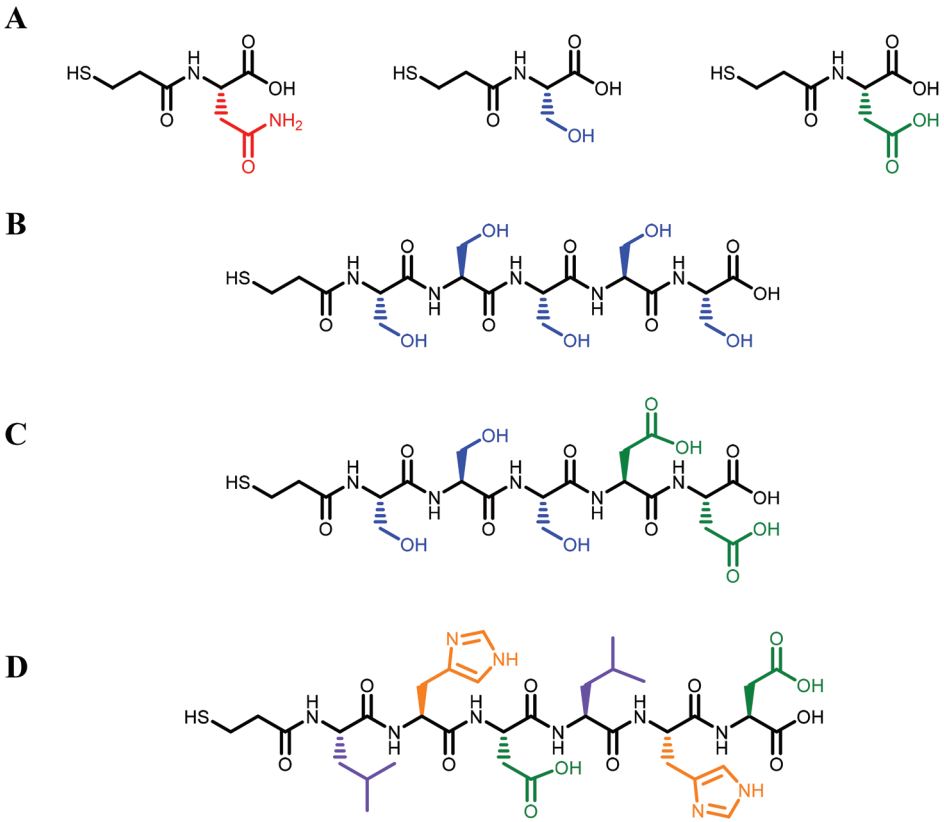

Fig. 3 Molecular structure of (A) 3-MPA-Asn-OH, 3-MPA-Ser-OH, and 3-MPA-Asp-OH single amino acids, (B) 3-MPA-Ser_5-OH homopentapeptide, (C) 3-MPA-Ser_3-Asp_2-OH binary-patterned pentapeptide, and (D) 3-MPA-$(Leu\text{-}His\text{-}Asp)_2$-OH ternary-patterned hexapeptide. Adapted from ref. 23 with permission of the Royal Society of Chemistry.

ionic (L-Asp) amino acids (Fig. 3A). Conversely, the highest amount of fouling ($\Gamma \sim 808$ ng cm^{-2}) was observed for hydrophobic L-tyrosine. The following year, the investigators were able to substantially decrease NSA by expanding the scope of their study to short 3-MPA-homopeptide-based SAMs.[53] Surface coverage due to NSA was lowest ($\Gamma = 132 \pm 33$ ng cm^{-2}) for pentapeptide SAMs featuring L-serine subunits (Fig. 3B). Continuing on, further remarkable progress was achieved by Masson and co-workers using 3-MPA-pentapeptides presenting binary sequences of amino acids.[54,55] For the nine different peptide designs investigated, NSA was consistently lower than $\Gamma = 80$ ng cm^{-2}, highest resistance to serum adsorption being the feat of 3-MPA-Ser_3-Asp_2-OH SAMs with $\Gamma = 23 \pm 10$ ng cm^{-2} (Fig. 3C). Best antifouling performance, to our knowledge, was reached in 2011 with a third-generation of ternary-patterned hexapeptide constructs, of which 3-MPA-$(Leu\text{-}His\text{-}Asp)_2$-OH (Fig. 3D) SAMs were the most effective at reducing NSA ($\Gamma = 12 \pm 11$ ng cm^{-2}).[56]

Unlike Lundström in 1995[48] and Masson in 2008,[52] Booksh was able very recently to prepare a single amino acid-based coating with pronounced antifouling properties.[57] In this 2015 account, anchorage to gold substrates did not rely on thiol chemistry however,[48,52] but on an electrografting reaction involving a diazonium salt of phenylalanine (Fig. 4).[57] Surface

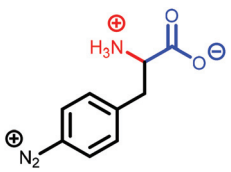

Fig. 4 Molecular structure of 4-diazonium-DL-phenylalanine.

coverage due to fouling by crude bovine serum (undiluted, 75 mg protein per mL), measured by SPR upon 20 min exposure, was relatively good at $\Gamma = 42 \pm 4$ ng cm^{-2}. In comparison, the level of adsorption on bare gold was reported to be $\Gamma = 96 \pm 2$ ng cm^{-2}.

In 2002, Picart and co-workers reported their findings on the antifouling properties of several polyelectrolyte multilayered films (1 to 153 nm-thick) made of alternating strata of poly(L-lysine) PLL and poly(L-glutamic acid) PGA polypeptides (Fig. 5).[58] Using optical waveguide lightmode spectroscopy (OWLS) and 10% serum diluted in MES-Tris[59] buffer, the authors observed that coatings exposing a terminal PLL layer invariably adsorbed a significant amount of proteins ($\Gamma >$ 300 ng cm^{-2}, 60 min contact), regardless of film thickness (*i.e.* irrespectively of the number of alternating layers beneath).

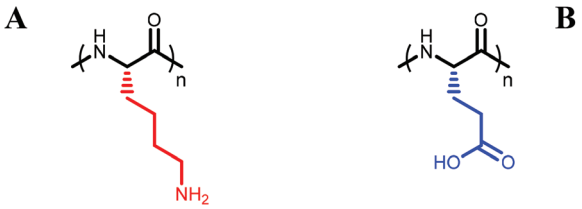

Fig. 5 Molecular structure of (A) poly(L-lysine) PLL, and (B) poly(L-glutamic acid) PGA. Adapted from ref. 23 with permission of the Royal Society of Chemistry.

Conversely, serum adsorption on PGA-terminated coatings was undetectable, at least up to six strata of polyelectrolytes for ~16 nm-thick $(PLL/PGA)_3$ films.

More recently (in 2013), Liu and co-workers prepared zwitterionic poly(L-serine) brushes on gold through an environmentally-friendly (catalyst-free), 'grafting from' photochemical process – known as 'surface-initiated photoiniferter-mediated polymerization' (SI-PIMP) – that involved a pre-coated thiol SAM of dithiocarbamoyl photoiniferter (Fig. 6A) and L-serine methacrylate monomer (Fig. 6B).[60] Considering that film thickness (and uniformity) could be easily controlled by simply varying the UV-photoirradiation time, the authors were able to determine the relationship existing between this parameter and fouling by 100% human blood plasma/serum. Interestingly, results showed that serum fouling was minimal (Γ = 9.2 ± 1.3 ng cm^{-2}) at the intermediate thickness of ~37 nm, as measured upon 10 min exposure using SPR as the detection technique. Both thinner and thicker brushes (~5–55 nm range) were indeed less resistant to serum adsorption with $10 < \Gamma < 50$ ng cm^{-2}. Gratifyingly, fouling by full human plasma at optimal film thickness was also limited (Γ = 12.9 ± 2.1 ng cm^{-2}). In contrast, both bare gold and ~2.7 nm-thick photoiniferter SAM surfaces were substantially fouled by both these fluids (Γ > 150 ng cm^{-2}).[60–62] In a series of follow-up papers published in 2014, Liu's group expanded the scope of zwitterionic poly(L-amino acid) antifouling brushes grown on gold through the versatile SI-PIMP process.[61–63] Another novelty, beside the chemical structure of the amino acid side-chain (Fig. 6C–F), was the 'amide' nature (*vs.* 'ester') of the newly polymerized monomers (Fig. 6C–F *vs.* 6B). Methacrylamide-based brushes were invariably more antifouling than the methacrylate ester variety, whether against 100% human plasma or 100% human serum.[61–63] Experimentally, although there was essentially no statistical difference in terms of antifouling properties within the amide series, the best performance against full plasma (Γ = 3.2 ± 2.3 ng cm^{-2}) was recorded for ~15 nm-thick ornithine-based brushes (Fig. 6C), upon 10 min contact.[61,62] With respect to full serum, aspartic acid-based brushes (~12 nm-thick, Fig. 6E) offered superior performance with Γ = 0.8 ± 0.8 ng cm^{-2}.[62,63] [Of note, aging of these latter brushes – upon 4 h UV irradiation followed by 7 day storage in PBS – did not significantly alter their thickness (still ~12 nm) or antifouling properties (Γ = 2.8 ± 2.9 ng cm^{-2}).[63]] Achieving greater antifouling performance with thinner coatings – by switching research from methacrylate- to methacrylamide-based brushes – was indeed another accomplishment by the authors.

In a 2005 exploratory investigation, Messersmith and co-workers reported the synthesis of a new peptidomimetic polymer with which to modify Ti surfaces for antifouling purposes.[64] This hybrid polymeric material features two distinct domains: (i) a short biomimetic substrate-anchoring pentapep-

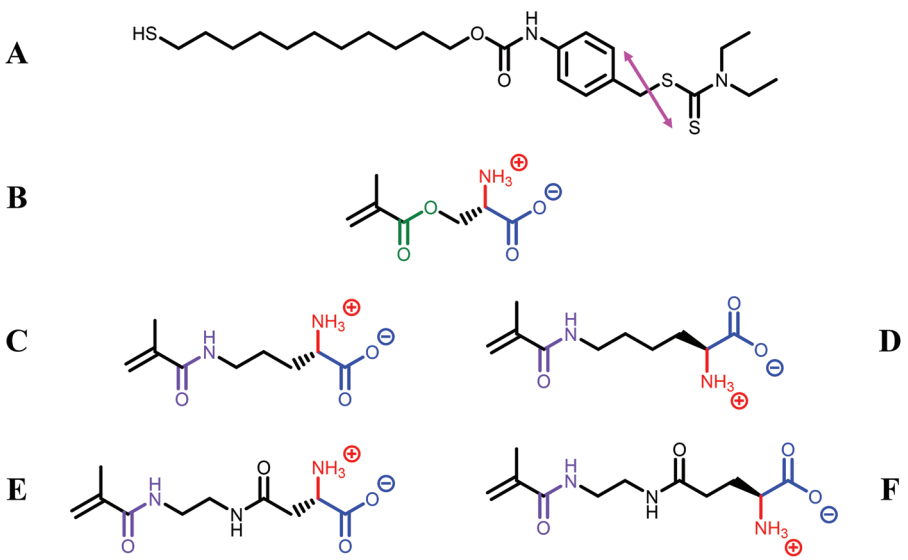

Fig. 6 Molecular structure of (A) the dithiocarbamoyl thiol photoiniferter (the double arrow marks the future site of polymerization), (B) the L-serine methacrylate monomer; as well as the (C) L-ornithine, (D) L-lysine, (E) L-aspartic acid-based, and (F) L-glutamic acid-based methacrylamide monomers.

tide made of alternating L-DOPA[65] and L-lysine residues, *N*-coupled to (ii) a *N*-(2-methoxyethyl)-substituted 20-mer polypeptoid (Fig. 7A). Excellent resistance to protein adsorption (20 min exposure) from whole human serum was demonstrated by means of OWLS ($\Gamma \sim 4$ ng cm^{-2} as opposed to $\Gamma \sim 435$ ng cm^{-2} for unmodified Ti substrates). The project was later expanded to investigate the influence on antifouling of the nature of the peptoid side-chains. In the new study, three different side-chains would be employed (2-methoxyethyl, 2-hydroxyethyl, and 2-hydroxypropyl) while keeping identical the adhesion pentapeptide sequence (Fig. 7A–C).[66] Although the investigators encountered mixed success among polymers, all three ~4.3 nm-thick coatings displayed substantially superior antifouling properties against whole human serum than the unmodified TiO_2 substrate of the study (Γ = 15–83 *vs.* 342 ± 21 ng cm^{-2}), when exposed for 20 min at 37 °C. Long-term resistance (1 week) to enzymatic degradation was also demonstrated. Varying the repeat length of *N*-(2-methoxyethyl)-substituted peptoid segments (n = 10 to 50, for a coating thickness ranging from 2.8 to 4.2 nm) was also shown soon after to

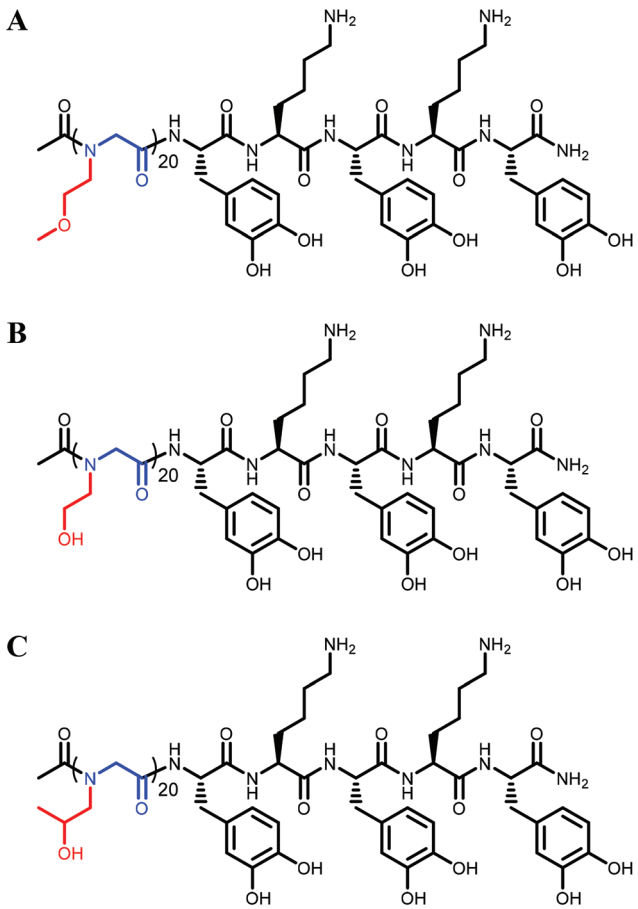

Fig. 7 Molecular structure of the (A) *N*-(2-methoxyethyl)-, (B) *N*-(2-hydroxyethyl)-, and (C) *N*-(2-hydroxypropyl)-substituted 20-mer polypeptoids C-coupled to a substrate-anchoring pentapeptide sequence made of alternating L-DOPA and L-lysine residues. Adapted from ref. 23 with permission of the Royal Society of Chemistry.

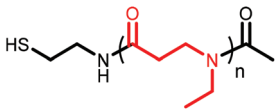

Fig. 8 Molecular structure of $PEtA_{20}$ (n = 20) and $PEtA_{40}$ (n = 40) poly(*N*-ethyl-β-alanine) poly(β-peptoid)s. Adapted from ref. 23 with permission of the Royal Society of Chemistry.

have statistically no significant effect on protein adsorption (Γ = 15–53 ng cm^{-2}).[67]

To our knowledge, the most recent report on peptoid-based antifouling coatings was published in 2011 by Liu and Jia.[68] In this study, the authors introduced a new type of peptoid polymer featuring *N*-ethyl-β-alanine subunits (Fig. 8). These poly(β-peptoid)s were tethered to gold *via* C-terminal cysteamine graft residues. Fouling was assessed using SPR upon contact for 10 min with dilute (10% in PBS) as well as full human plasma and serum. Gold substrates coated with $PEtA_{20}$ – a 20-mer of *N*-ethyl-β-alanine (Fig. 8, n = 20) – exhibited excellent antifouling properties whether against 10% serum (Γ = 10.7 ± 3.6 ng cm^{-2}) or 10% plasma (Γ = 5.2 ± 6.2 ng cm^{-2}). Gratifyingly, comparable levels of performance were achieved both for 100% serum (Γ = 10.8 ± 14.8 ng cm^{-2}) and 100% plasma (Γ = 9.8 ± 12.7 ng cm^{-2}). Better yet, it turned out that $PEtA_{20}$ coatings are quasi-systematically outperformed, both in terms of performance and reproducibility of measurement, by adlayers constructed with the longer $PEtA_{40}$ poly(β-peptoid)s shown in Fig. 8 (n = 40). In fact, fouling amounts on $PEtA_{40}$ coatings from 10% serum and 10% plasma were respectively Γ = 3.9 ± 1.2 and 5.7 ± 1.5 ng cm^{-2}, while those for 100% serum and 100% plasma were Γ = 5.9 ± 3.4 and 9.7 ± 3.2 ng cm^{-2}.

II.C. Oligo- and polyethylene oxides/glycols

We now turn our attention towards oligo- and polyethylene oxide (OEO and PEO) constructs and their derivatives, which all together constitute what has probably been the single most investigated/employed class of antifouling coating materials over the years (see Table 1 in upcoming subsection IV.A.).

We begin this subsection with the work of Horbett and coworkers, who in 2007 explored with SPR the antifouling properties of tetraglyme (Fig. 9) coatings against human plasma.[69] The study concluded that these films, RF plasma-deposited onto gold with a typical thickness of 100 nm, strongly resist protein adsorption even at low plasma dilution in PBS. Fouling from 10, 50 and 100% human plasma (10–20 min exposure) was calculated to be Γ = 4.8, 17.3 and 24.1 ng cm^{-2}, respectively. In comparison, bare gold adsorbed a considerably greater amount of proteins ($\Gamma \sim 244$ ng cm^{-2}), even from 1%

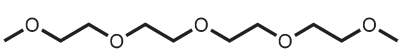

Fig. 9 Molecular structure of tetraglyme. Reproduced from ref. 23 with permission of the Royal Society of Chemistry.

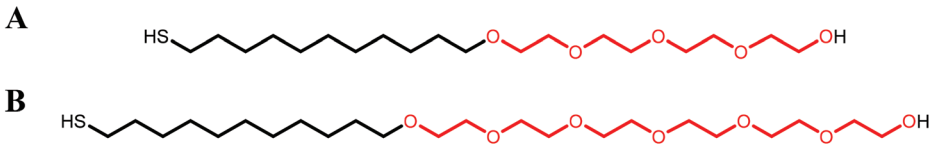

Fig. 10 Molecular structure of the OEG_n-terminated alkylthiol building block molecules (A: n = 4, B: n = 6) for antifouling SAM formation on gold. (A) adapted from ref. 23 with permission of the Royal Society of Chemistry.

plasma. At this dilution, fouling on tetraglyme films was Γ = 1.3 ng cm^{-2}.

This short/light tetrameric OEG chain was later (in 2010) integrated by Chang *et al.* into a linear, OEG_4-terminated alkylthiol molecule (Fig. 10A) with which OEG_4-SAMs were formed on gold.[70–72] These exhibited relatively good antifouling properties (Γ = 38.3 ng cm^{-2}) against 20% human platelet-poor plasma (PPP), as measured at 37 °C with SPR (~15 min exposure). Two years earlier, Jiang's group had not been as successful ($\Gamma \sim$ 200 ng cm^{-2}) using 10% human plasma.[73] Gratifyingly, 10% and even 100% human serum triggered significantly less fouling with $\Gamma \sim$ 15 and 85 ng cm^{-2}, respectively.[73–75] Recently, in 2012, Rodriguez-Emmenegger *et al.* reported that OEG_6-SAMs (9 Å-thick), prepared with a slightly longer thiol molecule (Fig. 10B), performed reasonably well against undiluted foetal bovine serum (FBS) with Γ = 26.1 ± 2.7 ng cm^{-2}, after contact for 15 min.[76,77] Fouling from an undiluted human biofluid (blood plasma) was again an issue (Γ = 71.0 ± 8.0 ng cm^{-2}).

Higher molecular weight PEG molecules (2–20 kDa range),[78] grafted onto gold SPR sensor chips through sulfhydryl moieties as well, were also used to form coatings ~1 to 5 nm-thick with good antifouling properties.[79] Resistance to protein adsorption – against 10% FBS for 30 min at 25 °C – was indeed measured to be Γ = 6–10 ng cm^{-2}, the best performance belonging to intermediarily dense/thick PEG films formed with 5 kDa polymer molecules. With respect to human blood-based fluids, another, more recent 2012 study reported 8.1 nm-thick $PEG_{20\ kDa}$ coatings able to minimize fouling from 100% (pooled) human blood plasma to $\Gamma \sim$ 25 ng cm^{-2}, as measured with SPR upon 20 min exposure.[80] In contrast, bare gold was heavily fouled with Γ = 293 ± 70 ng cm^{-2}.

The aforementioned experiment by Chang *et al.* constituted a control reference to a study primarily dedicated to explore the resistance to protein adsorption of Pluronic™ coatings on gold.[70] Pluronics™ – or poloxamers – are amphiphilic PEO-*bl*-PPO-*bl*-PEO triblock copolymers consisting of a central hydrophobic polypropylene oxide (PPO) segment flanked by two hydrophilic PEO chains. Poloxamer adlayers were prepared upon physisorption of the copolymers' middle PPO block onto pre-coated hydrophobic SAMs of 1-undecane-thiol, an arrangement which compels hydrophilic PEO side-chains to project outwards in the liquid environment. Interestingly, it was shown for Pluronic™ F108 coatings (Fig. 11) that PEO surface coverage plays a critical role on plasma protein adsorption. High-density surfaces (11 PEO chains/100 nm^2) adsorbed the least amount of proteins from 20% PPP (Γ < 1.5 ng cm^{-2}). In comparison, low-density surfaces (3 PEO chains/100 nm^2) adsorbed a substantially greater amount of proteins (Γ = 61.5 ng cm^{-2}), a value even higher than that recorded for the OEG_4-reference SAMs discussed earlier on (Γ = 38.3 ng cm^{-2}).[70]

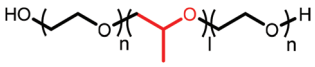

Fig. 11 Molecular structure of Pluronic™ F108 triblock copolymer (n = 133, l = 50). Adapted from ref. 23 with permission of the Royal Society of Chemistry.

In 2005, Tosatti and co-workers had explored closely related triblock copolymer structures (Fig. 12A), in which the two external PEG chains were now flanking a central polypropylene sulfide (PPS) block.[81] Unlike the preceding Pluronics™ F108 coatings that were physisorbed onto pre-coated alkanethiol SAMs through hydrophobic-hydrophobic interactions,[70] these PEG-*bl*-PPS-*bl*-PEG adlayers (~34 Å-thick) were directly anchored to the gold surface through multisite polysulfide chemisorption of their central PPS segment.[81,82] The impact of these PEG films on fouling from whole human serum, measured by means of SPR (30 min exposure), was also considerable, protein adsorption being reduced to Γ = 16 ± 5 ng cm^{-2} – from Γ = 380 ± 14 ng cm^{-2} for bare gold and Γ = 198 ± 81 ng cm^{-2} for PPS-only coatings.[81] Similar antifouling performance (Γ = 25 ± 17 ng cm^{-2}) was recorded for adlayers con-

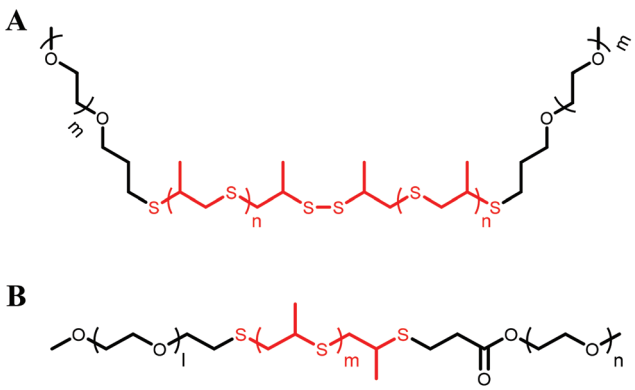

Fig. 12 Molecular structure of two variants of sulfur-based poloxamer analogues (PEG-*bl*-PPS-*bl*-PEG triblock copolymers). Adapted from ref. 23 with permission of the Royal Society of Chemistry.

structed with another variety of PEG-*bl*-PPS-*bl*-PEG triblock copolymer (Fig. 12B).[82] Unlike three commonly used CH_3-, HO- and COOH-terminated alkylthiol SAMs however, these PEG-*bl*-PPS-*bl*-PEG coatings also proved to be insensitive to sulfur oxidation under ambient conditions for at least 41 days (as demonstrated through XPS analysis). This characteristics, together with the multidentate nature of PPS chemisorption, contributes in endowing these polymer adlayers with greater stability.

Another kind of multidentate copolymeric chemisorbate with pendant PEG chains was introduced in 2010 by Robin and co-workers for the surface modification of titanium oxide.[83,84] This macromolecule – a terpolymer featuring undecyl-phosphonate, PEG and *n*-butyl side-chains branching out of a central methacrylate backbone in a 1/1/8 ratio (Fig. 13) – displayed the ability to self-organize onto TiO_2 substrates and impart the latter with excellent antifouling properties. Indeed, protein adsorption on this 30 Å-thick adlayer was $\Gamma = 4 \pm 1$ ng cm^{-2}, as measured with OWLS upon 15 min exposure to full human serum.[83]

In 2009, Schaaf and Mésini had also described poly(acrylic acid) (PAA)-based coatings derivatized with short OEO_3 side-chains (Fig. 14) at different grafting ratios (GR).[85] These polymer constructs were immobilized on silicon/titanium oxide substrates through an intercalated precursor film made of alternating poly(styrene sulfonate)/poly(allylamine hydrochloride) polyelectrolyte layers – this stratified structure being itself anchored to the substrate *via* a poly(ethylene imine) adhesion coating. PAA-*g*-OEO_3 films with GR <20% were reasonably antifouling with Γ = 18–51 ng cm^{-2}, as measured with OWLS upon exposure to 10% FBS. It is only when GR reached 24% (and up to 42%) that fouling surface coverage dropped to a much more technologically-interesting level (Γ = 1 ng cm^{-2}). In stark contrast, non-derivatized PAA coatings were heavily fouled with Γ = 297 ng cm^{-2}.[85,86]

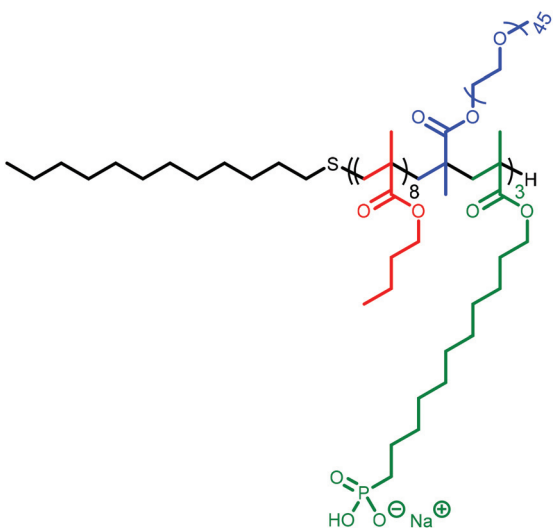

Fig. 13 Molecular structure of the PEG-polyalkyl phosphonate terpolymer. Adapted from ref. 23 with permission of the Royal Society of Chemistry.

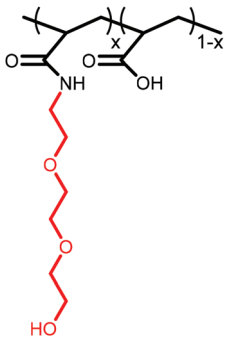

Fig. 14 Molecular structure of the PAA-*g*-OEO_3 polyelectrolyte adsorbates.

Soon after, in 2011, Textor and co-workers reported architecturally more complex OEG dendritic structures capable of self-assembling onto TiO_2 surfaces.[87] These macromolecules featured OEG dendrimer arms conjugated to substrate-anchoring L-DOPA/dopamine multidentate oligopeptides (Fig. 15). Resistance to protein adsorption was measured using ellipsometry, upon exposure to full blood serum for 20 min, and shown to be strongly dependent on dendron surface coverage. Lowest fouling, actually below the limit of detection (LOD) of the technique, was obtained for monomolecular adlayers at saturation coverage. *In situ* OWLS measurements with a lower detection limit of ~2 ng cm^{-2} confirmed this observation.

Films prepared with a linear PEG multisorbate of similar molecular weight (Fig. 16) also exhibited such remarkable antifouling properties.[87] This work constituted the latest addition to several previous studies, wherein linear PEG adsorbates featuring various L-DOPA-, dopamine- or derivatives-based anchors had also been successfully tested for their ability to form robust and stable adlayers with high fouling resistance against full human serum/plasma.[88–94]

Later in 2011, Huck and co-workers published the findings of a more systematic structural study, wherein the influence on protein adsorption of OEO polymer brush architecture was investigated.[95] Various brushes with regular, linear, or dendritic side-chain substructures were prepared *in situ* through atom transfer radical polymerization (ATRP) of mono/oligoglycerol (meth)acrylate monomers (Fig. 17A–C) – a 'grafting from' process surface-initiated by precursor thiol SAMs of ω-mercapto-undecyl α-bromoisobutyrate (Fig. 17D) pre-coated on gold. Fouling from non-diluted human serum and plasma (5 min exposure at 25 °C) was quantified using SPR. Highest resistance to serum adsorption (Γ = 20 ± 10 ng cm^{-2}) was recorded for first-generation dendritic brushes 17 nm-thick. In contrast, their second-generation counterparts performed poorly, so did the regular[96] and linear methoxylated (R = Me) brushes. All these less performing coatings indeed adsorbed greater amounts of serum proteins (Γ > 100 ng cm^{-2}), and this irrespectively of brush thickness (3 to 22 nm). Solely the linear

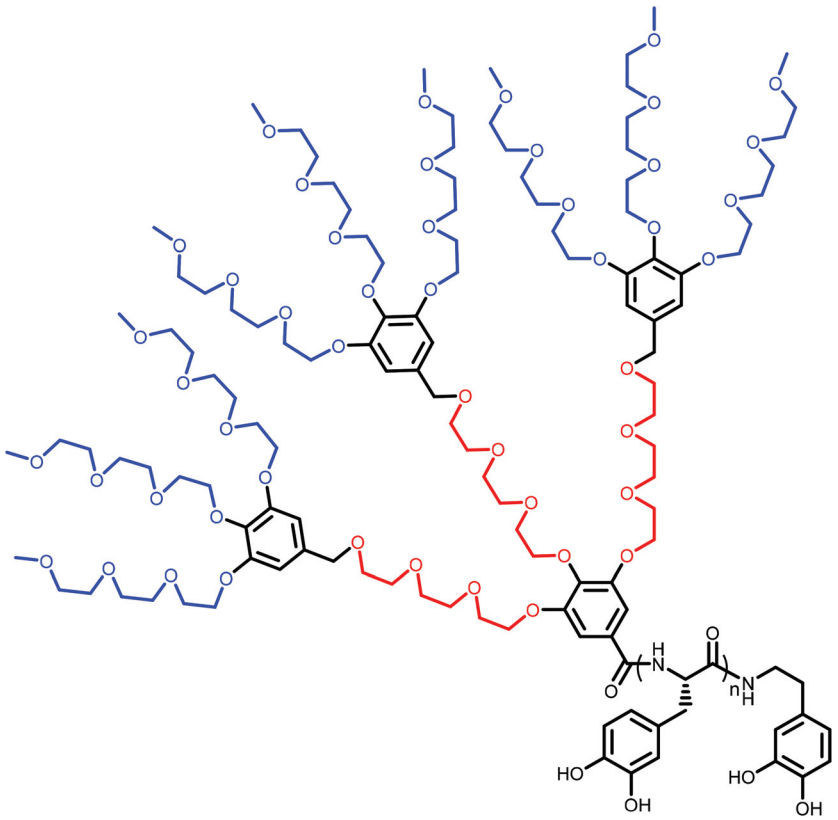

Fig. 15 Molecular structure of OEG dendritic multisorbates featuring substrate-anchoring L-DOPA and dopamine catechol residues. Adapted from ref. 23 with permission of the Royal Society of Chemistry.

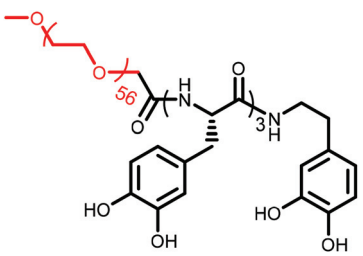

Fig. 16 Molecular structure of the linear PEG multisorbate featuring substrate-anchoring L-DOPA and dopamine catechol residues. Adapted from ref. 23 with permission of the Royal Society of Chemistry.

hydroxylated 'bottle' brushes (R = H, 6 nm-thick) approached such level of performance with Γ = 53 ± 12 ng cm^{-2}. Similar architectural dependence and trends of protein adsorption were observed for antifouling experiments carried out with plasma, the highest resistance to fouling (Γ = 8 ± 6 ng cm^{-2}) still being offered by first-generation dendritic brushes.[95] Regardless, all polymer brushes did display superior antifouling performance – against both non-diluted human serum and plasma – compared to bare gold (Γ = 217 ± 5 and 385 ± 5 ng cm^{-2}, respectively) and the thiol SAM of ATRP initiator (Γ = 207 ± 11 and 203 ± 1 ng cm^{-2}).

Other types of OEO bottle brushes – also prepared on gold *via* this 'grafting from' polymerization strategy using the linear, hydroxy- (HOEGMA) or methoxy-terminated (MeOEGMA) OEG methacrylate monomers shown in Fig. 18 – have also been shown on several occasions to possess remarkable antifouling properties. In 2008 for instance, a collaboration between Horbett, Ratner and Jiang resulted in the preparation of polyMeOEGMA brushes (20–25 nm-thick) that were able to limit fouling from 100% human plasma to Γ = 9.2 ± 6.5 ng cm^{-2}, as measured by SPR.[97] In separate investigations (in 2011–2012), Rodriguez-Emmenegger *et al.* reported similar low-fouling performance for both polyHOEGMA and polyMeOEGMA brushes with Γ = 16.3 and 18.9 ng cm^{-2}, respectively.[76,98–100] In 2014, these results were confirmed in several occasions by the investigators for polyMeOEGMA[101–103] and polyHOEGMA[101,103] films – as well as diblock polyMeOEGMA-*bl*-polyHOEGMA copolymer structures of various different thicknesses[101] – upon 15 min exposure at 25 °C. The same year, the authors described similarly good antifouling properties against undiluted human serum, for ~32 nm-thick polyHOEGMA brushes exposed for 30 min at 25 °C.[104] Antifouling performance against 10% human serum (of ~31 nm-thick polyMeOEGMA brushes, 15 min contact) was excellent at Γ = 4.3 ng cm^{-2}.[105] Long-term exposure (10 h) yielded reasonably good results (Γ = 58.4 ng cm^{-2}).

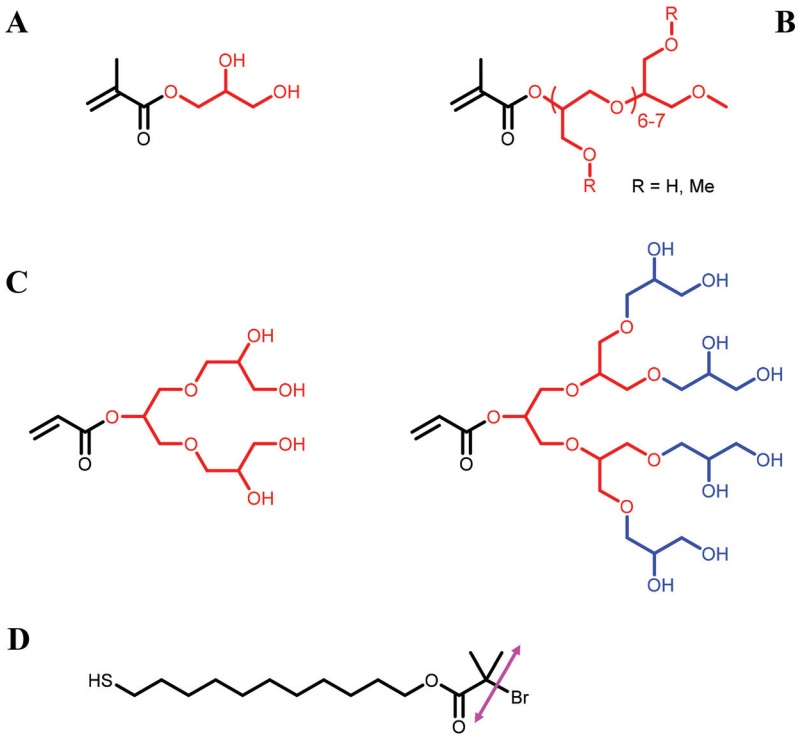

Fig. 17 Molecular structure of the (A) regular, monoglycerol- and (B) linear, oligoglycerol-based methacrylate monomers, as well as the (C) first- and second-generation (left/right) dendritic oligoglycerol acrylate monomers. (D) Molecular structure of the ω-mercapto-undecyl α-bromoisobutyrate ATRP building block initiator (the double arrow marks the future site of polymerization). Adapted from ref. 23 with permission of the Royal Society of Chemistry.

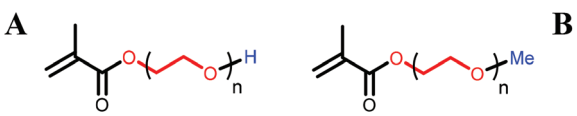

Fig. 18 Molecular structure of (A) HOEGMA, and (B) MeOEGMA OEG methacrylate monomers. Adapted from ref. 23 with permission of the Royal Society of Chemistry.

Earlier, in 2004, Chilkoti's group had already reported that fouling from 100% FBS was below the ~1 ng cm^{-2} LOD of their SPR instrument, for polyMeOEGMA brushes ~15 nm-thick exposed for 20 min.[106] This remarkable achievement was later reproduced (and extended to human serum and plasma) by Jiang,[73] then recently confirmed by Rodriguez-Emmenegger for 30–40 nm-thick brushes (Γ < 0.6 ng cm^{-2})[76,98,100,107] and Huck (Γ < 2 ng cm^{-2} for 20–30 nm-thick brushes).[108] With regards to coating stability, the latter also conducted experiments, wherein fouling surface coverage was measured upon storage of polyMeOEGMA brushes under ambient conditions for prolonged periods of time.[108] After one month, brushes still exhibited excellent resistance against protein adsorption from 100% FBS (Γ ~ 12 ng cm^{-2}), fouling from less challenging 10% FBS still being undetectable. Interestingly however, this study additionally revealed that whole sera obtained from a different species (horse) or at a different stage of maturity (adult *vs.* foetal bovine serum) did foul polyMeOEGMA coatings. Finally, Rodriguez-Emmenegger *et al.* also recently reported (in 2014) that ~31 nm-thick polyMeOEGMA brushes were remarkably able to sustain contact with 10% FBS for 10 h (Γ < 0.3 ng cm^{-2}).[105]

Several research groups also demonstrated that polyHOEGMA and polyMeOEGMA brushes exhibiting excellent antifouling properties could as well be ATRP-grown onto a variety of substrate materials other than gold. In 2006, Chilkoti and co-workers for instance reported 'non-fouling' polyMeOEGMA brushes polymerized onto silicon oxide.[109] Fouling upon exposure to undiluted FBS for 60 min was indeed below the 1 Å LOD of the ellipsometer apparatus used by the authors, for polymer brushes thicker than ~95 Å. The following year, García in collaboration with Collard prepared polyHOEGMA brushes (~135 Å-thick) on titanium oxide and reported background protein adsorption levels lower than Γ = 20 ng cm^{-2}, as measured by SPR against 10% FBS (diluted in DMEM[110]).[111] More recently, in 2011, Rodriguez-Emmenegger *et al.* described the growth of both types of polyHOEGMA and polyMeOEGMA brush on nylon-6/6 adhesion films, themselves RF plasma-sputtered onto various inorganic (gold, silicon, TiAlV alloy) or organic (polypropylene) substrates.[98] Fouling from undiluted FBS (15 min exposure) on polyHOEGMA brushes polymerized on nylon/Au surfaces was measured with SPR to be Γ = 9.7 ng cm^{-2}. PolyMeOEGMA counterparts, on the other hand, were

not fouled by 100% FBS (Γ < 0.03 ng cm^{-2}, the LOD of the SPR instrument used during this investigation). With respect to undiluted human plasma, fouling surface coverage was higher (respectively Γ = 28.3 and 19.5 ng cm^{-2}), but otherwise much lower than that recorded on bare and nylon only-coated gold control surfaces (Γ = 307 and 177 ng cm^{-2}). Also demonstrated by the investigators was the ability displayed by polyMeOEGMA brushes to maintain their antifouling performance against both fluids after storage in PBS for 5 months, sheltered from light. Excellent antifouling properties (Γ < 15 ng cm^{-2}, the LOD of FTIR-ATR) – against human plasma after 15 min exposure at 37 °C – were finally also reported for polyMeOEGMA brushes grown on nylon-coated polypropylene sheets.[98]

Moving away from gold as the substrate material meant that a new type of initiator adlayer – other than that based on the thiol SAM surface chemistry of ω-mercapto-undecyl α-bromoisobutyrate (shown in Fig. 17D) – be developed. This was successfully accomplished in the aforementioned accounts (*vide supra*) by Chilkoti[109] and García/Collard[111] (chlorosilane surface chemistry on SiO_2 or TiO_2), as well as Rodriguez-Emmenegger[98] (acylation of amino-rich nylon). The latter research group recently (in 2013) pursued their effort in a proof-of-concept study, whose objective was to propose a versatile, substrate-independent surface modification route.[80,112] The approach was to find its universality in the fact that the chosen adhesion surface chemistry – that of dopamine-melanin polymer films featuring bioinspired catechol anchoring moieties (see previous Fig. 7, 15 and 16, as well as upcoming Fig. 20 and 22) – is known for exhibiting high affinity to virtually any substrate, and for offering subsequent functionalizability.[80,93,112] This latter feature was taken advantage of to covalently install in a second step α-bromoisobutyryl initiation residues, from which polyOEGMA brushes were finally ATRP-grown. Demonstration was made on the model surface of gold SPR chips that fouling from undiluted, pooled human plasma (15 min exposure) could be minimized to Γ = 2.7 ± 1.2 ng cm^{-2} for ~20 nm-thick polyHOEGMA brushes, or even nearly suppressed for ~18 nm-thick polyMeOEGMA ones (*i.e.* Γ < 0.3 ng cm^{-2}, the LOD of the SPR sensor).[112] Another two types of polymer brushes that will be first introduced in upcoming subsections II. D. and II. E. 2., polyCBAA[113] and polyHEMA (both ~18 nm-thick), were also shown to display pronounced antifouling properties with Γ = 1.5 ± 0.2 and 10.9 ± 1.1 ng cm^{-2}, respectively.[112] In comparison, bare gold was heavily fouled (Γ = 293 ± 70 ng cm^{-2}), so was the ~13 nm-thick dopamine-melanin adhesion adlayer (Γ = 331 ± 38 ng cm^{-2}).[80,112]

II.D. Zwitterionic sulfo- and carboxybetaines[114]

Zwitterionic monomers of various nature have also been employed for the 'grafting from' formation of antifouling polymer brushes onto gold surfaces overcoated with a precursor thiol SAM of ω-mercapto-undecyl α-bromoisobutyrate ATRP initiator (Fig. 17D). These include the SBMA and CBMA sulfobetaine and carboxybetaine methacrylates (Fig. 19A and 19B) as well as the CBAA carboxybetaine acrylamide variant (Fig. 19D). Together with the polyOEGMA brushes described earlier, the recently established polySBMA, polyCBMA and polyCBAA zwitterionic brushes presented in the following subsections II.D.1–3. rank among the coatings with highest known antifouling performance against blood plasma/serum (see Table 1 in upcoming subsection IV.A.).

A fourth kind of zwitterionic brush, constructed from bioinspired PCMA phosphorylcholine methacrylate monomer (Fig. 19C), has also been described but shown not to be capable of preventing fouling from human plasma,[115] even if the latter was diluted to 33% in PBS[116] (Γ > 345 ng cm^{-2}, 30 min exposure, SPR detection). [PC-terminated thiol SAMs challenged by 100% human plasma performed as poorly (Γ > 300 ng cm^{-2}).[97]] Acceptable antifouling performance was only achieved against 10% FBS (Γ = 13–45 ng cm^{-2} at 25 °C).[79] Unlike the previous two examples however,[115,116] these PCMA-based antifouling surfaces (~0.5 to 2 nm-thick) were prepared using a 'grafting to' method, wherein polymers (MW = 5–25 kDa) were first ATRP-grown in solution then deposited onto gold SPR sensor chips.[117,118] In this account as well, a linear relationship was observed between fouling surface coverage Γ and film thickness/polymer MW, thickest coatings prepared with heaviest molecules being the most efficient.[79]

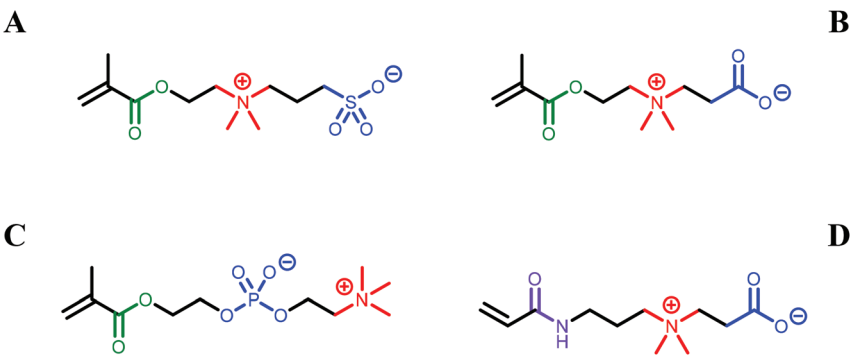

Fig. 19 Molecular structure of the (A–C) SBMA, CBMA, and PCMA methacrylate, as well as (D) CBAA acrylamide zwitterionic monomers. Adapted from ref. 23 with permission of the Royal Society of Chemistry.

II.D.1. Sulfobetaine methacrylate (SBMA). As part of a 2008 study that aimed at correlating platelet adhesion/activation with protein adsorption, Chen and co-workers reported polySBMA brushes only ~7 nm-thick capable of limiting protein adsorption from 20% PPP to Γ = 1.65 ng cm^{-2}, as measured by SPR upon exposure for ~15 min at 37 °C.[71,72] The same year, a collaboration by Horbett, Ratner and Jiang exposed slightly thicker polySBMA brushes (10–15 nm) to undiluted human plasma and determined the level of protein adsorption to be Γ = 9.1 ± 0.6 ng cm^{-2}, using SPR detection.[97] [This value was recently lowered to Γ = 3.4 ng cm^{-2} by Zheng's group with ~20 nm-thick brushes.[119]] Still in 2008, Jiang and co-workers published a more systematic study, wherein polySBMA brushes of various thickness (15–90 nm range) were screened by means of SPR for their ability to withstand protein adsorption from 100% human serum (10 min exposure).[120] The interesting conclusion of this work was that serum fouling was minimal (Γ = 6.1 ng cm^{-2}) at the intermediate thickness of 62 nm. Both thinner and thicker brushes indeed adsorbed a greater amount of serum proteins, always below Γ ~ 20 ng cm^{-2} however. It is only when zwitterionic brushes (~20 nm-thick) were built from an amide (*vs.* ester) variant of SBMA monomer that 'ultralow' fouling against both 100% pooled human plasma and serum (10 min exposure) was reached with Γ < 0.3 ng cm^{-2}, the LOD of the SPR sensor used in the study.[119]

Other types of α-bromoisobutyryl building block molecules – other than that ω-mercapto-undecyl-based shown in Fig. 17D – for the surface pre-modification of gold or other underlying substrate materials with ATRP initiator SAMs have been studied as well. For instance, Jiang and co-workers reported in 2008 that polySBMA brushes with excellent resistance to protein adsorption could also be ATRP-grown from an α-bromoisobutyramide initiator underlayer, immobilized on gold through bioinspired dopamine graft residues (Fig. 20A).[121] Fouling from 10% human serum (measured with SPR after contact for 15 min) was low at Γ ~ 12 ± 3 ng cm^{-2}. Even lower protein adsorption (Γ = 1.1 ± 2.0 ng cm^{-2}) was achieved for polySBMA brushes polymerized from ATRP initiator residues immobilized onto pre-coated, NH_2-terminated alkylthiol SAMs. These particular coatings maintained good performance (Γ = 14.9 ± 6.0 ng cm^{-2}) against more challenging undiluted human serum. With respect to 100% human plasma, fouling was nearly undetectable (Γ = 0.8 ± 0.7 ng cm^{-2}). Remarkably, these antifouling properties were preserved, against both undiluted fluids, upon storage in PBS for 42 days at room temperature. In a simultaneous separate publication, the authors observed comparable antifouling performance when the polySBMA polymer chains were grown in solution from free ATRP initiator molecules (Fig. 20B), then deposited onto NH_2-terminated SAMs ('grafting to' method).[122] Indeed, fouling surface coverage from 100% human serum and plasma respectively was Γ = 22.5 ± 7.5 and 1.6 ± 7.3 ng cm^{-2}, as measured with SPR upon 15 min exposure.

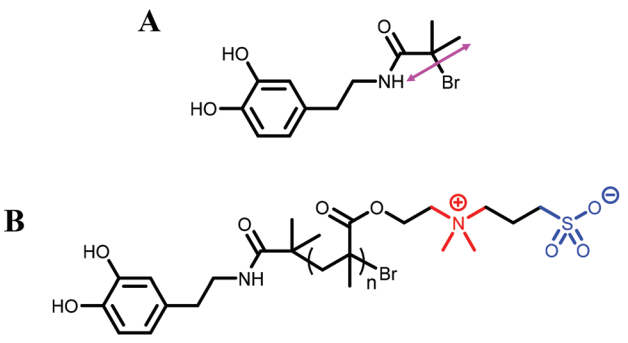

Fig. 20 Molecular structure of (A) the α-bromoisobutyramide ATRP initiator (the double arrow marks the future site of polymerization), and (B) the 'grafting to' polySBMA polymer grown in solution – both bearing a bioinspired dopamine residue for surface adhesion. Adapted from ref. 23 with permission of the Royal Society of Chemistry.

As well, in the manner of Chilkoti in 2006 for polyMeOEGMA brushes,[109] Bailey's team reported in 2011 that polySBMA brushes with good antifouling properties against undiluted FBS (Γ = 26 ng cm^{-2}) could also be ATRP-grown onto the silicon (oxide) surface of photonic microring resonators through precursor siloxane SAMs of undecyltrichlorosilane α-bromoisobutyrate initiator.[123] In comparison, serum fouling on bare oxide-passivated silicon surfaces was evaluated to be Γ = 300 ng cm^{-2}.

Finally, there is also the approach by Chang *et al.* who, in their research for smart haemocompatible materials, devised hybrid copolymer coatings combining the excellent antifouling character of zwitterionic polySBMA with the attractive thermoresponsive properties of non-ionic poly(*N*-isopropylacrylamide) (polyNIPAAm).[124] In this 2009 investigation, the authors prepared a series of statistical poly(SBMA-*co*-NIPAAm) copolymers, whose chemical structure is drawn in Fig. 21A, that were next physisorbed through hydrophobic-hydrophobic interactions onto CH_3-terminated SAMs pre-coated on gold ('grafting to' method). Measured with SPR upon exposure to 10% PPP at 37 °C, the amount of adsorbed plasma proteins was found to be extremely low and invariably below Γ = 5 ng cm^{-2}, even for copolymer coatings containing as little as 15 mol% of SBMA monomer. In comparison, CH_3-terminated conditioning SAMs adsorbed a considerably greater amount of plasma proteins (Γ ~ 150 ng cm^{-2}), so did polyNIPAAm homopolymer coatings (Γ ~ 90 ng cm^{-2}). Conversely, polySBMA homopolymer brushes were highly resistant to fouling (Γ < 5 ng cm^{-2}). On a side note, Leckband's group did recently succeed in preparing polyNIPAAm homopolymer brushes displaying pronounced antifouling properties, upon polymerization from a variety of mixed thiol initiator SAMs on gold.[125] Coatings with high polymer grafting density (650 Å^2 per chain) were indeed able to resist fouling from 10% FBS with Γ < ~20 ng cm^{-2} (as measured with ellipsometry upon 20 h exposure at 25 °C). When the temperature was increased to 37 °C for an additional 20 h of contact with 10% FBS, fouling surface coverage increased to Γ ~ 40 ng cm^{-2}, irrespectively this time around of the nature of the underlying SAM. (Some) antifouling perfomance was recovered when the temperature was cycled back to 25 °C. At the exception of those built from OEG-based under-

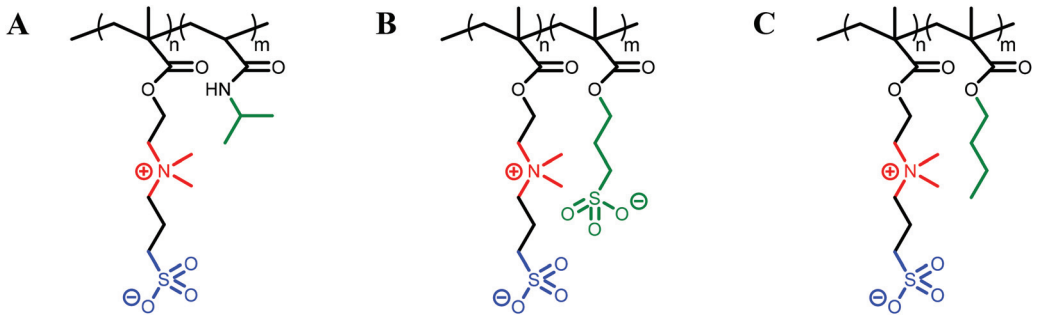

Fig. 21 Molecular structure of the (A) poly(SBMA-*co*-NIPAAm), (B) polySBMA-*bl*-polySA, and (C) poly(SBMA-*co*-BMA) copolymers. (A) adapted from ref. 23 with permission of the Royal Society of Chemistry.

lying SAMs (and for which $\Gamma \sim 25$ ng cm^{-2}), polyNIPAAm coatings with lower polymer grafting density (1450 Å^2 per chain) were not as antifouling with $\Gamma \sim 40$–200 ng cm^{-2}, regardless of the temperature of incubation and the nature of the initiator SAM.

The same year (2013), Chang and Jiang reported SBMA-containing diblock methacrylate copolymers incorporating polysulfonate (SA) subunits (Fig. 21B) – for ion-pairing, interpenetrating physisorption on polycationic, trimethylammonium-based methacrylate brushes (40 nm-thick), themselves ATRP-grown on gold through precursor SAMs of ω-mercapto-undecyl α-bromoisobutyrate initiator (shown in Fig. 17D).[126] Electrostatically 'grafted to' polySBMA-*bl*-polySA assemblies presenting longer polysulfonate anchorage chains (*i.e.* polySBMA$_{40}$-*bl*-polySA$_{40}$ *vs.* polySBMA$_{40}$-*bl*-polySA$_{20}$) were shown to invariably exhibit superior antifouling properties, both against 100% serum ($\Gamma \sim 9$ *vs.* 37 ng cm^{-2}) and 100% plasma ($\Gamma \sim 9$ *vs.* 44 ng cm^{-2}), as measured with SPR upon exposure for 20 min at 37 °C. Not surprisingly, fouling from diluted fluids (20% and 50% in PBS) was lower. Whereas trimethylammonium 'control' adhesion layers were shown to be heavily fouled both by serum and plasma, even if the latter were diluted to 20% ($\Gamma > 210$ ng cm^{-2}), polySBMA homopolymer 'reference' brushes exhibited their habitual pronounced antifouling properties against both full fluids[97,120] (*vide supra*) with $\Gamma < 10$ ng cm^{-2}.[126]

At last, another variety of antifouling, SBMA-based zwitterionic methacrylate copolymer brushes was described in 2014 by Liu's group.[127] These were the result of the random copolymerization of *n*-butyl methacrylate (BMA) and SBMA monomers (Fig. 21C). The authors showed that, among a series of ~40 nm-thick poly(SBMA-*co*-BMA) brushes deposited onto gold SPR chips, sole those having a minimal 10 mol% SBMA content presented pronounced antifouling properties – the best performance ($\Gamma = 15 \pm 4$ ng cm^{-2} for 100% pooled human plasma, and $\Gamma = 17 \pm 3$ ng cm^{-2} for 100% pooled human serum, 10 min exposure) belonging to the brush with the highest SBMA content studied, poly(SBMA$_{20}$-*co*-BMA$_{80}$). In contrast, brushes with a SBMA content below 10% were heavily fouled ($\Gamma > 70$ ng cm^{-2}), irrespectively of the nature of the challenging fluid, so was bare gold ($\Gamma > 150$ ng cm^{-2}).

II.D.2. Carboxybetaine methacrylate (CBMA). Along with polySBMA coatings, Horbett, Ratner and Jiang also described in 2008 polyCBMA brushes (10–15 nm-thick) able to minimize fouling from 100% human plasma to as little as $\Gamma = 0.4 \pm 0.9$ ng cm^{-2}, as measured with SPR.[97] Such 'ultralow' protein adsorption level had already been reported shortly before by Jiang's team for both human serum and plasma.[73] In 2009, the latter investigated the influence of incubation temperature on protein adsorption from undiluted human plasma (~10 min exposure).[128] This work revealed that 29 nm-thick polyCBMA brushes exhibit 'ultralow' fouling properties ($\Gamma <$ 0.3 ng/ cm^{-2}, the LOD of the SPR sensor) at all examined temperatures (25, 30 and 37 °C). That same year, Rodriguez-Emmenegger *et al.* also described polyCBMA brushes capable of efficaciously resisting protein adsorption; however, only from 33% human plasma diluted in PBS.[116] The amount of plasma proteins deposited after 30 min exposure was below the LOD of the SPR instrument of the study ($\Gamma < 0.6$ ng cm^{-2}). In comparison, fouling surface coverage on uncoated gold substrates was considerably much greater ($\Gamma = 400 \pm 98$ ng cm^{-2}). Interestingly, and in stark contrast with the polyCBMA system, polySBMA brushes prepared for the purpose of the investigation adsorbed a substantial amount of plasma proteins ($\Gamma = 320 \pm 78$ ng cm^{-2}) – nearly equivalent to that observed for unmodified, control gold surfaces (*vide supra*). This problem was alleviated when polyCBMA chains were sequentially grown over polySBMAs in a diblock layered copolymer configuration ($\Gamma = 24 \pm 10$ ng cm^{-2}), but still very much present when CBMA and SBMA monomers were randomly copolymerized ($\Gamma = 180 \pm 26$ ng cm^{-2}). Tremendous improvement was finally recently achieved by the investigators (in 2012) when fouling on 20 nm-thick polyCBMA brushes from now undiluted plasma (*vs.* 33% in PBS) was found to be simply undetectable by SPR ($\Gamma <$ 0.03 ng cm^{-2}, 30 min exposure).[115]

Extending their own work with SBMA (see Fig. 20B),[122] Jiang's team developed in 2010 polyCBMA adsorbates functionalized with bioinspired L-DOPA adhesion residues (Fig. 22) – for the direct, 'grafting to' surface modification of SPR sensor gold chips.[129] Fouling from 100% human serum and plasma (10 min exposure) on films estimated to be 9–10 nm-thick was low at $\Gamma = 11.0 \pm 5.0$ and 8.9 ± 3.4 ng cm^{-2}, respectively. Com-

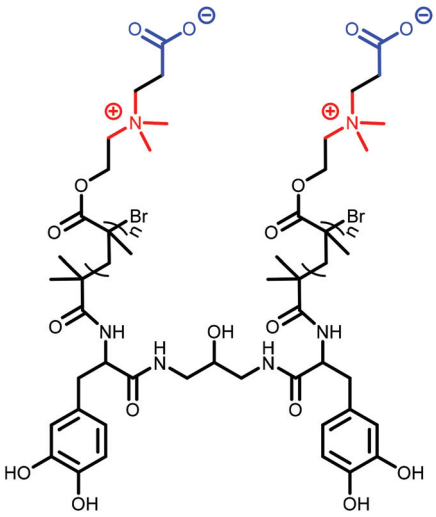

Fig. 22 Molecular structure of the L-DOPA/polyCBMA polymer conjugate with bioinspired catechol residues for substrate anchorage. Adapted from ref. 23 with permission of the Royal Society of Chemistry.

parable levels of performance were reached when the adsorbate was implemented to derivatize silicon oxide substrates.[130–132] Interestingly however, when the polymer conjugate was reduced to a single catechol/polyCBMA arm, fouling dramatically increased to $\Gamma \sim 64$ and 68 ng cm^{-2}.[129]

II.D.3. Carboxybetaine acrylamides (CBAA). The last variant of zwitterionic brushes to be discussed – based on CBAA monomer (Fig. 19D) – has been the object of multiple studies. One such work was conducted by Jiang and co-workers, who described in 2008 polyCBAA brushes 15–20 nm-thick exhibiting 'ultralow' fouling performance below or near the LOD of their SPR sensor (0.2 ng cm^{-2}), upon contact with either 10, 50 or 100% human plasma for 7 min at room temperature.[133,134] The following year, the investigators published a more comprehensive study, wherein the effects on fouling of film thickness (10–55 nm range) and incubation temperature (25 or 37 °C) were determined using SPR for both full human serum and plasma.[135] Like the polySBMA brushes described earlier in subsection II.D.1., there also seemed to exist an intermediate, optimal thickness (~21 nm) at which fouling was minimal (*i.e.* undetectable), and this regardless of the incubation temperature or the nature of the contacting fluid (10 min exposure). Moreover, the range in thickness for which $\Gamma < 5$ ng cm^{-2} was 15–26 nm, at 25 °C. Gratifyingly, these polyCBAA brushes were capable of maintaining their high resistance to protein adsorption at the more relevant body temperature of 37 °C, for an even wider range of thicknesses (15–40 nm). Soon after, Jiang's team supplemented this remarkable work with a study, wherein CBAA monomers of various spacing length between the two ammonium and carboxylate charged moieties were explored.[136] Polymer brushes 15–20 nm-thick, prepared either with regular-ethylene CBAA-2 (the structure actually drawn in Fig. 19D) or shorter-methylene CBAA-1 monomers, reduced protein adsorption from full human plasma and serum below $\Gamma = 5$ ng cm^{-2}, as measured with SPR upon 10 min exposure. Conversely, polymerization of CBAA-3 monomers with longer propylene spacer yielded slightly thicker brushes (15–25 nm) on which fouling from undiluted fluids was higher, especially for serum ($\Gamma \sim 70$ ng cm^{-2}). Recently, the refractive index (RI) – a material characteristic that can be correlated to film density – was demonstrated by Jiang's team to also constitute an important parameter to take into consideration for the identification and development of antifouling polymer coatings.[137] In this 2012 work, fouling from undiluted human serum (measured using SPR upon 10 min exposure at 25 °C) was shown to systematically be lower than $\Gamma = 5$ ng cm^{-2} only for polyCBAA brushes with RI values $\gtrsim$1.5, and this regardless of dry film thickness (~9–40 nm). Below this threshold in dry RI, serum fouling was significantly higher (up to 29 ng cm^{-2}). In 2011, Rodriguez-Emmenegger *et al.* also reported polyCBAA brushes capable of resisting fouling from 100% FBS for 15 min ($\Gamma < 0.03$ ng cm^{-2}, the LOD of the SPR sensor used in this study).[98] Unfortunately, with respectively $\Gamma = 15$ and 16 ng cm^{-2}, SPR measurements with undiluted human plasma and serum biosamples were not as satisfactory. Shortly after however, the investigators reported 18 nm-thick polyCBAA brushes able to nearly suppress fouling from undiluted human plasma ($\Gamma < 0.03$ ng cm^{-2}).[76,99,115,138] Similar resistance to fouling was observed with foetal bovine and calf sera in a more comprehensive study, which also aimed at assessing fouling from five other human or animal undiluted biofluids: human cerebrospinal fluid, saliva and urine, as well as chicken egg and whole cow milk (see section III.).[76] [Fouling from undiluted food media – *i.e.* raw orange, tomato or cucumber blend juices, as well as fresh half-fat milk – was also investigated ($\Gamma < 5$ ng cm^{-2}, 10 min exposure at 25 °C).[138]] In comparison, plasma proteins avidly adsorbed on bare gold ($\Gamma = 307$ ng cm^{-2}).[76,99,115] Lastly, the authors also showed that fouling on these polyCBAA brushes was still undetectable after longer exposure (120 *vs.* 15 min).[99]

In 2011–12, Jiang's group additionally demonstrated that polyCBAA brushes could also be polymerized photochemically through a smooth and environmentally-friendly (catalyst-free) SI-PIMP process (see subsection II.B.)[60] that allowed for film thickness and uniformity to be readily controlled.[139] Measured with SPR upon 10 min exposure at 25 °C, fouling surface coverage from undiluted human plasma was very low ($\Gamma < 5$ ng cm^{-2})[139–141] and comparable to that recorded for regular, ATRP-grown polyCBAA brushes of similar thickness.[140]

II.E. Hybrid, derivative and bioinspired materials

The remaining surface-modifying (macro)molecules to be discussed do not belong to any of the three families presented thus far. Rather, the following are combinations thereof (*i.e.* hybrids), derivatives or totally unrelated materials. Nonetheless, these 'outliers' are no less important and form, as a matter of fact, some of the best antifouling coatings known against blood plasma/serum (see Table 1 in upcoming subsection IV.A.).

II.E.1. PLL-*graft*-PEG hybrids and PLL-*graft*-PMOXA analogues. In a series of studies published between 2000 and 2012, several groups described hybrid copolymeric surface modifiers having for generic design a PLL polypeptide backbone partially grafted with PEG side-chains through primary amine residues (Fig. 23).[142–155] At pH 7.4 (HEPES[156] or PBS buffer), these PLL-*g*-PEG macromolecules were shown to display the ability to spontaneously self-assemble onto a variety of metal oxide substrates made of niobium,[142–144,151,152,154,155] titanium,[142,143,145–148,150,153] silicon/titanium,[142] or tantalum.[143] The adsorption mechanism involves multiple electrostatic interactions between the residual, positively-charged amine moieties of PLL side-chains and the negatively-charged oxide surfaces.[143,145–147,149,151] As a result, the polypeptide backbone lies parallel to the substrate and the PEG side-chains stretch perpendicularly into the liquid environment in a comb-like overall architecture.[143–147,149,154,155] For optimized copolymer structures, protein adsorption upon exposure to human serum (15–60 min) was near/lower than the 2 ng cm^{-2} LOD of the OWLS sensor.[142–145,147–149,151,152,154,155] This represented a dramatic decrease in surface coverage compared to bare, control oxide surfaces for which serum adsorption ranged between Γ = 223 and 596 ng cm^{-2}.[142–144,152,154,157] It was also shown in one example that resistance to fouling is maintained whether PLL-*g*-PEG coatings are exposed to multiple successive serum injections over several hours, or stored dry for several months.[142]

Whether (partially) end-functionalized through the PEG side-chains with (i) biotinyl residues in streptavidin sandwhich immunoassays,[151,157] (ii) nitrilotriacetic acid (NTA) ligands for the development of sensing platforms relying on Ni^{II}/His-tag docking chemistry,[155] or (iii) cell-adhesive oligopeptides containing the integrin receptor-binding RGD amino acid sequence for cell attachment experiments,[145,147,149,154,158] the resulting PLL-*g*-PEG derivatized coatings still exhibited excellent antifouling properties against undiluted human serum or plasma. In each case, fouling levels were within/near the LOD of the detection technique used (OWLS or *in situ* null ellipsometry).

In 2005, the surface of poly(dimethylsiloxane) (PDMS) substrates was also derivatized with PLL-*g*-PEG copolymer chemistry.[159] Unlike bare PDMS however (Γ = 385 ± 18 ng cm^{-2}), PLL-*g*-PEG coatings were capable of preventing protein adsorption from serum ($\Gamma \sim \pm$ 1.0 ng cm^{-2}), as assessed using OWLS. Long-term resistance (up to 12 weeks) was also demonstrated.

Finally, a PLL-graft copolymer analogue featuring poly(2-methyl-2-oxazoline)[160] PMOXA side-chains (Fig. 24A) was reported by Konradi *et al.* in 2008.[161,162] The resulting PLL-*g*-PMOXA coatings, likewise, exhibited excellent antifouling properties against full human serum (Γ < 2 ng cm^{-2}), even after repeated 15 min contact (as measured with OWLS).[160–162] A PMOXA copolymer variant introduced shortly after (Fig. 24B) performed as efficiently,[152,163] even following pro-

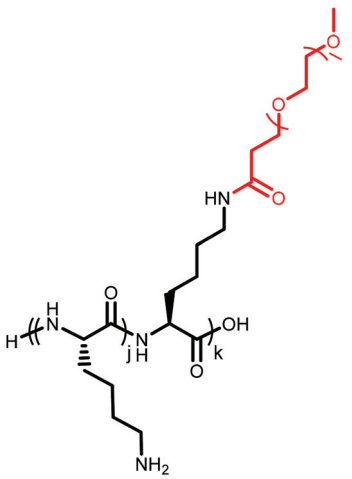

Fig. 23 Molecular structure of the PLL-*g*-PEG copolymers. Adapted from ref. 23 with permission of the Royal Society of Chemistry.

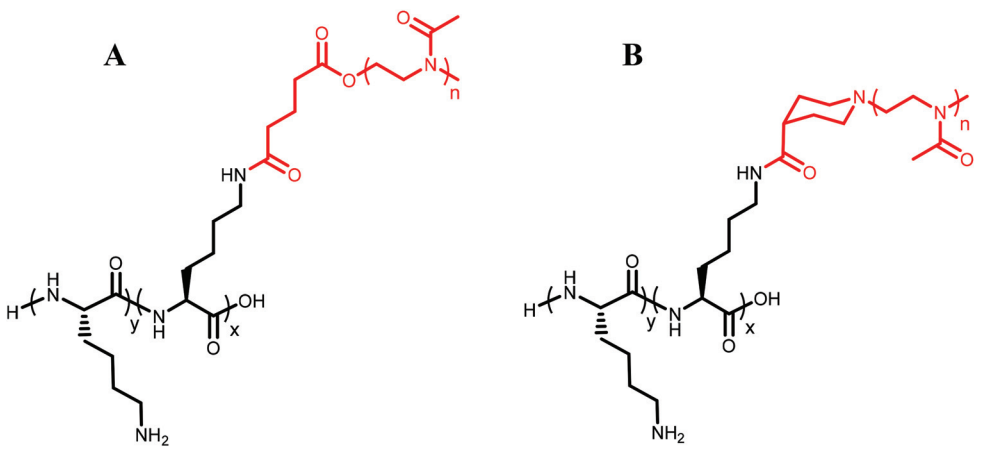

Fig. 24 Molecular structure of two variants of PLL-*g*-PMOXA copolymers. (A) adapted from ref. 23 with permission of the Royal Society of Chemistry.

longed exposure (up to 2 weeks) to simulated physiological conditions of ionic strength or/and an oxidative environment.[152,160] These PLL-*g*-PMOXA films were also shown to be significantly more stable under these conditions than PLL-*g*-PEG parent coatings. A very recent 2014 account revealed that PLL-*g*-PEG coatings also are sensitive to trypsin – an enzyme that cleaves polypeptide chains at lysine (and arginine) residues[164] – the extent of degradation (measured with OWLS as a decrease in adsorbed mass upon 1.5 h exposure at 37 °C) depending on the temperature (37 or 80 °C) at which the coatings were built.[164] [In comparison, polyoxazoline-based films were reported to be capable of withstanding nearly unaffected acidic and/or enzymatic hydrolysis at 37 °C, for periods of time potentially extending up to several days.[165]] The higher the deposition temperature was, the more stable PLL-*g*-PEG assemblies turned out to be. On a brighter note, this study also confirmed the general observation that PLL-*g*-PEG coatings exhibit excellent antifouling properties (measured with OWLS upon contact with 100% FBS for 15 min at 37 °C), those being as well essentially independent on the temperature at which the coatings were deposited ($\Gamma_{37\ °C}$ = 5.7 ± 0.6 ng cm^{-2} ~ $\Gamma_{80\ °C}$ = 4.8 ± 0.6 ng cm^{-2}).[164] Resistance to fouling was influenced however by the enzymatic treatment, less degraded coatings assembled at higher temperature experiencing a lesser loss in antifouling performance ($\Gamma_{37\ °C/trypsin}$ = 38.5 ± 0.7 ng cm^{-2} > $\Gamma_{80\ °C/trypsin}$ = 20.4 ± 0.7 ng cm^{-2}) – assessed upon exposure to 100% FBS for 15 min at 37 °C.

II.E.2. Short, non-ionic hydroxyalkyl and MEG ATRP monomers. Other types of short hydroxyalkyl monomers – related to monoglycerol methacrylate drawn in Fig. 17A – have also been employed to prepare 'grafted from' polymer brushes ATRP-grown from precursor thiol SAMs of ω-mercapto-undecyl α-bromoisobutyrate initiator pre-coated on gold. However, as will be seen next, these brushes were otherwise more efficient at resisting fouling from blood plasma/serum biosamples.

In 2011, Zheng in collaboration with Yu used 3-hydroxypropyl and 2-hydroxyethyl methacrylate monomers (HPMA and HEMA – Fig. 25A and 25B) to build a series of polymer brushes for which they methodically assessed with SPR the effect on antifouling properties of film thickness (~10–60 nm), upon 10 min exposure to both diluted and undiluted human serum and plasma.[166] Interestingly, this study revealed that optimal antifouling performance was achieved for intermediate ranges of coating thickness (20–45 nm),[166,167] corroborating the observations made by Jiang's team for both polySBMA[120] and polyCBAA[135] systems (see respectively subsections II.D.1. and II.D.3.). For both fluids diluted at 10% in PBS, polyHEMA and polyHPMA brushes exhibited remarkable antifouling properties with undetectable protein adsorption (Γ < 0.3 ng cm^{-2}).[166,167] With respect to undiluted serum and plasma, antifouling performances were still excellent for polyHEMA brushes with respectively Γ ~ 3.0 and 3.5 ng cm^{-2}.[166] In sharp contrast, polyHPMA brushes adsorbed much greater amounts of proteins (Γ ~ 13.5 and 50.0 ng cm^{-2}).[166,167]

Still in 2011, Rodriguez-Emmenegger *et al.* introduced a new type of 'non-fouling' polymer brush constructed from

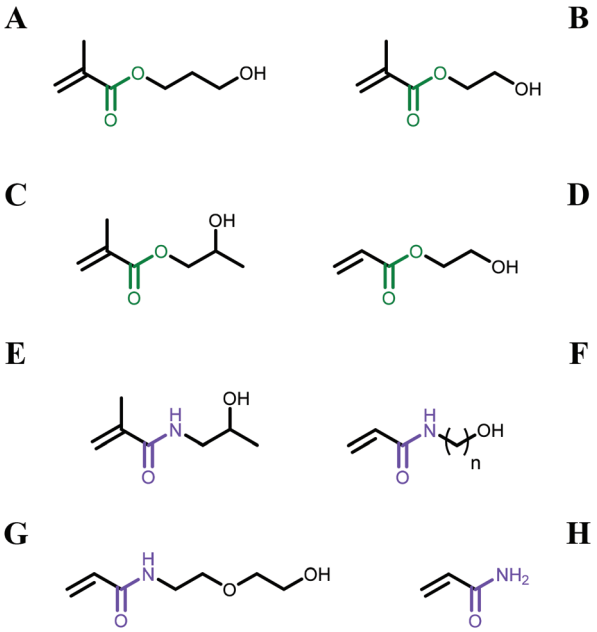

Fig. 25 Molecular structure of short, non-ionic monomers for 'grafting from' polymerization: (A–C) 3-hydroxypropyl (HPMA), 2-hydroxyethyl (HEMA), and 2-hydroxypropyl (HPM) methacrylates, (D) 2-hydroxyethyl acrylate (HEA), (E) *N*-(2-hydroxypropyl) methacrylamide (HPMA), (F) methylene (*n* = 1 – HMAA), ethylene (*n* = 2 – HEAA), propylene (*n* = 3 – HPAA), and pentylidene (*n* = 5 – HPenAA) *N*-(*n*-hydroxyalkyl) acrylamides, (G) acryloylaminoethoxyethanol (AAEE), and (H) non-substituted acrylamide. (A–C, E and H) adapted from ref. 23 with permission of the Royal Society of Chemistry.

N-(2-hydroxypropyl) methacrylamide monomer (incidentally also abbreviated 'HPMA' – Fig. 25E).[99] These polyHPMA brushes (17–30 nm-thick) were shown to be able to resist for 15 min fouling from undiluted human plasma[76,99] or serum,[105] FBS,[76] as well as calf serum.[76] Indeed, for all tested biological samples, SPR readings were below the limit of detection of the sensor device used for the study (0.03 ng cm^{-2}). This 'non-fouling' behaviour was also observed for five other human or animal undiluted biofluids: human cerebrospinal fluid, saliva, and urine, as well as chicken egg and whole cow milk (see section III.).[76] Interestingly, polyHPM brushes (30 nm-thick) resulting from the polymerization of the corresponding 2-hydroxypropyl methacrylate *ester* monomer (HPM – Fig. 25C *vs.* HPMA – Fig. 25E) adsorbed a considerably greater amount of plasma proteins with Γ = 40.5 ng cm^{-2}.[99] Importantly for practical applications, fouling on polyHPMA coatings was still undetectable upon long-term contact (120 *vs.* 15 min) with 100% plasma,[99] or upon exposure to single individual plasma samples obtained from different human adult donors (see upcoming subsection II.G.).[103] [It was also shown in another investigation that ~30 nm-thick polyHPMA brushes are able to effectively sustain exposure for 10 h to 10% human serum (Γ = 7.8 ng cm^{-2}) and 10% FBS (Γ = 8.7 ng cm^{-2}), fouling surface coverage after 15 min contact being in both cases below the LOD of the SPR sensor (Γ < 0.3 ng cm^{-2}).[105]]

Remarkably as well, multiple exposures to plasma and storage in PBS over 2 years barely affected the 'non-fouling' characteristics of the coatings, demonstrating their excellent reusability and shelf-life stability.[99] In this respect, non-ionic polyHPMA brushes were shown to easily outperform otherwise equally 'non-fouling' zwitterionic polyCBAA brushes (Γ = 17 *vs.* 125 ng cm^{-2} after 2 years).[99]

Another addition to this family of short, non-ionic hydroxyalkyl monomers, reported by Zheng's group in late 2011, is *N*-(2-hydroxyethyl) acrylamide (HEAA – Fig. 25F, n = 2).[119,168,169] All polymer brushes grown within a wide range of thicknesses (~10–40 nm) were shown with SPR to display as well 'non-fouling' properties (Γ < 0.3 ng cm^{-2}), when exposed for 10 min to either undiluted human serum or plasma. [Brushes ~20 nm-thick constructed from the 2-hydroxyethyl acrylate *ester* version of HEAA monomer (HEA – Fig. 25D *vs.* HEAA – 25F, n = 2) were not as performing but still quite effective at decreasing fouling from 100% human plasma (Γ = 4.9 ng cm^{-2}) and 100% human serum (Γ = 5.0 ng cm^{-2})[119] – these values being well in par however with those obtained for polyHEMA brushes (*vide supra*),[166] their *meth*acrylate variant (Fig. 25B *vs.* 25D).] Even more gratifying was the observation that a polyHEAA brush only 12 nm-thick was able to retain such remarkable antifouling properties for a much longer period of time (60 min). Recently (in 2014), Zheng's group reported a longer, OEG version of HEAA – the *N*-acryloylaminoethoxyethanol (AAEE) monomer shown in Fig. 25G – with which were built polymer brushes able to reduce fouling from undiluted human plasma/serum below Γ = 0.3 ng cm^{-2}, as measured with SPR upon 10 min of contact.[170] As was already the situation for other types of brush (poly(L-serine),[60] polySBMA,[120] polyCBAA,[135] and polyHPMA/polyHEMA[166,167] – *vide supra*), there also existed for antifouling polyAAEE coatings an optimal range of polymer thickness (~10–40 nm).

In 2014 as well, Zheng in collaboration with Chen systematically studied the influence of the alkyl chain length of a series of *N*-(*n*-hydroxyalkyl) acrylamide building block monomers (Fig. 25F, n = 1–3,5) on the antifouling performance against 100% plasma/serum of the corresponding polymer coatings.[171] All different brush types (consistently ~33 nm-thick) were shown to invariably reduce fouling below Γ = 2.1 ng cm^{-2}, as measured with SPR upon contact for 10 min, and this irrespectively of the nature of the undiluted testing fluid. A clear correlation between spacer length and protein adsorption appeared however, brushes bearing longer side-chains being less antifouling. In this respect, polyHEAA coatings (n = 2) were shown once again (*vide supra*)[119,168,169] to resist fouling with Γ < 0.3 ng cm^{-2}, so did brushes built with shorter *N*-(1-hydroxymethyl) acrylamide monomer (HMAA – Fig. 25F, n = 1). In comparison, longer *N*-(3-hydroxypropyl) and *N*-(5-hydroxypentyl) acrylamide building block molecules (HPAA and HPenAA – Fig. 25F, n = 3 and 5) yielded brushes with measurable fouling surface coverage, respectively Γ = 0.3–0.9 and 0.7–2.1 ng cm^{-2}.

There is finally the shortest building block monomer of them all, non-substituted acrylamide (Fig. 25H), which was recently implemented by Liu and co-workers.[172,173] Measured with SPR for both human serum and plasma (10 min exposure), the resistance to fouling of ~39 nm-thick polyacrylamide brushes was excellent. For diluted 10% serum and plasma, levels of adsorption were indeed extremely low at Γ = 0.7 ± 0.4 and 0.5 ± 0.4 ng cm^{-2}, respectively. Such high performance was maintained against both undiluted biosamples (Γ = 2.8 ± 0.9 and 1.7 ± 0.7 ng cm^{-2}). In comparison, fouling surface coverage on unmodified gold control surfaces was invariably greater than Γ = 140 ng cm^{-2}, regardless of the challenging fluid or its level of dilution.

II.E.3. EGylated zwitterionic hybrids

II.E.3.a. OEGylated phosphorylcholine polyelectrolytes. Their 2009 investigation on the antifouling properties of OEO-grafted poly(acrylic acid) PAA films (see subsection II.C. – Fig. 14) was also the occasion for Schaaf and Mésini to assess the performance of various, different phosphorylcholine (PC)-terminated related polymer adlayers.[85] Antifouling coatings were also prepared on silicon/titanium oxide through an intercalated film made of alternated poly(styrene sulfonate)/poly(allylamine hydrochloride) strata – this polyelectrolyte multilayered structure being itself anchored to the substrate *via* a poly(ethylene imine) adhesion coating. When subjected to 10% FBS, constructs based on PAA-*g*-(OEO$_3$-PC) polymer (Fig. 26A) with a 18% grafting ratio (GR) performed rather well with Γ = 15 ng cm^{-2}, as measured with OWLS. Considerably more antifouling however (Γ = 1 ng cm^{-2}) were coatings made with PAA-*g*-(OEO$_3$-PC) polymer at a slightly higher 25% GR.[85,174] At this GR (*i.e.* 23%), films based on non-OEGylated – that is, alkylated – PAA-*g*-(*n*-hexyl-PC) polymer (Fig. 26B) were not as effective with Γ = 11 ng cm^{-2}. Coatings built with PAA-*g*-(*n*-undecanyl-PC) polymer featuring longer (C_{11} *vs.* C_6) alkyl spacer arms were even more fouled with Γ = 81 ng cm^{-2} (33% GR). Finally, OEO$_3$-PC side-chain grafting on poly(allylamine hydrochloride) (PAH) – seen in Fig. 26C – gave rise to reasonably good antifouling performance (Γ = 22 ng cm^{-2}), only when GR reached 80% however. Regardless, all these coatings did display superior antifouling properties compared to those prepared with non-grafted PAA (Γ = 297 ng cm^{-2})[85,86,174] and PAH (Γ = 385 ng cm^{-2})[85] polymers.

II.E.3.b. PolyCBMA-bl-PPO-bl-polyCBMA poloxamers. Using their expertise with zwitterionic materials to diversify/expand the scope of available antifouling coating strategies, Jiang and co-workers recently reported the synthesis of polyCBMA-*bl*-PPO-*bl*-polyCBMA triblock copolymer, a zwitterionic poloxamer derivative (Fig. 27).[175] Antifouling surfaces were prepared on gold upon physisorption of the middle PPO segment onto a pre-coated hydrophobic SAM of 1-undecane-thiol – as such compeling the superhydrophilic, ATRP-grown polyCBMA side-chains to face outwards into the aqueous environment. Fouling from undiluted blood plasma, as measured using SPR upon 10 min exposure, was low at Γ = 5.2 ± 0.2 ng cm^{-2}.

II.E.3.c. PolyMeOEGMA-bl-polyCBAA copolymers. In a recent pioneering work (in 2012) that also aimed at studying the possibility of performing living ATRP in biological milieux, Rodriguez-Emmenegger *et al.* reported a (2 × 15) nm-thick

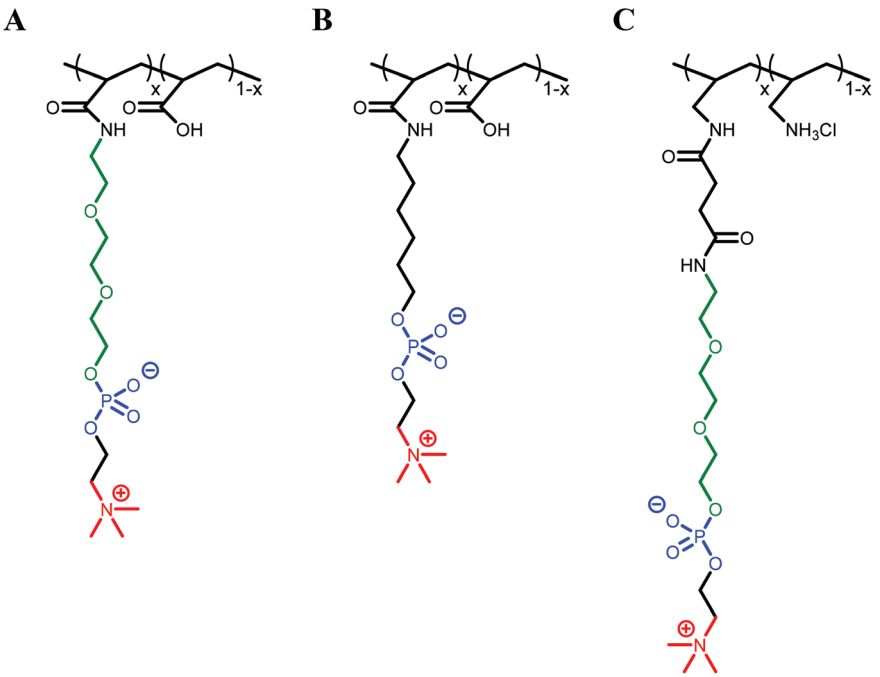

Fig. 26 Molecular structure of (A) PAA-*g*-(OEO_3-PC), (B) PAA-*g*-(*n*-hexyl-PC), and (C) PAH-*g*-(OEO_3-PC) poly(acrylic acid)- or poly(allylamine hydrochloride)-based polymers.

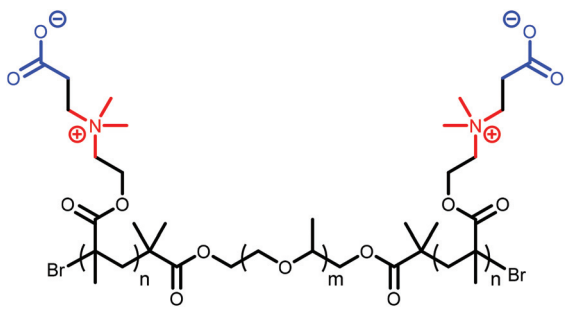

Fig. 27 Molecular structure of the polyCBMA-*bl*-PPO-*bl*-polyCBMA zwitterionic poloxamer derivative (*n* = 40, *m* = 48).

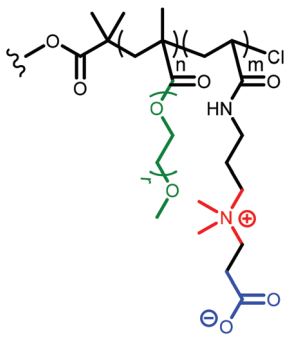

Fig. 28 Molecular structure of the hierarchical polyMeOEGMA-*bl*-polyCBAA hybrid copolymer brush.

polyMeOEGMA-*bl*-polyCBAA diblock copolymer hybrid brush (Fig. 28) – sequentially grown on gold *via* a precursor SAM of ω-mercapto-undecyl α-bromoisobutyrate ATRP initiator (Fig. 17D) – able to nearly suppress fouling from various undiluted biofluids (FBS, calf serum and human plasma) below the LOD of the SPR sensor device used in the study (Γ < 0.03 ng cm^{-2}, 30 min exposure at 25 °C).[100] In comparison, bare gold adsorbed considerably greater amounts of proteins, respectively Γ = 261 ± 9, 280 ± 7 and 307 ± 11 ng cm^{-2}. The remarkable antifouling properties, against undiluted pooled human plasma (for 15 min), of such hierarchically-constructed brushes (20 + 10 nm-thick) were very recently confirmed by the authors in a 2014 study.[101]

II.E.4. Carboxybetaine zwitterionic monomer derivatives. As illustrated throughout this Review, research on antifouling coating materials is a topic of great current interest with a high level of competitivity, which is fuelled by a seemingly inexhaustible imagination in terms of material chemical structure and architecture. The very active field of zwitterionic polymer brushes is not spared from this trend, as illustrated by the recent work by Cheng and co-workers, who reported a new type of carboxybetaine methacrylamide (CBMAA) building block monomers (Fig. 29).[176] When challenged for 10 min either by undiluted human plasma or serum, ~9–18 nm-thick polyCBMAA brushes (built *via* the photochemical SI-PIMP process – see subsection II.B.) exhibited 'ultralow' fouling performance with Γ < 0.3 ng cm^{-2} (the SPR sensor LOD). The aim of this 'structure-function' relationship study was to pave the way towards the rational design and development of stable

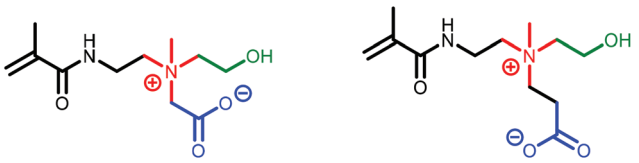

Fig. 29 Molecular structure of two variants of CBMAA zwitterionic monomers differing with respect to the length of the spacer arm between the inner, positively-charged ammonium and terminal, negatively-charged carboxylate moieties.

zwitterionic elastomers having tunable mechanical properties while keeping uncompromised their anti(bio)fouling characteristics.

II.E.5. Pseudozwitterionic materials.[17,114] As shown earlier in subsection II.D., zwitterionic polymer brushes exhibit excellent protein repellence. These do not constitute however the sole type of 'grafted from', ATRP-grown mixed-charged polymer coatings displaying antifouling properties. Indeed, 'pseudozwitterionic' copolymer brushes, wherein the positively- and negatively-charged moieties are now located on two separate subunits, also are capable of resisting protein adsorption. This was recently demonstrated by Chang and Chen (in 2010) with 30–45 nm-thick methacrylate copolymer brushes featuring positively-charged *N*,*N*,*N*-trimethylammonium and negatively-charged sulfonate side-chains (Fig. 30A).[72] Fouling surface coverage from 20% human PPP in PBS (pH 7.4) was measured with SPR upon ~15 min exposure at 37 °C and found to be very low at Γ = 7.65 ng cm^{-2}. As well, Bernards' group reported in 2012 acrylate copolymer brushes with positively-charged *N*,*N*,*N*-trimethylammonium and negatively-charged carboxylate subunits (Fig. 30B).[177] In this work, whether from 10% or undiluted FBS, fouling on ~18 nm-thick coatings was also very low at respectively Γ = 2.1 ± 2.0 and 4.3 ± 1.7 ng cm^{-2}, as assessed with SPR upon 10 min exposure.

Earlier investigations by Jiang's group had already demonstrated the concept of mixed-charged material for antifouling purposes with SAM coatings.[73] In this study, combinations of *N*,*N*,*N*-trimethylammonium (TMA), and sulfonic acid (SA) or carboxylic acid (CA) ω-functionalized alkylthiol gold surface modifiers (Fig. 31) were investigated by means of SPR for their resistance to human serum/plasma adsorption. At physiological pH 7.4, the best antifouling performance recorded for the TMA/SA system was achieved against 10% human serum (Γ ~ 15 ng cm^{-2}, 10 min exposure).[73] This was also the case for the TMA/CA system (Γ ~ 25 ng cm^{-2}). Unfortunately, neither of these combinations was capable of resisting adsorption from 100% serum (Γ > 90 ng cm^{-2}). Fouling from human plasma was even greater, even at 10% dilution in PBS (Γ ~ 190–950 ng cm^{-2}).[73,97]

II.E.6. Ionic liquids. At last, there also exists – in addition to the various (truly and pseudo) zwitterionic building blocks discussed herein (*vide supra*) – another type of charged material that has very recently been implemented in the preparation of antifouling coatings on gold: ionic liquids (IL). In fact, Masson's group reported in 2013 IL SAMs – built with long, imidazolium-based thiol molecules (Fig. 32) – that were shown to be capable of impeding protein adsorption.[178] The latter, measured against crude serum (~70 mg proteins per mL) using SPR, was Γ = 99 ng cm^{-2}. Although this account obviously exceeds the level of adsorption set for antifouling coatings to qualify for presentation in this Review (Γ < 30 ng cm^{-2}), the novelty of this IL surface chemistry, and the fact that the latter performed similarly as benchmark antifouling PEGylated surfaces under identical conditions,[178] both make it definitely worth describing. Incidentally, when these IL SAMs were functionalized with anti-IgG antibodies for immunosensing application, fouling from crude serum dropped to Γ = 45 ng cm^{-2}.

II.E.7. Carbohydrates: glycocalyx mimics. We conclude this subsection on hybrid, derivative and other coating materials with an important class of biomimetic antifouling constructs inspired by the outer surface of biological cell membranes. This interfacial region – known as the 'glycocalyx' – consists of a dense, non-adhesive mesh of highly hydrated, carbohydrate-rich macromolecules (proteoglycans and glycoproteins), and acts as a barrier that regulates molecular and cellular interactions.[179–181]

In 1998, Marchant and co-workers set out to mimic such supramolecular assembly by engineering oligosaccharide surfactant polymers for the surface modification of highly-oriented pyrolytic graphite (HOPG).[181] These macromolecular structures consisted of a poly(vinyl amine) polymer back-

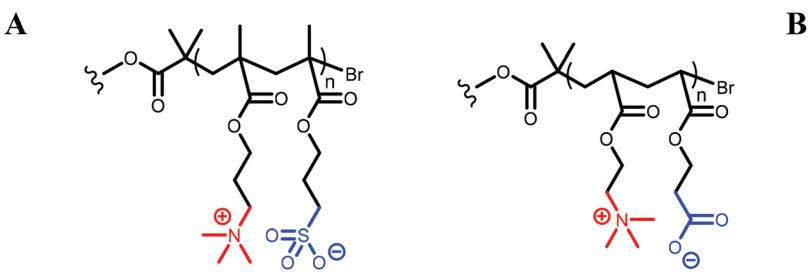

Fig. 30 Molecular structure of the (A) ammonium/sulfonate, and (B) ammonium/carboxylate mixed-charged, pseudozwitterionic (meth)acrylate copolymer brushes. Adapted from ref. 23 with permission of the Royal Society of Chemistry.

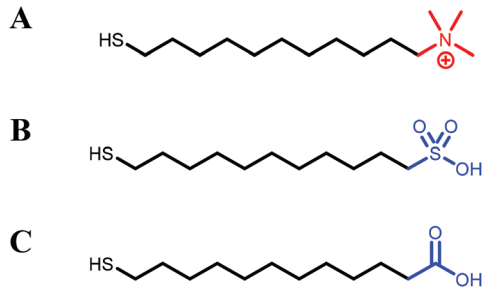

Fig. 31 Molecular structure of the (A) *N,N,N*-trimethylammonium (TMA), (B) sulfonic acid (SA), and (C) carboxylic acid (CA) ω-functionalized alkylthiol surface modifiers for mixed, pseudozwitterionic antifouling SAM formation on gold. At physiological pH 7.4, SA and CA moieties in the mixed SAMs exist as their negatively-charged sulfonate and carboxylate forms, respectively. Adapted from ref. 23 with permission of the Royal Society of Chemistry.

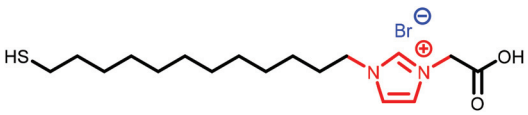

Fig. 32 Molecular structure of the imidazolium-based IL thiol surface modifier for antifouling SAM formation on gold.

bone onto which hydrophobic *n*-hexanoyl and hydrophilic dextran side-chains were simultaneously grafted *via* the pendant primary amine groups (Fig. 33A). On HOPG, these graft-copolymers were shown to grow monomolecular epitaxial films 7–12 Å-thick. During the adsorption process, *n*-hexanoyl side-chains assemble on the underlying HOPG substrate through hydrophobic-hydrophobic interactions, thereby constraining the flexible poly(vinyl amine) backbone to lie parallel to the surface and the hydrophilic dextran arms to stretch outwards in the aqueous environment – in an overall tridimensional, comb-like structure. Although not quantified *per se*, the level of protein adsorption on these glycocalyx-like assemblies (upon incubation in 50% human PPP for 30 min at 37 °C) was shown to be considerably lower than that recorded on unmodified HOPG control surfaces. Using FTIR-ATR following the relative absorbance of the characteristic amide I and II protein bands, the investigators indeed estimated plasma protein adsorption to be reduced by at least 90%.

Later, in 2001, Marchant's group conducted a more systematic investigation, wherein a series of oligomaltose-based analogous copolymer coatings with varying saccharide side-chain length were tested for their antifouling properties – under the same, previous experimental conditions (*i.e.* against 50% PPP for 30 min at 37 °C).[182] Still using FTIR-ATR, the authors demonstrated in this work that plasma protein adsorption steadily declined with increasing film thickness, the best performance (a ~96% reduction) being obtained for the thickest (42 Å) films studied.

Gratifyingly, Spencer and co-workers did later quantify (in 2008) the antifouling properties of a series of poly(L-lysine)-*graft*-dextran copolymer analoguous coatings (Fig. 33B) immobilized on silicon/titanium oxide OWLS surfaces.[183] The best resistance to fouling recorded against human serum (30 min exposure) was rather good at $\Gamma = 13 \pm 8$ ng cm^{-2}. The same research group recently (in 2013) devised a new strategy to prepare antifouling dextran coatings; those, however, were not as effective.[78]

There is finally the approach by Kizhakkedathu and co-workers, who in 2012 investigated the antifouling properties of

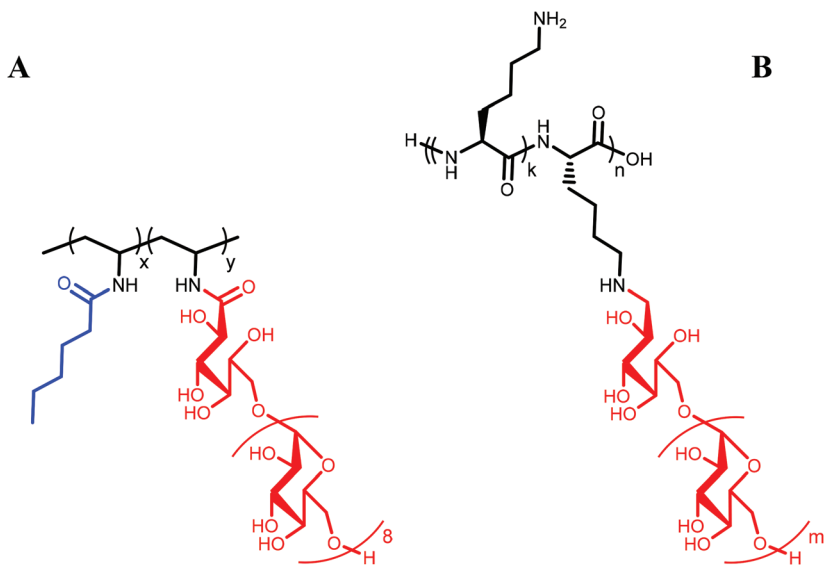

Fig. 33 Molecular structure of the (A) poly(vinyl amine)-, and (B) poly(L-lysine)-*graft*-dextran carbohydrate-based copolymers. Adapted from ref. 23 with permission of the Royal Society of Chemistry.

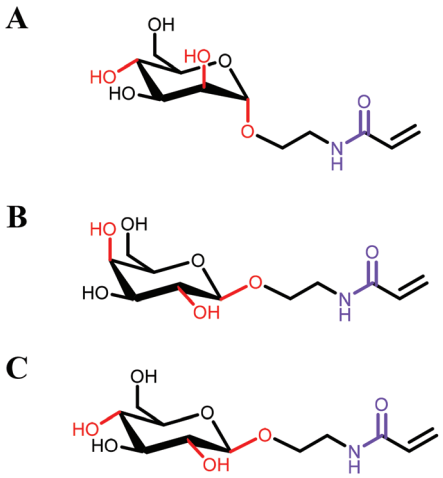

Fig. 34 Molecular structure of the (A) mannose, (B) galactose, and (C) glucose pyranoside carbohydrate-based acrylamide monomers.

a series of glycopolymer brushes ATRP-grown onto SPR gold chips through an α-bromoisobutyrate-terminated initiator thiol SAM.[184] Three types of 'grafted from' coatings – constructed with mannose (Fig. 34A), galactose (Fig. 34B), or glucose (Fig. 34C) pyranoside acrylamide monomers presenting varied carbohydrate stereochemistry – were examined. When challenged by undiluted blood plasma (for 6 min), it was the latter kind of brush (58.6 nm-thick) that exhibited the greatest propensity to repel plasma proteins with $\Gamma = 24.3$ ng cm^{-2}.

II.F. A closer look at fouling: identification of adsorbed proteins

There exists, beyond its mere quantification, another important aspect to surface fouling that relates to the actual, qualitative identification of adsorbed proteins – an arduous task Brynda's (in 2013) then Masson's (in 2014) research groups recently accomplished.

In a SPR flow-through cell, the former investigators first fouled with undiluted human plasma (pooled and citrated, 30 min exposure) a series of antifouling polyOEGMA brushes (see subsection II.C. – Fig. 18) and (PEG-capped) OEG SAMs that were then directly submitted to a sequence of on-surface trypsin digestion (24 h at 37 °C) followed by nanoLC-MS/MS qualitative analysis.[185] Together with the help of a database cataloguing over 20 000 registered proteins, the latter technique enabled the authors to identify the proteins responsible for fouling. The observation was thus made that the ~28 nm-thick polyHOEGMA brushes of the study adsorbed the littlest *number* of proteins (only 9 different types), but were not the most antifouling with $\Gamma = 63.0$ ng cm^{-2}. In fact, ~27 nm-thick polyMeOEGMA counterparts adsorbed less proteins (actually the least amount with $\Gamma = 48.0$ ng cm^{-2}), but in a greater number (11 different kinds). On the other hand, much thinner EG SAM coatings (~1–2 nm-thick) were fouled by a much greater amount ($\Gamma = 105$–165 ng cm^{-2}) and number of plasma proteins (up to 27 different types). To note, the 9 proteins that were found to foul all coatings were apolipoprotein A-1 (31 kDa), apolipoprotein B-100 (516 kDa), complement C3 (187 kDa), complement C4-A (193 kDa), complement C4-B (193 kDa), histidine-rich glycoprotein (60 kDa), Ig mu chain C region (49 kDa), fibrinogen (340 kDa), and albumin (69 kDa).[185] In view of the great diversity in molecular weight of adsorbed proteins, the investigators concluded that no apparent correlation existed between this parameter and protein deposit composition, and also noted that the latter – as per the dynamic 'Vroman effect' that describes the temporal exchange of proteins on surfaces[3,186] – could differ for longer exposure time to plasma (>30 min).[185] Another interesting finding was that fibrinogen and albumin were detected on poly-OEGMA brushes only when adsorbed from blood plasma (*vs.* single protein solutions), suggesting that their deposition was mediated by other adsorbed/co-adsorbing plasma proteins. The authors finally attempted to predict the biological processes and other interactions the presence of these adsorbed proteins might trigger (and those that presumably might not be due to the absence of some other proteins), should the coatings be implemented in real-world applications.

More recently (in 2014), Masson's group – continuing on with their research on antifouling surface chemistry based on short peptide SAMs[52–56] – used MALDI-MS analysis in combination with on-surface trypsin digestion to identify directly from SPR chips the species responsible for fouling from crude bovine serum.[187] The investigation suggested that the team's best antifouling peptide SAM ($\Gamma = 12 \pm 11$ ng cm^{-2}),[56] built from ternary-patterned 3-MPA-(Leu-His-Asp)$_2$-OH hexapeptide (Fig. 3D), was fouled by apolipoprotein A-1, bovine serum albumin, and SHC-transforming protein 1.[187] Another, less antifouling peptide SAM ($\Gamma = 29 \pm 1$ ng cm^{-2}), based on binary-patterned 3-MPA-His$_3$-Asp$_2$-OH pentapeptide, would in addition also adsorb complement C3 and kininogen 2. The latter protein would not adhere however on otherwise more fouled alkyl- and OEG-based SAMs ($\Gamma = 236 \pm 63$ and 100 ± 23 ng cm^{-2}, respectively). Contrary to the work by Brynda and co-workers with blood plasma (*vide supra*),[185] fibrinogen was not expected (nor found) to be part of the identified fouling species,[187] since this protein is absent in blood serum (but present in blood plasma).[39] In upcoming subsection III.A. will finally be presented the related, previous work by the authors that aimed at quantifying (with SPR) and identifying (with MS) the species responsible for fouling on peptide SAMs from a biological medium with much distinct composition: cell lysate.

It is fair to note that these accounts by Brynda's[185] and Masson's[187] teams by no means are unique in their attempt to identify the proteins responsible for fouling as other research groups have, previously or since, also accomplished such a task – for a variety of coatings (constructed on particulate surfaces).[188–193] By setting out to identify the (protein) species still adhering to effective antifouling coatings – an emerging trend in the field – these researchers all together have laid one

stepping stone towards a better understanding of fouling from complex biological media, which should eventually benefit the rational design of surface chemistries with superior antifouling performance. This effort to move forward a field – which, admittedly, is starting to be crowded by redundant accounts uniquely focusing on quantifying the amount of adsorbed material (*i.e.* proteins) – deserved to be pointed out.

A final comment also deserves to be made regarding Terminology. It seems indeed unfortunate that the terms 'antifouling' and 'non-fouling' – the latter being (by definition) the arguably elusive, perfect antifouling situation where *no* fouling occurs – have, admittedly, acquired a confusing and misleading status of synonyms in the literature. It is probably the case that this therefore nonsensical, yet much acclaimed 'non-fouling' expression has often more to do with marketing than science. The same holds true for the superlatives 'superlow' and 'ultralow'. In the same vein, both Brynda's[185] and Huck's[188] teams recently pointed out (in 2013) that so-called 'protein-resistant' surfaces exposed to complex biological milieux (*e.g.* blood plasma) are still fouled by a non-negligible, residual amount/number of proteins.

II.G. Antifouling and plasma/serum source variability

Before moving the focus of this Review on state-of-the-art antifouling surface chemistries from blood plasma/serum to other human or animal biofluids, a parenthesis of utmost importance – especially for potential biosensing assays – must be made regarding the necessity of considering the source of blood plasma/serum samples, and its variability, in the assessment of the antifouling properties of coatings. To date, this issue has only been given sporadic attention, but the message that clearly emerged was that blood plasma/serum biosamples originating (i) from different species (bovine *vs.* equine sera),[108] (ii) from a same species but at a different stage of maturity (adult *vs.* foetal bovine sera,[108] adult *vs.* infant human plasmas[194]), or (iii) from different donors (human adults)[103,116] do/may indeed exhibit markedly different fouling behaviour. The latter situation was recently (in 2014) the focus of a methodical, pioneering study by Rodriguez-Emmenegger's team, who compiled the data obtained for a series of various antifouling surface chemistries – polyHEMA (Fig. 25B), polyHOEGMA (Fig. 18A), polyMeOEGMA (Fig. 18B), polyCBAA (Fig. 19D), and polyHPMA (Fig. 25E) polymer brushes – challenged by human blood plasma samples drawn from five different healthy individuals.[103] Despite limited sampling, unambiguous (substantial) variability in terms of fouling surface coverage was demonstrated across the different blood plasmas, most notably for polyHEMA brushes that exhibited the highest dispersity between single measurements with $\sim 7 < \Gamma < \sim 195$ ng cm^{-2} (followed by polyHOEGMA with $\sim 2 < \Gamma < \sim 63$ ng cm^{-2}, polyMeOEGMA with $\sim 8 < \Gamma < \sim 26$ ng cm^{-2}, and then polyCBAA with $\sim 1 < \Gamma < \sim 7$ ng cm^{-2}) – as measured with SPR upon 15 min exposure at 25 °C. Littlest variability was observed for polyHPMA brushes for which fouling was actually invariably below $\Gamma = 0.3$ ng cm^{-2} for all tested blood plasmas. Even when the five single donations were mixed, significant variability was still observed with pooled plasma samples acquired from two other, different commercial suppliers.[103] Once again, polyHEMA brushes displayed the highest discrepancy in terms of antifouling behaviour with $\sim 7 < \Gamma < \sim 170$ ng cm^{-2}.[103,138] Regardless of the pooled plasma source (commercial or not), fouling on polyHPMA brushes was still not quantifiable (*i.e.* below the 0.3 ng cm^{-2} LOD of the SPR sensor).

Through their systematic investigation of the antifouling properties of relevant surface chemistries using various, different sources of blood plasma/serum biosamples – pooled or not – Rodriguez-Emmenegger's team provided one legitimate explanation to the existence of some conflicting results that had appeared in the literature over recent years (for polyHEMA).[103] From the practical standpoint of clinical diagnostics, the inherent variability of biological samples necessarily obtained from single donors could have serious implications, noted the authors.

III. Antifouling surface chemistries against other human or animal biofluids

Even though research activity in this domain has been modest so far, accounts also exist that report the quantified antifouling properties (in terms of surface coverage) of various different coatings against other human or animal biofluids than blood plasma and serum (Fig. 1). Those biological fluids – ranked alphabetically, and not according to their ubiquity or a given importance – are presented in the following subsections, each of which will also encompass a concise but solid description (*e.g.* composition, role, importance) of said biofluid.

Before going any further however, it should be noted that – to date (January 2015) – the following, non-exhaustive list of another 25 technologically-relevant biological media has generated no (exploitable) search hit from Scifinder® database: amniotic fluid,[195] bile,[196] breath,[197,198] cerumen,[199] chyle,[200] endolymph,[201] feces,[198,202] flatus/intestinal gas,[203] gastric juice,[204] honey,[205] ink,[206] interstitial fluid,[207] karyoplasm,[208] lymph,[209] ocular fluids (aqueous and vitreous humours),[210] pericardial fluid,[211] perilymph,[212] peritoneal fluid,[213] pleural fluid,[214] sebum,[198,215] semen,[216] sputum,[217] synovial fluid,[218,219] sweat,[198] and tears.[220] [To note, it is also possible to set foot into the plant kingdom with sap as a fluid against which it might be needed to implement antifouling coatings.[221]] Hopefully, this Review will also trigger for these leftover biological milieux an interest in the quantification of minimized fouling by appropriate surface chemistry.

III.A. Cell lysate

We begin with cell lysate our survey of other human or animal biofluids for which antifouling surface chemistries have been developed or adapted. Rightfully so, one could immediately

argue that cell lysates should not be considered as being a biofluid since – as their name suggest – these are the result of the mechanical or chemical lysis of whole biological cells.[222] However, in view of the importance these complex biological mixtures may soon acquire in the field of biosensors (*vide infra*), it has been decided that those accounts describing antifouling surface chemistry against cell lysate would find their place in this Review. Lysis causes cells to release cytosolic biomolecules (*e.g.* proteins, nucleic acids) and organelle constituents of the cytoplasm, the intracellular matrix. Dismantelment of the cell bilayer membrane in the process endows crude, unprocessed lysates with their particularity of presenting a very high lipid content.[223] The work described below constitutes, to our knowledge, the sole example quantifying (and identifying the species responsible for) fouling from crude cell lysate.

Based on the assumption (and previous experimental work)[53] that crude cell lysate and serum should be expected to display different fouling behaviour – owing to their different biomolecular make-ups notably in terms of lipid *vs.* protein contents – Masson's group methodically revisited in a recent account the antifouling peptide SAM surface chemistry they had originally developed to minimize fouling from 100% serum (see subsection II.B.).[223] The objective was for the authors to engineer antifouling coatings suited for crude cell lysates, and capable of being implemented into SPR biosensors for the detection of biomarkers in lysates produced from suspected cancerous tumors collected during solid tissue biopsies. The reason for this is that there exist cancers, whose biomarker presence is difficult to detect in yet less invasive blood serum, urine or saliva liquid biosamples.

In a first effort, the authors prepared on SPR gold chips a series of 3-MPA-homopentapeptide-based SAMs that were next exposed for 20 min to crude cell lysate (from HEK 293FT cells).[223] Peptide building blocks had the 3-MPA-$(AA)_5$-OH generic structure – where neutral L-Ser, acidic L-Asp, basic L-His, aromatic L-Phe, and aliphatic L-Leu representative amino acids were selected to cover the effects on antifouling of side-chain charge, polarity, and aromaticity. Lowest fouling (Γ = 194 ± 77 ng cm^{-2}) was recorded for the most hydrophobic 3-MPA-Leu_5-OH SAM. In comparison, fouling from undiluted serum was Γ = 345 ± 78 ng cm^{-2}.[53] Close second was the nearly as hydrophobic 3-MPA-Phe_5-OH SAM for which fouling from cell lysate was Γ = 235 ± 77 ng cm^{-2}.[223] With respect to serum however, this coating was outperformed by its counterpart based on L-Leu subunits (Γ = 619 ± 66 ng cm^{-2}).[53] The authors next investigated peptide length and showed that – unlike experiments carried out with serum[53] – this parameter had little influence on fouling from cell lysate, lowest adsorption (Γ = 147 ± 44 ng cm^{-2}) being observed for 3-MPA-Leu_2-OH SAM.[223] This relatively pronounced antifouling behaviour was to be contrasted, again, with the high level of adsorption recorded with serum (Γ = 598 ± 84 ng cm^{-2}).[53] As was also the situation with serum,[54] SAMs constructed from 3-MPA-pentapeptides presenting binary, diblock sequences of amino acids exhibited better antifouling properties, highest

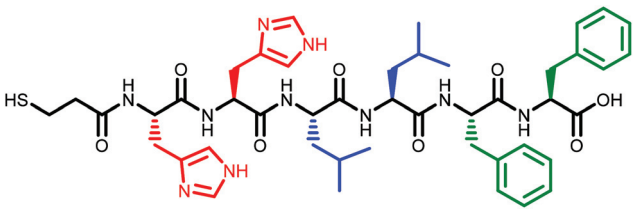

Fig. 35 Molecular structure of 3-MPA-$(His)_2(Leu)_2(Phe)_2$-OH ternary-patterned, triblock hexapeptide.

performance in the present case of cell lysate being that of 3-MPA-$(Leu)_3(Phe)_2$-OH hydrophobic SAM with Γ = 112 ± 28 ng cm^{-2}.[223]

At last, experiments were also carried out with *concentrated* lysate, a more challenging test for which SAMs built with ternary-patterned, triblock 3-MPA-$(His)_2(Leu)_2(Phe)_2$-OH hexapeptide[56] (Fig. 35) turned out to be the most effective (Γ = 159 ± 27 ng cm^{-2}).[223] In comparison, bare gold was heavily fouled (Γ = 929 ± 186 ng cm^{-2}) – so was, to a lesser extent, a benchmark antifouling OEG SAM coating (Γ = 294 ± 25 ng cm^{-2}). The antifouling performance against concentrated cell lysate of the best 3-MPA-$(Leu)_3(Phe)_2$-OH diblock SAM became Γ = 698 ng cm^{-2} (from Γ = 112 ng cm^{-2} with the less concentrated mixture); that of the best antifouling SAM against serum (built with 3-MPA-$(Leu\text{-}His\text{-}Asp)_2$-OH hexapeptide drawn in Fig. 3D – Γ = 12 ± 11 ng cm^{-2})[56] plummeted to Γ = 789 ± 107 ng cm^{-2}.[223]

More than a still modest level of performance (Γ > 100 ng cm^{-2}), this[223] and previous[52–56] antifouling studies by Masson and co-workers collectively generated two crucial pieces of information. Of utmost importance for biodiagnosticians was the unambiguous demonstration that crude cell lysate and serum do indeed present, as anticipated, (drastically) different fouling behaviour – implying the inconvenient necessity for biosensing platforms to be customized in terms of antifouling surface chemistry to a given detection biofluid. Secondly, from a mechanistic point of view, the conclusion was drawn that SAMs made of hydrophobic and/or basic (positively-charged) peptides show greater potential to reduce fouling from cell lysate. This, noted the authors, contrasts with the general trend observed in experiments performed with serum for which hydrophilic surfaces are more effective at resisting fouling.[223]

Finally, in addition to quantifying their surface coverage using SPR, the investigators actually set out to identify the cell lysate species (lipids and proteins) responsible for fouling, using a combination of enzymatic digestion (trypsin) followed by MALDI-TOF/TOF MS qualitative analysis (for the identification of the fouling material from blood serum, see subsection II.F.).[223] The latter revealed that lipids (mostly from the phosphatidyl choline family), and not proteins, constituted the major source of fouling. This was to be expected since, unlike serum that is mainly composed of proteins, crude cell lysate essentially is a concentrated mixture of highly adhesive lipids

resulting from the fragmentation of biological cell membranes.[223]

III.B. Cerebrospinal fluid

The cerebrospinal fluid (CSF) is mainly a product of blood plasma ultrafiltration – secreted in specialized regions deep within the brain – that flows in the space around and within the brain and spinal cord (together known as 'central nervous system' – CNS) back into the bloodstream.[224–228] From the ~500 mL of CSF produced daily, only 90–150 mL circulate in adults at any one time, meaning that the CSF is constantly being replenished.[224–228] In terms of composition, normal CSF – a clear, colourless liquid – is essentially an electrolyte (*e.g.* Na^+, K^+, Cl^-)-rich aqueous solution (99% of water), nearly depleted of red/white cells and proteins (0.15–1.00 mg mL^{-1} *vs.* ~70 mg mL^{-1} for blood serum) as a result of ultrafiltration.[224–228] Glucose (0.40–0.70 mg mL^{-1}), neurotransmitters (*e.g.* γ-amino-butyric acid – GABA), and enzymes are also found in the metabolome of CSF.[225–229] The CSF has several vital functions. Of note is its buoyancy that supports the brain against gravity and literally causes it to float in the cranium, reducing as such the strain exerted over the blood vessels and nerves attached to the CNS.[224,227] The CSF also acts as a protective hydraulic cushion, regulating intracranial pressure and diffusing forces generated by external shocks.[224–227] The CSF also creates a regulated chemical environment supplying the CNS with essential nutrients and, conversely, disposing it of its metabolic waste products (when the CSF is re-absorbed in the blood circulatory system).[224–227] Finally, the CSF also serves as a vehicle for the intracerebral transport of bioactive substances.[226]

The collection of CSF specimens for clinical analysis can be performed through a sampling procedure known as 'lumbar puncture' (or 'spinal tap').[224,225,227,228] Lists of known and candidate CSF biomarkers of chronic neurodegenerative diseases (such as the notorious 'Alzheimer's disease') have been recently compiled,[228–231] analytes for which biosensor technology could be of service for diagnostic purposes.[76] A criterion that biosensing interfaces will have to fulfil however is the ability to resist, with appropriate antifouling surface chemistry, the signal-interfering non-specific adsorption of CSF matrix components.

There is – to our knowledge – only one, recent account (in 2012) that quantified fouling surface coverage from (human) CSF. This pioneering work by Rodriguez-Emmenegger and co-workers revealed that 18 to 30 nm-thick polyHOEGMA (Fig. 18A), polyCBAA (Fig. 19D), polyHEMA (Fig. 25B), and polyHPMA (Fig. 25E) polymer brushes – ATRP-grown on SPR gold chips through a precursor SAM of ω-mercapto-undecyl α-bromoisobutyrate initiator (Fig. 17D) – all resisted fouling from undiluted human CSF, adsorption being indeed undetectable (Γ < 0.03 ng cm^{-2}, the LOD of the SPR sensor – 15 min exposure).[76] Even both 0.9 nm-thick OEG_2- and OEG_6-terminated alkylthiol SAMs (Fig. 10) – that were heavily fouled by undiluted human plasma (Γ = 225 ± 12 and 71 ± 8 ng cm^{-2}) – displayed pronounced antifouling properties against human CSF with Γ = 7.6 ± 1.0 and 4.3 ± 0.8 ng cm^{-2}, respectively.[76] This observation should perhaps not come as a surprise considering that CSF is an otherwise less proteinaceous biological medium than blood plasma (~0.35 *vs.* ~70 mg mL^{-1}).[228] This experiment with CSF was part of a larger investigation, which also aimed at assessing the fouling behaviour of six other human or animal undiluted biological milieux (discussed in this Review): human plasma/serum, saliva, and urine, as well as chicken egg and cow milk.

III.C. Egg

Annually, over a trillion eggs – more often than not from chicken – are produced worldwide for food.[232] Structurally, raw eggs are essentially composed of two distinct, semi-liquid media – (i) the albumen ('egg white') that surrounds (ii) the yolk – encapsulated in a hard, ~0.3 mm-thick calcareous shell.[233] The albumen has a gel-like consistency and mainly consists of water (~88%) and a variety of proteins (~10%), examples of which are ovalbumin (the most abundant) and avidin (which is well-known for its extremely high affinity for biotin).[233] Lipids (<0.1%), carbohydrates (~1%), minerals (<1%), and vitamins are minor constituents of albumen. Yolk is an 'oil-in-water' emulsion with a dry matter content (~51%) mainly made of lipids (~63%) and proteins (~32%), as well as minerals (~2%), carbohydrates (~2%), and vitamins.[233] As discussed for milk in upcoming subsection III.D., eggs are an important source of nutrition for which also exists an interest – in both fields of food quality/safety assessment and veterinary medicine – in developing biosensors for the (early) detection of pathogens/disease biomarkers.[76] A prerequisite would be to minimize, with appropriate antifouling surface chemistry, the response signal interference caused by the non-specific adsorption of egg matrix components on sensing platforms.

As was the situation for cerebrospinal fluid in previous subsection III.B., the aforementioned pioneering work by Rodriguez-Emmenegger and co-workers appears to be the sole one to date to quantify fouling surface coverage from (carefully blended yolk and white) chicken egg.[76] This complex mixture turned out to be otherwise more challenging however, as only the polyHOEGMA (Fig. 18A), polyCBAA (Fig. 19D), and polyHPMA (Fig. 25E) polymer brushes were able in this case to resist fouling (Γ < 0.03 ng cm^{-2}, 15 min contact). Another evidence was the extremely heavy fouling now experienced not only by the polyHEMA brushes (Γ = 51 ± 3 ng cm^{-2} – Fig. 25B) but also, in particular, by both OEG_2- and OEG_6-SAMs (Γ = 914 ± 76 and 657 ± 43 ng cm^{-2}, respectively – Fig. 10).

III.D. Milk

Fouling by milk components, its quantification in terms of surface coverage and the antifouling surface chemistries to combat the phenomenon have received more attention in comparison to other biofluids (at the probable exception of blood plasma/serum) – notably from bioanalysts willing to develop biosensors for the real-time detection of pathogens/disease biomarkers with minimized response signal interference.[76]

The reason for such interest certainly resides in the fact that milk,[234] like eggs,[233] is an important source of food (about 500 billion liters are produced worldwide annually[232]), whose quality/safety is therefore crucial to closely monitor. In terms of composition, milk is principally made of water (up to 87% depending on the mammal species) but also is rich in proteins (<10%) – caseins and the whey proteins β-lactoglobulin and α-lactalbumin being, in the case of cow milk, by far the most abundant (>90%).[234] Whole milk also contains sugars (~5%), mainly lactose, and diverse lipids (~4%). Also found in cow milk are organic acids (*e.g.* citric and lactic acids), minerals and trace elements (*e.g.* calcium and iron), vitamins, and a great number of enzymes.

In terms of antifouling coating studies aiming to quantify the minimized amount of deposited material from milk, there is again that by Rodriguez-Emmenegger's team, who demonstrated in 2012 that 30 nm-thick polyHOEGMA brushes (Fig. 18A) – ATRP-grown on SPR gold chips *via* a precursor SAM of ω-mercapto-undecyl α-bromoisobutyrate initiator (Fig. 17D) – were able to decrease fouling from whole cow milk to $\Gamma = 3.9 \pm 0.6$ ng cm^{-2} (15 min exposure).[76] Much thinner (0.9 nm-thick) OEG_2- and OEG_6-terminated alkylthiol SAMs (Fig. 10) were also shown to display such pronounced antifouling properties with $\Gamma = 15.2 \pm 1.1$ and 2.9 ± 0.5 ng cm^{-2}, respectively. More interesting was the observation that ~19 nm-thick polyCBAA (Fig. 19D), polyHEMA (Fig. 25B), and polyHPMA (Fig. 25E) polymer brushes all resisted fouling from whole milk with $\Gamma < 0.03$ ng cm^{-2} (the LOD of the SPR sensor). Collectively, this[76] and another two preceeding (in 2011)[235] or following (in 2014)[138] SPR studies by Rodriguez-Emmenegger and co-workers also revealed that the fat content (1.5 *vs.* 3.25%, *i.e.* 'semi-skimmed' *vs.* 'whole, full-fat' undiluted fresh milk) and the source of milk (fresh undiluted milk *vs.* powder milk *vs.* infant powder milk formula – the latter two reconstituted at 10% in water), if any, have little effect on the remarkable antifouling properties of OEG_6-SAMs,[235] as well as polyHOEGMA (and polyMeOEGMA),[138,235] polyHEMA,[138,235] and polyCBAA[138] polymer brushes.

Another type of surface chemistry to combat fouling from milk, based on hyaluronic acid (HA – Fig. 36), has also been recently developed (in 2014).[236] Polysaccharidic HA films (10.5 nm-thick) were covalently grafted on SPR gold chips through an epoxide-terminated alkylthiol adhesion SAM. The level of fouling from cow milk ($\Gamma = 9.8$ ng cm^{-2} – 10 min exposure)[236] was comparable to that reported in the aforementioned studies with polymer brushes and OEG_n-SAMs (*vide supra*).[76,138,235]

Fouling from milk – notably on the surface of heat exchangers during its thermal processing (for pasteurization/sterilization) – also is of primary concern in the dairy industry since the resulting expenditure in terms of plant maintenance ousts billions of dollars annually (this necessity for periodic cleaning down times also raising the issue of plant productivity and profitability), not to mention the problems associated with a decrease in treatment efficiency (*e.g.* in heat transfer) and product quality/safety.[237–246] In the dairy industry, fouling from milk is also referred to as 'burn-on',[238] and – in contrast to the field of biosensor analysis, where this interfering phenomenon would for obvious reasons be discussed at the molecular, ng cm^{-2} scale – constitutes more of a 'macroscopic' issue with deposits in the mg cm^{-2} range (or a difference of six orders of magnitude).[238–241,244] [Fouling build-ups on heat exchangers – two types of which have been defined and abundantly studied with various methods[238] (as well as their critical effect on operating parameters, and *vice-versa*) – are mainly composed of proteins (*e.g.* β-lactoglobulin) and minerals (calcium salts, through a process known as 'crystallization fouling').[237–243]] Another difference in the study of milk fouling is the total area of exposed surfaces, which is otherwise much larger in the latter situation ($\gg$100 cm^2 *vs.* $\ll$1 cm^2) since meaningful experimental conditions in this case are those of pilot plant-scale set-ups.[239–241] The same holds true for the duration (hours *vs.* minutes) and temperature (>75 °C *vs.* $\leq$37 °C) of fouling experiments.

Various surface chemistries have been developed to try and decrease fouling from milk on heat exchangers.[242,243,246–249] There is for instance the successful approach by Goddard's group, who used an ~10.5 μm-thick nickel-phosphorous-polytetrafluoroethylene (Ni-P-PTFE) coating plated on stainless steel (SS, the standard contact material used in milk-processing equipment) to mitigate fouling from raw milk during pasteurization (8 h exposure at 85 °C) – from $\Gamma \sim 12$ mg cm^{-2} for control heat exchanger plates of native SS, to $\Gamma \sim 0.3$ mg cm^{-2} for SS modified with a Ni-P-PTFE adlayer.[239,241,246] Gratifyingly, coated surfaces were also shown to retain their antifouling performance for 10 repeated processing runs, each lasting 4 h.[239] In contrast, the strategy adopted by Patel and co-workers – that involved the deposition of doped diamond-like carbon (DLC) adlayers onto SS plates – offered no benefit as bare and DLC-modified SS heat exchanger surfaces presented similar levels of fouling ($\Gamma > 23$ mg cm^{-2}), from raw whole milk heated at 84 °C for 240 min.[240,248]

PTFE fluoropolymer (Teflon – Fig. 37) is a heat-resistant material capable of withstanding the high temperatures (>75 °C)[237–239] reached during the thermal treatment of milk.

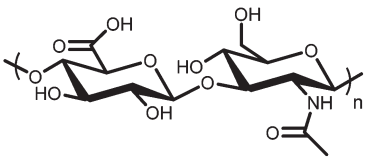

Fig. 36 Molecular structure of hyaluronic acid.

Fig. 37 Molecular structure of polytetrafluoroethylene (Teflon).

It would be interesting to determine whether some of the various polymer brushes/SAMs and other organic coatings discussed in this (or other) sections are robust enough to sustain such harsh conditions of temperature while maintaining their otherwise more pronounced, ng cm^{-2} antifouling properties displayed at room temperature. In the affirmative, the dairy industry could very well experience a genuine economical revolution in terms of maintenance cost and productivity of milk-processing factories. Actually, the food industry as a whole could benefit from such an accomplishment.[245]

III.E. Saliva

Counter-intuitively perhaps, the spontaneous fouling of teeth (newly erupted or freshly brushed) by salivary material can be seen as a blessing in disguise since the resulting, mainly proteinaceous film – called 'acquired enamel pellicle' (AEP) – protects them both from acid-induced demineralization/erosion and abrasion by friction with other teeth/the oral mucosa.[250,251] Paradoxically however, this pellicle may also have a detrimental effect by acting as a substratum conditioning bacterial adhesion and the formation of the so-called 'dental plaque', a biofilm associated with the development of dental caries and periodontal disease (*e.g.* gingivitis).[250,251] Understandably, the adsorption of salivary material also is a topic of great interest, not only in prosthetic dentistry with the issue of the biocompatibility of restorative synthetic materials,[252] but also in the realm of biosensor technology as this biofluid hosts a collection of important, non-invasively collectable biomarkers.[76,253–255] Interestingly, the AEP itself has been proposed as a potential source of such analytes.[256]

Secretion product of three major glands (0.5–1.5 L day^{-1}), saliva is a slightly acidic (pH 6–7) clear biofluid mainly made of water (99%).[253–255,257] Other salivary components include a variety of proteins (*e.g.* enzymes, immunoglobulins) and ions (*e.g.* Ca^{2+}, F^-, phosphates), for instance.[250,253–255] Also found in saliva, and the non-sterile environment of the oral cavity, are colonies of bacteria.[250,253–255] Saliva is multifunctional in nature and – in addition to maintaining (through remineralization) and protecting (through AEP formation and pH regulation) the integrity of tooth enamel – is notably involved in the moisturization, lubrication and cleansing of the oral cavity, as well as in food digestion (including mastication, preliminary breakdown, and deglutition).[250,253–255] Defence against pathogens (*e.g.* viruses, bacteria, fungi) is another important role of saliva.[250,253–255]

Studies intending to quantify the minimized surface coverage of adsorbed salivary material are relatively scarce, and the antifouling coating strategies implemented variously effective. Successful approaches include that, aforementioned, by Rodriguez-Emmenegger's group, who recently (in 2012) reported that ~19 nm-thick polyCBAA (Fig. 19D), polyHEMA (Fig. 25B), and polyHPMA (Fig. 25E) brushes – ATRP-grown on SPR gold chips through a precursor SAM of ω-mercapto-undecyl α-bromoisobutyrate initiator (Fig. 17D) – all resisted fouling from undiluted human saliva.[76] Adsorption of salivary material upon 15 min exposure was indeed undetectable (Γ < 0.03 ng cm^{-2}, the SPR sensor's LOD). Another polymer coating (30 nm-thick polyHOEGMA – Fig. 18A) as well OEG_2- and OEG_6-terminated alkylthiol SAMs (Fig. 10), both 0.9 nm-thick, also displayed excellent antifouling properties with Γ = 6.7 ± 1.4, 15.7 ± 1.9 and 8.2 ± 2.0 ng cm^{-2}, respectively. Others also have studied fouling from whole human saliva on methyl-[258–262] or perfluorooctyl-terminated[263,264] hydrophobic silane coatings,[265] but those surfaces were not as effective with $\Gamma \sim 300$ and 110 ng cm^{-2}, respectively. In the latter case, bare substrates (silicon oxide) adsorbed a comparatively greater amount of salivary material ($\Gamma \sim 400$ ng cm^{-2}). More surprising perhaps, in view of the pronounced antifouling properties repeatedly reported in this Review and elsewhere for such type of construct, was the observation that substrates modified with an hydrophilic, OEG-based coating were on average more fouled than those derivatized with the perfluoroalkyl, hydrophobic adlayer discussed earlier ($\Gamma \sim 210$ *vs.* 110 ng cm^{-2}).[263,264]

III.F. Urine

There is finally one last biofluid to discuss in this Review that has been tested for its fouling potency: urine. Contrary to common belief, the most important function of urine (*i.e.* of the kidneys where it is produced upon blood filtration) is not to dispose the organism of water-soluble waste products, but to regulate the water and electrolyte contents of blood.[266,267] Urine – 1.5 to 2 liters of which are collected in/eliminated from the bladder on a daily basis[267,268] – is an aqueous medium (>95% of water) containing many catabolites, most notably urea (9.3–23.3 g L^{-1}).[268,269] Other breakdown products include, for instance: creatinine (0.67–2.15 g L^{-1}), uric acid (0.04–0.67 g L^{-1}), and ammonia (0.20–0.73 g L^{-1}), as well as yellow pigments urobilin (7–90 mg L^{-1}) and bilirubin (3–30 mg L^{-1}).[269] Ions at high concentration can also be found such as Cl^- (1.87–8.40 g L^{-1}), Na^+ (1.17–4.39 g L^{-1}), and K^+ (0.75–2.61 g L^{-1}).[269] Many other (in)organic solutes, such as glucose (0.03–0.20 g L^{-1}), also make the long list of urine components.[267–269] Normal urine is a yellow/amber-coloured, nearly acellular liquid, whose analysis only reveals trace amount[268,270] of a great variety of proteins.[267,271]

Proteinuria – a condition characterized by an abnormally-high level of proteins in urine (>300 mg L^{-1}) – can be readily detected through routine dipstick urinalysis.[268] Urine can also be tested for illicit substances or their metabolites, examples of which are performance-enhancing steroids (doping)[272] and drugs of abuse/prohibited street drugs (*e.g.* cocaine).[273] Until modern times and the advent of blood serology, urine was the primary diagnostic biofluid,[268,274] but the possibility to non-invasively collect large samples of it still makes urine a particularly convenient medium where to detect/discover biomarkers.[267,271] Biomarker detection is an area where biosensor technology, again, could be of service.[76] Response signal interference by the matrix components of urine first

needs to be minimized with appropriate surface chemistry however.

To our knowledge, and as was already the case for cerebrospinal fluid (subsection III.B.) and egg (subsection III.C.), the above-mentioned work by Rodriguez-Emmenegger and coworkers pioneered the quantification of fouling by undiluted (human) urine.[76] This biofluid was shown not to be an issue in this respect since fouling surface coverage upon 15 min exposure was indeed undetectable (*i.e.* $\Gamma < 0.03$ ng cm^{-2}) – for all, 18–30 nm-thick polyHOEGMA (Fig. 18A), polyCBAA (Fig. 19D), polyHEMA (Fig. 25B), and polyHPMA (Fig. 25E) tested brushes (ATRP-grown on SPR gold chips through a precursor SAM of ω-mercapto-undecyl α-bromoisobutyrate initiator – Fig. 17D). A 0.9 nm-thick OEG_6-terminated alkylthiol SAM (Fig. 10) also displayed such performance. Even a shorter OEG_2-SAM analogue, 0.9 nm-thick as well, demonstrated the ability to resist fouling from human urine with $\Gamma = 11.0 \pm 1.1$ ng cm^{-2}. This latter result is to be constrasted with that obtained with undiluted human plasma ($\Gamma = 225 \pm 12$ ng cm^{-2}),[76] but should perhaps not come as a surprise considering that blood plasma is an otherwise more proteinaceous biological milieux than urine (~70 *vs.* ~0.30 mg mL^{-1}).

IV. At-a-glance summary

Compiled below in two summary tables are the best antifouling performances in terms of minimized surface coverage (ng cm^{-2}) of the various different surface chemistries presented in this Review, against blood plasma/serum (Table 1, subsection IV.A.) as well as other human or animal biofluids (Table 2, subsection IV.B.) – for a given substrate material. Interested readers are kindly invited to consult the main text for a more detailed discussion on antifouling surface chemistries and experimental testing conditions.

IV.A. Blood plasma/serum

Table 1 State-of-the-art antifouling performance of various, different surface chemistries against blood plasma/serum

		~Adsorbed mass (ng cm^{-2})						
		Bovine serum		Human serum		Human plasma		
Type of coating	Substrate	10%	100%	10%	100%	10%	100%	Ref.
Single amino acid monolayer	Au	—	42	—	—	~200	—	48,57
Peptide SAM	Au	—	12	—	—	<50	—	48,56
Multilayered polypeptide film	Metal oxide	—	—	<1	—	—	—	58
Poly(single amino acid) brush	Au	—	—	—	<1	—	3	61–63
Polypeptoid film/SAM	Au	—	—	4	6	5	10	68
	Ti	—	—	—	~4	—	—	64
	TiO_2	—	—	—	>15	—	—	66,67
OEG film	Au	—	—	—	—	5	24	69
	Metal oxide	1	—	—	—	—	—	85
OEG SAM	Au	—	26	~15	~85	38[a]	71	70–73,76
PEG film	Au	>6	—	—	14	—	2	79,93
	TiO_2	—	—	—	<5	—	—	83,87,88
PEG poloxamer film	Au	—	—	—	16	<2[a]	—	70,81
OEG dendritic film	Au	—	—	—	20	—	8	95
	TiO_2	—	—	—	<2	—	—	87
Poly(OEG) brush	Au	<1	<1	<5	<1	<5	<1	73,105–108,112,170
	TiO_2	<20	—	—	—	—	—	111
	Nylon	—	<1	—	—	—	<20	98
Phosphorylcholine-based zwitterionic polymer brush	Au	>13	—	—	—	>345[b]	—	79,115,116
Sulfobetaine-based zwitterionic	Au	—	—	~1	<1	2[a]	<1	71,119,121
polymer brush	SiO_2	—	26	—	—	—	—	123
Carboxybetaine-based	Au	—	<1	<1	<1	<1	<1	73,76,97–99,115,116,128,133–135,138,176
zwitterionic polymer brush	SiO_2	—	<5	—	12	—	6	130,132
PEG-polypeptide hybrid	Metal oxides	—	5	—	<2	—	—	142–145,147–149,151,152,154,155,160–164
(and derivatives) film	PDMS	—	—	—	<1	—	—	159
Poly(short hydroxyalkyl) brush	Au	<1	<1	<1	<1	<1	<1	76,99,103,105,166–169,171–173
EGylated zwitterionic hybrid	Au	—	<1	—	—	—	<1	100
polymer film/brush	Metal oxide	1	—	—	—	—	—	85,174
Pseudozwitterionic copolymer brush	Au	2	4	—	—	8[a]	—	72,177
Pseudozwitterionic mixed SAM	Au	—	—	~15	>90	>190	>250	73,97
Ionic liquid SAM	Au	—	—	—	99	—	—	178
Polysaccharide film	Metal oxide	—	—	—	13	—	—	183
Poly(carbohydrate) brush	Au	—	—	—	—	—	24	184

[a] 20% platelet-poor plasma. [b] 33% in PBS.

IV.B. Other human or animal biofluids

Table 2 State-of-the-art antifouling performance of various, different surface chemistries against other human or animal biofluids including cell lysate, cerebrospinal fluid, egg, milk, saliva, and urine

		~Adsorbed mass (ng cm^{-2})						
Type of coating	Substrate	Cell lysate	CSF[a]	Egg	Milk	Saliva	Urine	Ref.
Peptide SAM	Au	159	—	—	—	—	—	223
OEG SAM	Au	294	4	657	3	8	<1	76,223
Poly(OEG) brush	Au	—	<1	<1	4	7	<1	76
Zwitterionic brush (carboxybetaine)	Au	—	<1	<1	<1	<1	<1	76
Poly(short hydroxyalkyl) brush	Au	—	<1	<1	<1	<1	<1	76
Polysaccharide film	Au	—	—	—	10	—	—	236

[a] CSF is cerebrospinal fluid.

V. Conclusion and outlook

The functionality and life expectancy of biomedical/bioanalytical equipment, implants and devices critically depend on the interactivity of their exogenous synthetic surface with the multi-components of the biofluid matrix they are exposed to, the outcome largely hinging on the physicochemical make-up of the artificial material contacting said biological environment. Herein, we have gathered, upon comprehensive review of pertinent literature, the state-of-the-art stealth surface chemistries developed up to January 2015 to minimize fouling surface coverage from both human and animal real-life biosamples (≥10 vol%) down to biotechnologically relevant levels (*i.e.* a few ng cm^{-2}). These remarkable antifouling properties were imparted to a variety of both inorganic and organic underlying substrates through the implementation of (sub)nanometer thin SAMs or thicker polymer films/brushes, a varied arsenal of which is now available as demonstrated in this Review. Attention was first focused on the most investigated biofluids – blood plasma and serum – whose provenance and variability (in terms of species, age, and single *vs.* pooled donations) were also shown to markedly alter their fouling potency. The identification of the species responsible for fouling – the next, logical trend in the field that should benefit the educated and rational design of antifouling coatings with superior performance – was also touched upon. Quantification of minimized fouling by appropriate surface chemistry was also presented for another 6, much less explored human or animal biological milieux: cell lysate, cerebrospinal fluid, egg, milk, saliva, and urine.

It is the authors' hope that this Review will not only motivate continued research on antifouling surface chemistries for all these media, but also trigger an equivalent interest for some others – a non-exhaustive list of which encompassing 25 potential candidates is proposed hereinafter: amniotic fluid, bile, breath, cerumen, chyle, endolymph, feces, flatus/intestinal gas, gastric juice, honey, ink, interstitial fluid, karyoplasm, lymph, ocular fluids (aqueous and vitreous humours), pericardial fluid, perilymph, peritoneal fluid, pleural fluid, sebum, semen, sputum, synovial fluid, sweat, and tears. An area where quantified minimization of fouling with appropriate surface chemistry would be of definite interest for any of the biological milieux inventoried in this Review is biosensor technology, with in perspective both human and veterinary applications. Time will tell.

Notes and references

1 B. Kasemo and J. Gold, *Adv. Dent. Res.*, 1999, **13**, 8.
2 C. J. Wilson, R. E. Clegg, D. I. Leavesley and M. J. Pearcy, *Tissue Eng.*, 2005, **11**, 1.
3 R. A. Latour Jr., Biomaterials: Protein-Surface Interactions, in *Encyclopedia of Biomaterials and Biomedical Engineering*, ed. G. E. Wnek and G. L. Bowlin, Taylor & Francis, USA, 2005, pp. 1–15.
4 For a discussion on the link between material 'fouling' and 'bio-incompatibility' – and the fact that 'antifouling' and 'biocompatibility' are subtly two different, not necessarily related surface properties – please see: C. Blaszykowski, S. Sheikh and M. Thompson, *Trends Biotechnol.*, 2014, **32**, 61.
5 B. D. Ratner and S. J. Bryant, *Annu. Rev. Biomed. Eng.*, 2004, **6**, 41.
6 B. Nilsson, K. N. Ekdahl, T. E. Mollnes and J. D. Lambris, *Mol. Immunol.*, 2007, **44**, 82.
7 K. N. J. Stevens, Y. B. J. Aldenhoff, F. H. van der Veen, J. G. Maessen and L. H. Koole, *J. Biomed. Biotechnol.*, 2007, **2007**, 29464.
8 P. H. Kvist and H. E. Jensen, *J. Diabetes Sci. Technol.*, 2007, **1**, 746.
9 P. Thevenot, W. Hu and L. Tang, *Curr. Top. Med. Chem.*, 2008, **8**, 270.
10 J. M. Anderson, A. Rodriguez and D. T. Chang, *Semin. Immunol.*, 2008, **20**, 86.
11 S. Franz, S. Rammelt, D. Scharnweber and J. C. Simon, *Biomaterials*, 2011, **32**, 6692.

12 J. L. Harding and M. M. Reynolds, *Trends Biotechnol.*, 2014, **32**, 140.
13 K. Fedorov, C. Blaszykowski, S. Sheikh, A. Reheman, A. Romaschin, H. Ni and M. Thompson, *Langmuir*, 2014, **30**, 3217.
14 M. R. Malone, J.-F. Masson, M. Barhnart, S. Beaudoin and K. S. Booksh, *Proc. SPIE*, 2005, **6007**, 60070V.
15 S. Choi and J. Chae, *J. Micromech. Microeng.*, 2010, **20**, 075015.
16 M. Thompson, S. Sheikh, C. Blaszykowski and A. Romaschin, Biosensor Technology and the Clinical Biochemistry Laboratory – Issue of Signal Interference from the Biological Matrix, in *Detection Challenges in Clinical Diagnostics*, ed. P. Vadgama and S. Peteu, Royal Society of Chemistry Publishing, UK, 2013, ch. 1, pp. 1–34.
17 S. Chen, L. Li, C. Zhao and J. Zheng, *Polymer*, 2010, **51**, 5283.
18 I. Banerjee, R. C. Pangule and R. S. Kane, *Adv. Mater.*, 2011, **23**, 690.
19 P. Gong and D. W. Grainger, Nonfouling Surfaces: A Review of Principles and Applications for Microarray Capture Assay Designs, in *Microarrays Volume 1 Synthesis Methods – Methods in Molecular Biology*, ed. J. B. Rampal, Humana Press Inc., USA, 2nd edn, 2007, vol. 381, pp. 59–92.
20 C. Zhao, L.-Y. Li, M.-M. Guo and J. Zheng, *Chem. Pap.*, 2012, **66**, 323.
21 P. Vermette and L. Meagher, *Colloids Surf., B*, 2003, **28**, 153.
22 E. Ostuni, R. G. Chapman, R. E. Holmlin, S. Takayama and G. M. Whitesides, *Langmuir*, 2001, **17**, 5605.
23 C. Blaszykowski, S. Sheikh and M. Thompson, *Chem. Soc. Rev.*, 2012, **41**, 5599.
24 J. Benesch, S. Svedhem, S. C. T. Svensson, R. Valiokas, B. Liedberg and P. Tengvall, *J. Biomater. Sci. Polymer Edn*, 2001, **12**, 581.
25 D. Rana and T. Matsuura, *Chem. Rev.*, 2010, **110**, 2448.
26 R. Mukhopadhyay, *Anal. Chem.*, 2005, **77**, 429A.
27 See also: C. Zilio, L. Sola, F. Damin, L. Faggioni and M. Chiari, *Biomed. Microdevices*, 2014, **16**, 107.
28 M. Piliarik, M. Bocková and J. Homola, *Biosens. Bioelectron.*, 2010, **26**, 1656.
29 S. Lowe, N. M. O'Brien-Simpson and L. A. Connal, *Polym. Chem.*, 2015, **6**, 198.
30 A. Barfidokht and J. J. Gooding, *Electroanalysis*, 2014, **26**, 1182.
31 Y.-J. Shih and Y. Chang, *Langmuir*, 2010, **26**, 17286.
32 Y. L. Jeyachandran, J. A. Mielczarski, E. Mielczarski and B. Rai, *J. Colloid Interface Sci.*, 2010, **341**, 136.
33 S. Sheikh, C. Blaszykowski and M. Thompson, *Surf. Interface Anal.*, 2013, **45**, 1781.
34 A. Rosenhahn, S. Schilp, H. J. Kreuzer and M. Grunze, *Phys. Chem. Chem. Phys.*, 2010, **12**, 4275 and references therein.
35 M. Morra, *J. Biomater. Sci., Polym. Ed.*, 2000, **11**, 547.
36 S. Sheikh, C. Blaszykowski, R. Nolan, D. Thompson and M. Thompson, *J. Colloid Interface Sci.*, 2015, **437**, 197.
37 Fouling surface coverage, expressed in terms of adsorbed mass per unit area, can sometimes be found 'quantified' using sensor devices based on acoustic wave physics – a yet non-gravimetric technique, notably when implemented in the liquid phase and/or the monitoring of adsorbed biopolymer films with non-negligible viscoelastic properties. See, for instance: citations 114, 116 and 118 of ref. 23. In the latter citation (118), it is also clearly evident that considerable discrepancy in terms of 'quantification' exists between this and other techniques. See also: F. Höök, J. Vörös, M. Rodahl, R. Kurrat, P. Böni, J. J. Ramsden, M. Textor, N. D. Spencer, P. Tengvall, J. Gold and B. Kasemo, *Colloids Surf., B*, 2002, **24**, 155.
38 For instance, with respect to diagnostic assays aiming to detect trace amounts of target analytes in biological milieux, excessive sample dilution may result in undetectable concentrations and preclude early detection of the associated disease/condition.
39 W. F. Ganong, Circulating Body Fluids, in *Review of Medical Physiology*, Lange Medical Books/McGraw-Hill (Medical Publishing Division), USA, 22nd edn, 2005, pp. 515–546.
40 A. C. Guyton and J. E. Hall, in *Textbook of Medical Physiology*, Elsevier Saunders, USA, 11th edn, 2006, pp. 419–468.
41 J. F. Dailey, in *Dailey's Notes on Blood*, Medical Consulting Group, USA, 3rd edn, 1996.
42 D. U. Silverthorn, *Blood, in Human Physiology – An Integrated Approach*, Pearson-Benjamin Cummings Publisher, USA, 3rd edn, 2004, ch. 16, pp. 523–545.
43 J. G. White, Platelet Structure, in *Platelets*, ed. A. D. Michelson, Elsevier Academic Press, USA, 2nd edn, 2007, pp. 45–52.
44 J. A. Davis, D. W. Inglis, K. J. Morton, D. A. Lawrence, L. R. Huang, S. Y. Chou, J. C. Sturm and R. H. Austin, *Proc. Natl. Acad. Sci. U. S. A.*, 2006, **103**, 14779.
45 Y. Shen, J. Kim, E. F. Strittmatter, J. M. Jacobs, D. G. Camp II, R. Fang, N. Tolié, R. J. Moore and R. D. Smith, *Proteomics*, 2005, **5**, 4034.
46 J. D. Andrade and V. Hlady, *Ann. N. Y. Acad. Sci.*, 1987, **516**, 158.
47 J. N. Adkins, S. M. Varnum, K. J. Auberry, R. J. Moore, N. H. Angell, R. D. Smith, D. L. Springer and J. G. Pounds, *Mol. Cell. Proteomics*, 2002, **1**, 947.
48 M. Lestelius, P. Tengvall and I. Lundström, *J. Colloid Interface Sci.*, 1995, **171**, 533.
49 P. Lin, L. Ding, C.-W. Lin and F. Gu, *Langmuir*, 2014, **30**, 6497.
50 M. Lestelius, B. Liedberg, I. Lundström and P. Tengvall, *J. Biomed. Mater. Res.*, 1994, **28**, 871.
51 P. Tengvall, M. Lestelius, B. Liedberg and I. Lundström, *Langmuir*, 1992, **8**, 1236.
52 O. R. Bolduc and J.-F. Masson, *Langmuir*, 2008, **24**, 12085.

53 O. R. Bolduc, C. M. Clouthier, J. N. Pelletier and J.-F. Masson, *Anal. Chem.*, 2009, **81**, 6779.
54 O. R. Bolduc, J. N. Pelletier and J.-F. Masson, *Anal. Chem.*, 2010, **82**, 3699.
55 O. R. Bolduc, D. Correia-Ledo and J.-F. Masson, *Langmuir*, 2012, **28**, 22.
56 O. R. Bolduc, P. Lambert-Lanteigne, D. Y. Colin, S. S. Zhao, C. Proulx, D. Boeglin, W. D. Lubell, J. N. Pelletier, J. Féthière, H. Ong and J.-F. Masson, *Analyst*, 2011, **136**, 3142.
57 Q. Zou, L. L. Kegel and K. S. Booksh, *Anal. Chem.*, 2015, **87**, 2488.
58 L. Richert, P. Lavalle, D. Vautier, B. Senger, J.-F. Stoltz, P. Schaaf, J.-C. Voegel and C. Picart, *Biomacromolecules*, 2002, **3**, 1170.
59 MES and Tris respectively are 2-(*N*-morpholino)ethanesulfonic acid and Tris(hydroxymethyl)aminomethane.
60 Q. Liu, A. Singh and L. Liu, *Biomacromolecules*, 2013, **14**, 226.
61 Q. Liu, W. Li, A. Singh, G. Cheng and L. Liu, *Acta Biomater.*, 2014, **10**, 2956.
62 W. Li, Q. Liu and L. Liu, *J. Biomater. Sci., Polym. Ed.*, 2014, **25**, 1730.
63 W. Li, Q. Liu and L. Liu, *Langmuir*, 2014, **30**, 12619.
64 A. R. Statz, R. J. Meagher, A. E. Barron and P. B. Messersmith, *J. Am. Chem. Soc.*, 2005, **127**, 7972.
65 L-DOPA is L-3,4-dihydroxy-phenylalanine.
66 A. R. Statz, A. E. Barron and P. B. Messersmith, *Soft Matter*, 2008, **4**, 131.
67 A. R. Statz, J. Kuang, C. Ren, A. E. Barron, I. Szleifer and P. B. Messersmith, *Biointerphases*, 2009, **4**, FA22.
68 S. Lin, B. Zhang, M. J. Skoumal, B. Ramunno, X. Li, C. Wesdemiotis, L. Liu and L. Jia, *Biomacromolecules*, 2011, **12**, 2573.
69 L. Cao, M. Chang, C.-Y. Lee, D. G. Castner, S. Sukavaneshvar, B. D. Ratner and T. A. Horbett, *J. Biomed. Mater. Res., Part A*, 2007, **81**, 827.
70 Y. Chang, W.-L. Chu, W.-Y. Chen, J. Zheng, L. Liu, R.-C. Ruaan and A. Higuchi, *J. Biomed. Mater. Res., Part A*, 2010, **93**, 400.
71 Y. Chang, S.-C. Liao, A. Higuchi, R.-C. Ruaan, C.-W. Chu and W.-Y. Chen, *Langmuir*, 2008, **24**, 5453.
72 Y. Chang, S.-H. Shu, Y.-J. Shih, C.-W. Chu, R.-C. Ruaan and W.-Y. Chen, *Langmuir*, 2010, **26**, 3522.
73 J. Ladd, Z. Zhang, S. Chen, J. C. Hower and S. Jiang, *Biomacromolecules*, 2008, **9**, 1357.
74 See also: B. Zhu, T. Eurell, R. Gunawan and D. Leckband, *J. Biomed. Mater. Res.*, 2001, **56**, 406.
75 See also: C. Subramani, A. Bajaj, O. R. Miranda and V. M. Rotello, *Adv. Mater.*, 2010, **22**, 5420.
76 C. Rodriguez-Emmenegger, M. Houska, A. Bologna Alles and E. Brynda, *Macromol. Biosci.*, 2012, **12**, 1413.
77 For the antifouling properties against 10% FBS (30 min exposure) of the corresponding, 1.7 nm-thick OEG_3-SAM on gold, see: M. Lashkor, F. J. Rawson, J. A. Preece and P. M. Mendes, *Analyst*, 2014, **139**, 5400.
78 For the antifouling properties against human serum of 20 kDa PEG (~3.9 nm-thick), 2000 kDa dextran (~7.1 nm-thick), and 27 kDa poly(vinyl alcohol) (~0.9 nm-thick) polymeric films spin-coated onto ~1.8 nm-thick polyallylamine-*g*-perfluorophenylazide adhesion coatings themselves anchored to Si/SiO_2 wafers through multiple electrostatic interactions, see: Â. Serrano, O. Sterner, S. Mieszkin, S. Zürcher, S. Tosatti, M. E. Callow, J. A. Callow and N. D. Spencer, *Adv. Funct. Mater.*, 2013, **23**, 5706.
79 K. Yoshimoto, T. Hirase, J. Madsen, S. P. Armes and Y. Nagasaki, *Macromol. Rapid Commun.*, 2009, **30**, 2136.
80 O. Pop-Georgievski, D. Verreault, M.-O. Diesner, V. Proks, S. Heissler, F. Rypáček and P. Koelsch, *Langmuir*, 2012, **28**, 14273.
81 L. M. Feller, S. Cerritelli, M. Textor, J. A. Hubbell and S. G. P. Tosatti, *Macromolecules*, 2005, **38**, 10503.
82 J. P. Bearinger, S. Terrettaz, R. Michel, N. Tirelli, H. Vogel, M. Textor and J. A. Hubbell, *Nat. Mater.*, 2003, **2**, 259.
83 V. Zoulalian, S. Zürcher, S. Tosatti, M. Textor, S. Monge and J.-J. Robin, *Langmuir*, 2010, **26**, 74.
84 V. Zoulalian, S. Monge, S. Zürcher, M. Textor, J.-J. Robin and S. Tosatti, *J. Phys. Chem. B*, 2006, **110**, 25603.
85 A. Reisch, J.-C. Voegel, E. Gonthier, G. Decher, B. Senger, P. Schaaf and P. J. Mésini, *Langmuir*, 2009, **25**, 3610.
86 J. Davila, D. Toulemon, T. Garnier, A. Garnier, B. Senger, J.-C. Voegel, P. J. Mésini, P. Schaaf, F. Boulmedais and L. Jierry, *Langmuir*, 2013, **29**, 7488.
87 T. Gillich, E. M. Benetti, E. Rakhmatullina, R. Konradi, W. Li, A. Zhang, A. D. Schlüter and M. Textor, *J. Am. Chem. Soc.*, 2011, **133**, 10940.
88 J. L. Dalsin, L. Lin, S. Tosatti, J. Vörös, M. Textor and P. B. Messersmith, *Langmuir*, 2005, **21**, 640.
89 S. Zürcher, D. Wäckerlin, Y. Bethuel, B. Malisova, M. Textor, S. Tosatti and K. Gademann, *J. Am. Chem. Soc.*, 2006, **128**, 1064.
90 J.-Y. Wach, B. Malisova, S. Bonazzi, S. Tosatti, M. Textor, S. Zürcher and K. Gademann, *Chem. – Eur. J.*, 2008, **14**, 10579.
91 B. Malisova, S. Tosatti, M. Textor, K. Gademann and S. Zürcher, *Langmuir*, 2010, **26**, 4018.
92 For the antifouling properties against 50% FBS (2 h incubation) of ~9 kDa PEG multisorbate films (~4 nm-thick) tethered to a variety of metal substrates (Au, Si, Ti) through catechol graft residues, see also: H. Lee, K. D. Lee, K. B. Pyo, S. Y. Park and H. Lee, *Langmuir*, 2010, **26**, 3790.
93 For the remarkable (Γ < 30 ng cm^{-2}), long-term (10 days) antifouling properties against undiluted human blood plasma/serum of PEO coatings grafted at high temperature (≥90 °C melts) onto dopamine-melanin anchoring polymer films (12 nm-thick) pre-coated on gold surfaces, see also: O. Pop-Georgievski, Š. Popelka, M. Houska, D. Chvostová, V. Proks and F. Rypáček, *Biomacromolecules*,

2011, **12**, 3232. For a more recent (2012), related study minimizing fouling from 100% human blood plasma to $\Gamma = 7 \pm 2$ ng cm^{-2} with 14.1 nm-thick $PEO_{20\ kDa}$ brushes (as measured with SPR upon 20 min exposure), see ref. 80.

94 For a more recent study on the antifouling properties against full human serum (20 min incubation) of ~2 kDa PEG-dopamine brushes (~62 Å-thick) grafted onto titanium oxide through the pioneering electroreduction of *o*-benzoquinone anchoring residues, see also: S. Liu, L. Chen, L. Tan, F. Cao, L. Bai and Y. Wang, *J. Mater. Chem. B*, 2014, **2**, 6758.

95 G. Gunkel, M. Weinhart, T. Becherer, R. Haag and W. T. S. Huck, *Biomacromolecules*, 2011, **12**, 4169.

96 For the antifouling properties against 100% human PPP of a closely related poly-*N*-[(2,3-dihydroxy-propyl)acrylamide] polymer brush on silicon, see: Y. Zou, P.-Y. J. Yeh, N. A. A. Rossi, D. E. Brooks and J. N. Kizhakkedathu, *Biomacromolecules*, 2010, **11**, 284.

97 Z. Zhang, M. Zhang, S. Chen, T. A. Horbett, B. D. Ratner and S. Jiang, *Biomaterials*, 2008, **29**, 4285.

98 C. Rodriguez-Emmenegger, O. Kylián, M. Houska, E. Brynda, A. Artemenko, J. Kousal, A. Bologna Alles and H. Biederman, *Biomacromolecules*, 2011, **12**, 1058.

99 C. Rodriguez-Emmenegger, E. Brynda, T. Riedel, M. Houska, V. Šubr, A. Bologna Alles, E. Hasan, J. E. Gautrot and W. T. S. Huck, *Macromol. Rapid Commun.*, 2011, **32**, 952.

100 C. Rodriguez-Emmenegger, E. Hasan, O. Pop-Georgievski, M. Houska, E. Brynda and A. Bologna Alles, *Macromol. Biosci.*, 2012, **12**, 525.

101 A. de los Santos Pereira, T. Riedel, E. Brynda and C. Rodriguez-Emmenegger, *Sens. Actuators, B*, 2014, **202**, 1313.

102 A. R. Kuzmyn, A. de los Santos Pereira, O. Pop-Georgievski, M. Bruns, E. Brynda and C. Rodriguez-Emmenegger, *Polym. Chem.*, 2014, **5**, 4124.

103 A. de los Santos Pereira, C. Rodriguez-Emmenegger, F. Surman, T. Riedel, A. Bologna Alles and E. Brynda, *RSC Adv.*, 2014, **4**, 2318.

104 T. Riedel, C. Rodriguez-Emmenegger, A. de los Santos Pereira, A. Bědajánková, P. Jinoch, P. M. Boltovets and E. Brynda, *Biosens. Bioelectron.*, 2014, **55**, 278.

105 C. Rodriguez-Emmenegger, A. Decker, F. Surman, C. M. Preuss, Z. Sedláková, N. Zydziak, C. Barner-Kowollik, T. Schwartz and L. Barner, *RSC Adv.*, 2014, **4**, 64781.

106 H. Ma, J. Hyun, P. Stiller and A. Chilkoti, *Adv. Mater.*, 2004, **16**, 338.

107 C. Rodriguez-Emmenegger, A. Jäger, E. Jäger, P. Stepanek, A. Bologna Alles, S. S. Guterres, A. R. Pohlmann and E. Brynda, *Colloids Surf., B*, 2011, **83**, 376.

108 J. E. Gautrot, B. Trappmann, F. Oceguera-Yanez, J. Connelly, X. He, F. M. Watt and W. T. S. Huck, *Biomaterials*, 2010, **31**, 5030.

109 H. Ma, D. Li, X. Sheng, B. Zhao and A. Chilkoti, *Langmuir*, 2006, **22**, 3751.

110 DMEM is Dulbecco's mininum essential medium.

111 J. E. Raynor, T. A. Petrie, A. J. García and D. M. Collard, *Adv. Mater.*, 2007, **19**, 1724.

112 O. Pop-Georgievski, C. Rodriguez-Emmenegger, A. de los Santos Pereira, V. Proks, E. Brynda and F. Rypáček, *J. Mater. Chem. B*, 2013, **1**, 2859.

113 For the antifouling properties against 33% foetal calf serum (15 min incubation) of polyCBAA brushes grafted on cellulose (filter paper), see also: T. Tischer, C. Rodriguez-Emmenegger, V. Trouillet, A. Welle, V. Schueler, J. O. Mueller, A. S. Goldmann, E. Brynda and C. Barner-Kowollik, *Adv. Mater.*, 2014, **26**, 4087.

114 S. Jiang and Z. Cao, *Adv. Mater.*, 2010, **22**, 920.

115 N. Y. Kostina, C. Rodriguez-Emmenegger, M. Houska, E. Brynda and J. Michálek, *Biomacromolecules*, 2012, **13**, 4164.

116 C. Rodriguez-Emmenegger, E. Brynda, T. Riedel, Z. Sedlakova, M. Houska and A. Bologna Alles, *Langmuir*, 2009, **25**, 6328.

117 For the antifouling properties (Γ > 100 ng cm^{-2}) against 10% FBS (3 h exposure at 37 °C) of photoreactive PCMA-based block terpolymer coatings grafted to stainless steel, see: Y. Iwasaki, A. Matsumoto and S.-I. Yusa, *ACS Appl. Mater. Interfaces*, 2012, **4**, 3254.

118 For the antifouling properties against 10% FBS (30 min exposure) of $[PCMA/Zr^{4+}]_n$ multilayered films self-assembled *via* ionic complexation on silicon wafers, see: S. Pang, C. Zhu, F. Xu, C. Chen and J. Ji, *Colloids Surf., B*, 2012, **94**, 22.

119 C. Zhao, J. Zhao, X. Li, J. Wu, S. Chen, Q. Chen, Q. Wang, X. Gong, L. Li and J. Zheng, *Biomaterials*, 2013, **34**, 4714.

120 W. Yang, S. Chen, G. Cheng, H. Vaisocherová, H. Xue, W. Li, J. Zhang and S. Jiang, *Langmuir*, 2008, **24**, 9211.

121 G. Li, H. Xue, G. Cheng, S. Chen, F. Zhang and S. Jiang, *J. Phys. Chem. B*, 2008, **112**, 15269.

122 G. Li, G. Cheng, H. Xue, S. Chen, F. Zhang and S. Jiang, *Biomaterials*, 2008, **29**, 4592.

123 F. T. Limpoco and R. C. Bailey, *J. Am. Chem. Soc.*, 2011, **133**, 14864.

124 Y. Chang, W.-Y. Chen, W. Yandi, Y.-J. Shih, W.-L. Chu, Y.-L. Liu, C.-W. Chu, R.-C. Ruaan and A. Higuchi, *Biomacromolecules*, 2009, **10**, 2092.

125 S. Choi, B.-C. Choi, C. Xue and D. Leckband, *Biomacromolecules*, 2013, **14**, 92.

126 Y. Chang, Y.-J. Shih, C.-J. Lai, H.-H. Kung and S. Jiang, *Adv. Funct. Mater.*, 2013, **23**, 1100.

127 Q. Liu, W. Li, H. Wang and L. Liu, *J. Appl. Polym. Sci.*, 2014, **131**, 40789.

128 G. Cheng, G. Li, H. Xue, S. Chen, J. D. Bryers and S. Jiang, *Biomaterials*, 2009, **30**, 5234.

129 C. Gao, G. Li, H. Xue, W. Yang, F. Zhang and S. Jiang, *Biomaterials*, 2010, **31**, 1486.

130 N. D. Brault, C. Gao, H. Xue, M. Piliarik, J. Homola, S. Jiang and Q. Yu, *Biosens. Bioelectron.*, 2010, **25**, 2276.

131 See also: J. T. Kirk, N. D. Brault, T. Baehr-Jones, M. Hochberg, S. Jiang and D. M. Ratner, *Biosens. Bioelectron.*, 2013, **42**, 100.
132 See also: M. G. von Muhlen, N. D. Brault, S. M. Knudsen, S. Jiang and S. R. Manalis, *Anal. Chem.*, 2010, **82**, 1905.
133 H. Vaisocherová, W. Yang, Z. Zhang, Z. Cao, G. Cheng, M. Piliarik, J. Homola and S. Jiang, *Anal. Chem.*, 2008, **80**, 7894.
134 N. D. Brault, A. D. White, A. D. Taylor, Q. Yu and S. Jiang, *Anal. Chem.*, 2013, **85**, 1447.
135 W. Yang, H. Xue, W. Li, J. Zhang and S. Jiang, *Langmuir*, 2009, **25**, 11911.
136 H. Vaisocherová, Z. Zhang, W. Yang, Z. Cao, G. Cheng, A. D. Taylor, M. Piliarik, J. Homola and S. Jiang, *Biosens. Bioelectron.*, 2009, **24**, 1924.
137 N. D. Brault, H. S. Sundaram, Y. Li, C.-J. Huang, Q. Yu and S. Jiang, *Biomacromolecules*, 2012, **13**, 589.
138 H. Vaisocherová, V. Ševců, P. Adam, B. Špačková, K. Hegnerová, A. de los Santos Pereira, C. Rodriguez-Emmenegger, T. Riedel, M. Houska, E. Brynda and J. Homola, *Biosens. Bioelectron.*, 2014, **51**, 150.
139 J. E. Krause, N. D. Brault, Y. Li, H. Xue, Y. Zhou and S. Jiang, *Macromolecules*, 2011, **44**, 9213.
140 C.-J. Huang, N. D. Brault, Y. Li, Q. Yu and S. Jiang, *Adv. Mater.*, 2012, **24**, 1834.
141 C.-J. Huang, Y. Li and S. Jiang, *Anal. Chem.*, 2012, **84**, 3440.
142 G. L. Kenausis, J. Vörös, D. L. Elbert, N.-P. Huang, R. Hofer, L. Ruiz-Taylor, M. Textor, J. A. Hubbell and N. D. Spencer, *J. Phys. Chem. B*, 2000, **104**, 3298.
143 N.-P. Huang, R. Michel, J. Vörös, M. Textor, R. Hofer, A. Rossi, D. L. Elbert, J. A. Hubbell and N. D. Spencer, *Langmuir*, 2001, **17**, 489.
144 S. Pasche, S. M. De Paul, J. Vörös, N. D. Spencer and M. Textor, *Langmuir*, 2003, **19**, 9216.
145 S. Tosatti, Z. Schwartz, C. Campbell, D. L. Cochran, S. VandeVondele, J. A. Hubbell, A. Denzer, J. Simpson, M. Wieland, C. H. Lohmann, M. Textor and B. D. Boyan, *J. Biomed. Mater. Res., Part A*, 2004, **68**, 458.
146 K. N. Hansson, S. Tosatti, J. Isaksson, J. Wetterö, M. Textor, T. L. Lindahl and P. Tengvall, *Biomaterials*, 2005, **26**, 861.
147 M. Schuler, G. Rh. Owen, D. W. Hamilton, M. de Wild, M. Textor, D. M. Brunette and S. G. P. Tosatti, *Biomaterials*, 2006, **27**, 4003.
148 R. R. Maddikeri, S. Tosatti, M. Schuler, S. Chessari, M. Textor, R. G. Richards and L. G. Harris, *J. Biomed. Mater. Res., Part A*, 2008, **84**, 425.
149 D. Vonwil, M. Schuler, A. Barbero, S. Ströbel, D. Wendt, M. Textor, U. Aebi and I. Martin, *Eur. Cells Mater.*, 2010, **20**, 316.
150 J. Pei, H. Hall and N. D. Spencer, *Biomaterials*, 2011, **32**, 8968.
151 N.-P. Huang, S. M. De Paul and M. Textor, *Biomacromolecules*, 2011, **12**, 4213.
152 B. Pidhatika, M. Rodenstein, Y. Chen, E. Rakhmatullina, A. Mühlebach, C. Acikgöz, M. Textor and R. Konradi, *Biointerphases*, 2012, **7**, 1.
153 R. Ogaki, O. Z. Andersen, G. V. Jensen, K. Kolind, D. C. E. Kraft, J. S. Pedersen and M. Foss, *Biomacromolecules*, 2012, **13**, 3668.
154 S. VandeVondele, J. Vörös and J. A. Hubbell, *Biotechnol. Bioeng.*, 2003, **82**, 784.
155 G. Zhen, D. Falconnet, E. Kuennemann, J. Vörös, N. D. Spencer, M. Textor and S. Zürcher, *Adv. Funct. Mater.*, 2006, **16**, 243.
156 HEPES is *N*-(2-hydroxyethyl)-piperazine-*N*′-(2-ethanesulfonic acid).
157 N.-P. Huang, J. Vörös, S. M. De Paul, M. Textor and N. D. Spencer, *Langmuir*, 2002, **18**, 220.
158 S. Tosatti, S. M. De Paul, A. Askendal, S. VandeVondele, J. A. Hubbell, P. Tengvall and M. Textor, *Biomaterials*, 2003, **24**, 4949.
159 S. Lee and J. Vörös, *Langmuir*, 2005, **21**, 11957.
160 R. Konradi, C. Acikgoz and M. Textor, *Macromol. Rapid Commun.*, 2012, **33**, 1663.
161 R. Konradi, B. Pidhatika, A. Mühlebach and M. Textor, *Langmuir*, 2008, **24**, 613.
162 B. Pidhatika, J. Möller, V. Vogel and R. Konradi, *Chimia*, 2008, **62**, 264.
163 B. Pidhatika, J. Möller, E. M. Benetti, R. Konradi, E. Rakhmatullina, A. Mühlebach, R. Zimmermann, C. Werner, V. Vogel and M. Textor, *Biomaterials*, 2010, **31**, 9462.
164 O. Guillaume-Gentil, T. Zambelli and J. A. Vorholt, *Lab Chip*, 2014, **14**, 402.
165 H. P. C. Van Kuringen, J. Lenoir, E. Adriaens, J. Bender, B. G. De Geest and R. Hoogenboom, *Macromol. Biosci.*, 2012, **12**, 1114.
166 C. Zhao, L. Li, Q. Wang, Q. Yu and J. Zheng, *Langmuir*, 2011, **27**, 4906.
167 C. Zhao, L. Li and J. Zheng, *Langmuir*, 2010, **26**, 17375.
168 C. Zhao and J. Zheng, *Biomacromolecules*, 2011, **12**, 4071.
169 C. Zhao, Q. Chen, K. Patel, L. Li, X. Li, Q. Wang, G. Zhang and J. Zheng, *Soft Matter*, 2012, **8**, 7848.
170 H. Chen, M. Zhang, J. Yang, C. Zhao, R. Hu, Q. Chen, Y. Chang and J. Zheng, *Langmuir*, 2014, **30**, 10398.
171 J. Yang, M. Zhang, H. Chen, Y. Chang, Z. Chen and J. Zheng, *Biomacromolecules*, 2014, **15**, 2982.
172 Q. Liu, A. Singh, R. Lalani and L. Liu, *Biomacromolecules*, 2012, **13**, 1086.
173 L. Liu, Q. Liu and A. Singh, Polyacrylamide: Evaluation of Ultralow Fouling Properties of a Traditional Material, in *Proteins at Interfaces III State of the Art*, ed. T. Horbett, J. L. Brash and W. Norde, ACS Symposium Series (vol. 1120), American Chemical Society, USA, 2012, ch. 30, pp. 661–676.
174 See also: A. Reisch, J. Hemmerlé, J.-C. Voegel, E. Gonthier, G. Decher, N. Benkirane-Jessel, A. Chassepot, D. Mertz, P. Lavalle, P. Mésini and P. Schaaf, *J. Mater. Chem.*, 2008, **18**, 4242.

175 Y. Li, A. J. Keefe, M. Giarmarco, N. D. Brault and S. Jiang, *Langmuir*, 2012, **28**, 9707.
176 B. Cao, L. Li, Q. Tang and G. Cheng, *Biomaterials*, 2013, **34**, 7592.
177 T. Tah and M. T. Bernards, *Colloids Surf., B*, 2012, **93**, 195.
178 M. Ratel, A. Provencher-Girard, S. S. Zhao, J. Breault-Turcot, J. Labrecque-Carbonneau, M. Branca, J. N. Pelletier, A. R. Schmitzer and J.-F. Masson, *Anal. Chem.*, 2013, **85**, 5770.
179 S. Reitsma, D. W. Slaaf, H. Vink, M. A. M. J. van Zandvoort and M. G. A. oude Egbrink, *Pflügers Archiv. – Eur. J. Physiol.*, 2007, **454**, 345.
180 S. Weinbaum, J. M. Tarbell and E. R. Damiano, *Annu. Rev. Biomed. Eng.*, 2007, **9**, 121.
181 N. B. Holland, Y. Qiu, M. Ruegsegger and R. E. Marchant, *Nature*, 1998, **392**, 799.
182 M. A. Ruegsegger and R. E. Marchant, *J. Biomed. Mater. Res.*, 2001, **56**, 159.
183 C. Perrino, S. Lee, S. W. Choi, A. Maruyama and N. D. Spencer, *Langmuir*, 2008, **24**, 8850.
184 K. Yu, B. F. L. Lai and J. N. Kizhakkedathu, *Adv. Healthcare Mater.*, 2012, **1**, 199.
185 T. Riedel, Z. Riedelová-Reicheltová, P. Májek, C. Rodriguez-Emmenegger, M. Houska, J. E. Dyr and E. Brynda, *Langmuir*, 2013, **29**, 3388.
186 M. Wahlgren and T. Arnebrant, *Trends Biotechnol.*, 1991, **9**, 201.
187 J. Breault-Turcot, P. Chaurand and J.-F. Masson, *Anal. Chem.*, 2014, **86**, 9612.
188 For the identification of 98 proteins adsorbed from undiluted human plasma on a set of polyMeOEGMA, polySBMA, and polyHEMA antifouling polymer brushes grafted to silica particles, see: G. Gunkel and W. T. S. Huck, *J. Am. Chem. Soc.*, 2013, **135**, 7047.
189 For the identification of 147 proteins adsorbed from 10% human serum on PEG-coated gold nanoparticles, see: C. D. Walkey, J. B. Olsen, H. Guo, A. Emili and W. C. W. Chan, *J. Am. Chem. Soc.*, 2012, **134**, 2139.
190 For the identification of 49 proteins adsorbed from human plasma on poly(*N*,*N*-dimethyl-acrylamide) brush-grafted polystyrene particles, see: B. F. L. Lai, A. L. Creagh, J. Janzen, C. A. Haynes, D. E. Brooks and J. N. Kizhakkedathu, *Biomaterials*, 2010, **31**, 6710.
191 For the identification of proteins (up to 50) adsorbed from platelet-poor human plasma on a series of mannose, galactose or glucose-based glycopolymer brushes grafted to polystyrene particles as biomimicry of the carbohydrate-rich outer surface of biological cell membranes (glycocalyx) – and the influence of the type of anticoagulant treatment (sodium citrate or heparin) on the composition of adsorbed proteins – please see ref. 184.
192 For a review on the interaction of nanomaterials with proteins in physiological environments and an 'adsorbome' of 125 plasma proteins known to associate with nanomaterials, see: C. D. Walkey and W. C. W. Chan, *Chem. Soc. Rev.*, 2012, **41**, 2780.
193 See also: Z. W. Lai, Y. Yan, F. Caruso and E. C. Nice, *ACS Nano*, 2012, **6**, 10438.
194 R. M. Cornelius, J. G. Archambault, L. Berry, A. K. C. Chan and J. L. Brash, *J. Biomed. Mater. Res.*, 2002, **60**, 622.
195 I. A. Buhimschi, R. Christner and C. S. Buhimschi, *Br. J. Obstetrics Gynaecol.*, 2005, **112**, 173.
196 A. Farina, J.-M. Dumonceau, P. Antinori, I. Annessi-Ramseyer, J.-L. Frossard, D. F. Hochstrasser, M. Delhaye and P. Lescuyer, *Biochim. Biophys. Acta*, 2014, **1844**, 1018.
197 S. A. Kharitonov and P. J. Barnes, *Am. J. Respir. Crit. Care Med.*, 2001, **163**, 1693.
198 M. Shirasu and K. Touhara, *J. Biochem.*, 2011, **150**, 257.
199 M. A. Feig, E. Hammer, U. Völker and N. Jehmlich, *J. Proteomics*, 2013, **83**, 119.
200 X. Cai, G. Pacheco-Rodriguez, Q.-Y. Fan, M. Haughey, L. Samsel, S. El-Chemaly, H.-P. Wu, J. P. McCoy, W. K. Steagall, J.-P. Lin, T. N. Darling and J. Moss, *Am. J. Respir. Crit. Care Med.*, 2010, **182**, 1410.
201 S. H. Kim, J. Y. Kim, H. J. Lee, M. Gi, B. G. Kim and J. Y. Choi, *PLoS One*, 2014, **9**, e111039.
202 A. D. Sutherland, R. B. Gearry and F. A. Frizelle, *Dis. Colon Rectum*, 2008, **51**, 1283.
203 C. Malagù, B. Fabbri, S. Gherardi, A. Giberti, V. Guidi, N. Landini and G. Zonta, *Sensors*, 2014, **14**, 18982.
204 L. Cui, X. Zhang, G. Ye, T. Zheng, H. Song, H. Deng, B. Xiao, T. Xia, X. Yu, Y. Le and J. Guo, *Cancer*, 2013, **119**, 1618.
205 S.-R. Won, D.-C. Lee, S. H. Ko, J.-W. Kim and H.-I. Rhee, *Food Res. Int.*, 2008, **41**, 952.
206 C. D. Derby, *Mar. Drugs*, 2014, **12**, 2700.
207 P. Gromov, I. Gromova, C. J. Olsen, V. Timmermans-Wielenga, M.-L. Talman, R. R. Serizawa and J. M. A. Moreira, *Biochim. Biophys. Acta*, 2013, **1834**, 2259.
208 A. Urruticoechea, I. E. Smith and M. Dowsett, *J. Clin. Oncol.*, 2005, **23**, 7212.
209 Z. Meng and T. D. Veenstra, *Proteomics Clin. Appl.*, 2007, **1**, 747.
210 F. H. Grus, S. C. Joachim and N. Pfeiffer, *Proteomics Clin. Appl.*, 2007, **1**, 876.
211 K. Karatolios, S. Pankuweit and B. Maisch, *Heart Fail. Rev.*, 2013, **18**, 337.
212 A. C. Lysaght, S.-Y. Kao, J. A. Paulo, S. N. Merchant, H. Steen and K. M. Stankovic, *J. Proteome Res.*, 2011, **10**, 3845.
213 R. A. Siciliano, M. F. Mazzeo, V. Spada, A. Facchiano, A. d'Acierno, M. Stocchero, P. De Franciscis, N. Colacurci, N. Sannolo and N. Miraglia, *Gynecol. Endocrinol.*, 2014, **30**, 872.
214 J. M. Porcel, *Clin. Chest Med.*, 2013, **34**, 27.
215 F. González-Illán, G. Ojeda-Torres, L. M. Díaz-Vázquez and O. Rosario, *J. Anal. Toxicol.*, 2011, **35**, 232.
216 B. Behrouzi, S. Kenigsberg, N. Alladin, S. Swanson, J. Zicherman, S.-H. Hong, S. I. Moskovtsev and C. L. Librach, *Syst. Biol. Reprod. Med.*, 2013, **59**, 153.
217 S. D. Sagel, B. D. Wagner, M. M. Anthony, P. Emmett and E. T. Zemanick, *Am. J. Respir. Crit. Care Med.*, 2012, **186**, 857.

218 J. B. Catterall, T. V. Stabler, C. R. Flannery and V. B. Kraus, *Arthritis Res. Ther.*, 2010, **12**, R229.
219 C. Deirmengian, N. Hallab, A. Tarabishy, C. Della Valle, J. J. Jacobs, J. Lonner and R. E. Booth Jr., *Clin. Orthop. Relat. Res.*, 2010, **468**, 2017.
220 N. von Thun und Hohenstein-Blaul, S. Funke and F. H. Grus, *Exp. Eye Res.*, 2013, **117**, 126.
221 A. Buhtz, A. Kolasa, K. Artl, C. Walz and J. Kehr, *Planta*, 2004, **219**, 610.
222 *Cell Lysis Technical Handbook (Featuring Cell Lysis Reagents and Detergents)*, ed. Thermo Scientific Pierce, 2009.
223 A. Aubé, J. Breault-Turcot, P. Chaurand, J. N. Pelletier and J.-F. Masson, *Langmuir*, 2013, **29**, 10141.
224 D. U. Silverthorn, The Central Nervous System, in *Human Physiology – An Integrated Approach*, Pearson-Benjamin Cummings Publisher, USA, 3rd edn, 2004, ch. 9, pp. 284–320.
225 F. Fischbach and M. B. Dunning III, Cerebrospinal Fluid Studies, in *A Manual of Laboratory and Diagnostic Tests*, Wolters Kluwer Health/Lippincott Williams and Wilkins Publishers, USA, 8th edn, 2008, ch. 5, pp. 310–337.
226 R. D. Terlizzi and S. Platt, *Vet. J.*, 2006, **172**, 422.
227 J. Valenta and P. Fiala, Ventricular System and Cerebrospinal Fluid, in *Central Nervous System – Overview of Anatomy*, Karolinum Press, Czech Republic, 1st edn, 2012, ch. 9, pp. 93–98.
228 M. H. Maurer, *Mass Spectrom. Rev.*, 2010, **29**, 17.
229 R. Mandal, A. C. Guo, K. K. Chaudhary, P. Liu, F. S. Yallou, E. Dong, F. Aziat and D. S. Wishart, *Genome Med.*, 2012, **4**, 38.
230 H. Tumani, C. Teunissen, S. Süssmuth, M. Otto, A. C. Ludolph and J. Brettschneider, *Expert Rev. Mol. Diagn.*, 2008, **8**, 479.
231 A. M. Fagan and R. J. Perrin, *Biomarkers Med.*, 2012, **6**, 455.
232 Please visit the Food and Agriculture Organization of the United Nations (UNFAO) – Statistics Division's website at http://faostat.fao.org.
233 H.-D. Belitz, W. Grosch and P. Schieberle, in *Food Chemistry*, Springer-Verlag, Germany, 3rd edn, 2004, pp. 551–565.
234 H.-D. Belitz, W. Grosch and P. Schieberle, in *Food Chemistry*, Springer-Verlag, Germany, 3rd edn, 2004, pp. 505–550.
235 C. Rodriguez-Emmenegger, O. A. Avramenko, E. Brynda, J. Skvor and A. Bologna Alles, *Biosens. Bioelectron.*, 2011, **26**, 4545.
236 X. Liu, R. Huang, R. Su, W. Qi, L. Wang and Z. He, *ACS Appl. Mater. Interfaces*, 2014, **6**, 13034.
237 B. Bansal and X. D. Chen, *Compr. Rev. Food Sci. Food Safety*, 2006, **5**, 27.
238 S. Prakash, N. Datta and H. C. Deeth, *Food Rev. Int.*, 2005, **21**, 267.
239 J. A. Barish and J. M. Goddard, *Food Bioprod. Process.*, 2013, **91**, 352.
240 J. S. Patel, B. Bansal, M. I. Jones and M. Hyland, *J. Food Eng.*, 2013, **116**, 413.
241 See also: R. Rosmaninho, O. Santos, T. Nylander, M. Paulsson, M. Beuf, T. Benezech, S. Yiantsios, N. Andritsos, A. Karabelas, G. Rizzo, H. Müller-Steinhagen and L. F. Melo, *J. Food Eng.*, 2007, **80**, 1176.
242 E. Sadeghinezhad, S. N. Kazi, A. Badarudin, M. N. M. Zubair, B. L. Dehkordi and C. S. Oon, *Rev. Chem. Eng.*, 2013, **29**, 169.
243 E. Sadeghinezhad, S. N. Kazi, M. Dahari, M. R. Safaei, R. Sadri and A. Badarudin, *Crit. Rev. Food Sci. Nutr.*, 2015, **55**, 1724.
244 P. M. Withers, *Trends Food Sci. Technol.*, 1996, **7**, 293.
245 For a review on surface fouling as it affects the food industry as a whole, see: T. Mérian and J. M. Goddard, *J. Agric. Food Chem.*, 2012, **60**, 2943.
246 S. Balasubramanian and V. M. Puri, *J. Food. Eng.*, 2009, **91**, 608.
247 M. Britten, M. L. Green, M. Boulet and P. Paquin, *J. Dairy Res.*, 1988, **55**, 551.
248 M. Beuf, G. Rizzo, J. C. Leuliet, H. Müller-Steinhagen, S. Yiantsios, A. Karabelas and T. Benezech, Fouling and Cleaning of Modified Stainless Steel Plate Heat Exchangers Processing Milk Products, in *Referred Proceedings of Heat Exchanger Fouling and Cleaning: Fundamentals and Applications*, Engineering Conferences International (ECI) Digital Archives Publisher, 2003.
249 A. B. Kananeh, E. Scharnbeck, U. D. Kück and N. Räbiger, *Food Bioprod. Process.*, 2010, **88**, 349.
250 T. Arnebrant, Protein Adsorption in the Oral Environment, in *Biopolymers at Interfaces*, ed. M. Malmsten, Marcel Dekker Inc., USA, 2nd edn, 2003, ch. 29, pp. 811–856.
251 U. Lendenmann, J. Grogan and F. G. Oppenheim, *Adv. Dent. Res.*, 2000, **14**, 22.
252 M. Edgerton and M. J. Levine, *J. Prosthet. Dent.*, 1993, **69**, 406.
253 J. M. Yoshizawa, C. A. Schafer, J. J. Schafer, J. J. Farrell, B. J. Paster and D. T. W. Wong, *Clin. Microbiol. Rev.*, 2013, **26**, 781.
254 P. D. V. de Almeida, A. M. T. Grégio, M. A. N. Machado, A. A. S. de Lima and L. R. Azevedo, *J. Contemp. Dent. Pract.*, 2008, **9**, 72.
255 S. P. Humphrey and R. T. Williamson, *J. Prosthet. Dent.*, 2001, **85**, 162.
256 W. L. Siqueira, E. J. Helmerhorst, W. Zhang, E. Salih and F. G. Oppenheim, *Ann. N. Y. Acad. Sci.*, 2007, **1098**, 504.
257 M. A. Catalán, T. Nakamoto and J. E. Melvin, *J. Med. Invest.*, 2009, **56**, 192.
258 N. Vassilakos, T. Arnebrant and P.-O. Glantz, *Scand. J. Dent. Res.*, 1992, **100**, 346.
259 N. Vassilakos, T. Arnebrant and P.-O. Glantz, *Scand. J. Dent. Res.*, 1993, **101**, 133.
260 See also: N. Vassilakos, P.-O. Glantz and T. Arnebrant, *Scand. J. Dent. Res.*, 1993, **101**, 339.

261 See also: L. Lindh, T. Arnebrant, P.-E. Isberg and P.-O. Glantz, *Biofouling*, 1999, **14**, 189.
262 See also: L. Lindh, P.-O. Glantz, P.-E. Isberg and T. Arnebrant, *Biofouling*, 2001, **17**, 227.
263 R. Müller, G. Gröger, K.-A. Hiller, G. Schmalz and S. Ruhl, *Appl. Environ. Microbiol.*, 2007, **73**, 2653.
264 See also: R. Müller, K.-A. Hiller, G. Schmalz and S. Ruhl, *Anal. Biochem.*, 2006, **359**, 194.
265 For oral film formation on polydimethylsiloxane (PDMS) coatings, see: R. E. Baier and P.-O. Glantz, *Acta Odontol. Scand.*, 1978, **36**, 289.
266 D. U. Silverthorn, The Kidneys, in *Human Physiology – An Integrated Approach*, Pearson-Benjamin Cummings Publisher, USA, 3rd edn, 2004, ch. 19, pp. 598–624.
267 S. Decramer, A. Gonzalez de Peredo, B. Breuil, H. Mischak, B. Monsarrat, J.-L. Bascands and J. P. Schanstra, *Mol. Cell. Proteomics*, 2008, **7**, 1850.
268 S. Bouatra, F. Aziat, R. Mandal, A. C. Guo, M. R. Wilson, C. Knox, T. C. Bjorndahl, R. Krishnamurthy, F. Saleem, P. Liu, Z. T. Dame, J. Poelzer, J. Huynh, F. S. Yallou, N. Psychogios, E. Dong, R. Bogumil, C. Roehring and D. S. Wishart, *PLoS One*, 2013, **8**, e73076.
269 D. F. Putnam, Composition and Concentrative Properties of Human Urine, in *NASA Contractor Report NASA CR-1802*, National Aeronautics and Space Administration Publisher, USA, 1971.
270 M. Houser, *J. Pediatr.*, 1984, **104**, 845.
271 T. Pisitkun, R. Johnstone and M. A. Knepper, *Mol. Cell. Proteomics*, 2006, **5**, 1760.
272 M. K. Parr and W. Schänzer, *J. Steroid Biochem. Mol. Biol.*, 2010, **121**, 528.
273 K. Wolff, M. Farrell, J. Marsden, M. G. Monteiro, R. Ali, S. Welch and J. Strang, *Addiction*, 1999, **94**, 1279.
274 J. A. Armstrong, *Kidney Int.*, 2007, **71**, 384.

